

**Swap70b acts downstream of Wnt11  
signalling to regulate zebrafish convergence  
and extension cell movements**

**Xiaoou Xu, MSc**

**Thesis submitted to the University of Nottingham for the degree of  
Doctor of Philosophy**

**May 2014**

## Abstract

During vertebrate gastrulation, convergence and extension (CE) cell movements narrow the body axis medial-laterally (convergence) and extend it anterior-posteriorly (extension). In zebrafish, Wnt11 (*silberblick*) and Wnt5b (*pipetail*) mutants exhibited widening and shortening of the body axes characteristic for CE cell movements defects during gastrulation. It was subsequently reported that Wnt signalling resulted in activation of Rho GTPases and rearrangements of the F-actin cytoskeleton, establishing that CE cell movements are regulated through the non-canonical Wnt/PCP pathway. Rho GTPases are activated by guanine nucleotide exchange factors (GEFs) and it was recently found that Def6a, a GEF for Rac1, Cdc42, and RhoA, was the downstream target of Wnt5b signalling.

In this thesis, morpholino-mediated knockdown of gene expression in conjunction with phenotypic rescue experiments revealed that Swap70b, a GEF protein closely related to Def6a, functions downstream of Wnt11. *Swap70b* morphants exhibited broader and shorter body axis with no apparent defect in cell fate specification, and ectopic Swap70b expression robustly rescued *wnt11* morphants, establishing Swap70b as a novel member of the non-canonical Wnt/PCP pathway downstream of Wnt11. The following phenotypic rescue experiments demonstrated that Swap70b and Def6a execute both distinct and overlapping functions in the modulation of CE cell movements. In addition, as previously shown for Wnt11 (*silberblick*) and Wnt5b (*pipetail*) double mutants, Swap70b and Def6a double mutant morphants exhibited a more severe CE cell movement defect, suggesting that Swap70b and Def6a delineate Wnt11 and Wnt5b signalling pathways.

# Acknowledgements

First and foremost, I would like to thank my supervisor, Professor Fred Sablitzky, for his continuous support during my PhD study, for his patience and enthusiasm that helped me go through all the tough times in developing our publication as well as this thesis, and for his immense and profound knowledge that helped to get my technical problems and theoretical questions solved. Fred has given me the moral support and the freedom I needed to go through all those difficulties during my scientific research and writing this thesis.

My sincere thanks also go to Dr. Martin Gering and Dr. Paul Scotting for their help with the fish facility and microscopy systems, to Dr. Peter Jones for his insightful comments and advice in lab meetings. A special thank you goes to Ivan (Yu-Huan Shih) who taught me all the essential zebrafish techniques. Thanks also go to Sarah Buxton and Carol Brown for taking care of the fish, to Julie and Lorraine for all the daily lab supports, to Emma King and Ian Ward for help with the confocal microscope system. I also thank my labmates: Taina Theodore, Nathan Czyzewicz, Selam Aman, Tamilvendhan Dhanaseelan, Huaitao Cheng, Chen Chen, Deniz Akdeniz etc. for all the fun we have had in the lab, and Katerina Goudevenou and Timothy (Wai Ho Shuen) for the cooperation in our publication (in preparation).

Last but not the least, I would like to thank my family, especially my parents Jingqing Xu and Ping Wang, my fiancé, and my friends for their constant support and unconditional love throughout my life.

## Abbreviations

A-P	anterior-posterior
BMP	bone morphogenetic protein
CE	convergence and extension
Cdc42	cell division cycle 42
cDNA	complementary DNA
<i>cdx4</i>	<i>caudal homeobox transcription factor 4</i>
<i>chd</i>	<i>chordin</i>
Def6	differentially expressed in FDCP 6
DEL	deep cell multilayer
DH	Dbl homology
dH <sub>2</sub> O	deionised water
DIG	Digoxigenin
DIX	Dishevelled/Axin protein domain
<i>dlx3b</i>	<i>distal-less homeobox gene 3b</i>
DMSO	dimethyl sulphoxide
DNase	Deoxyribonuclease
dNTPs	deoxyribonucleotide triphosphates
dpf	days post fertilization
Dsh	Dishevelled
DSH	Def6-Swap70 homology
DTT	dithiothreitol
D-V	dorsal-ventral
EDTA	ethylenediaminetetraacetic acid
EVL	Enveloping layer
Fz	Frizzled
GFP	green fluorescent protein
<i>gsc</i>	<i>goosecoid</i>
GDP	guanosine 5'-diphosphate
GTP	guanosine 5'-triphosphate

---

<i>hgg1</i>	<i>hatching gland 1</i>
hpf	hours post fertilization
ITAMs	immunoreceptor tyrosine-based activation motifs
JNK	Jun-N-terminal kinase
MO	morpholino oligonucleotide
mRNA	messenger RNA
MBT	midblastula transition
<i>myoD</i>	<i>myogenic differentiation</i>
<i>ntl</i>	<i>no-tail</i>
tRNA	transfer RNA
PBS	Phosphate buffered saline
PCP	planar cell polarity
PCR	polymerase chain reaction
PDZ	Postsynaptic density 95, Discs Large, Zonula occludens-1
PFA	paraformaldehyde
PH	Pleckstrin homology
PKC	protein kinase C
<i>ppt</i>	<i>pipetail</i>
Rac	Ras-related C3 botulinum toxin substrate
RhoA	Ras homologue gene family member A
RNase	Ribonuclease
ROCK	Rho-associated kinase
RT-PCR	reverse transcriptase- polymerase chain reaction
<i>shh</i>	<i>sonic hedgehog</i>
SSC	saline sodium citrate
Swap70b	switch-associated protein 70b
SYK	spleen tyrosine kinase
Taq	Thermus aquaticus
TE	Tris-EDTA buffer
TBE	Tris-borate buffer
YSL	yolk syncitial layer

# Table of Contents

<b>Chapter 1</b>	<b>Introduction .....</b>	<b>1</b>
1.1	Zebrafish as a model to investigate vertebrate development.....	1
1.1.1	The morpholino mediated gene knockdown technique .....	2
1.1.2	Early developmental stages of zebrafish .....	5
1.1.3	Cell movements during gastrulation .....	10
1.2	The non-canonical Wnt/PCP pathway in CE regulation .....	16
1.2.1	Structure of the non-canonical Wnt/PCP pathway .....	18
1.2.2	Specific CE cell behaviours regulated by the non-canonical Wnt/PCP pathway.....	26
1.3	Rho GTPases, downstream effectors of the non-canonical Wnt/PCP pathway .....	29
1.3.1	Rho GTPases in the reorganisation of cytoskeleton .....	30
1.3.2	Rho GTPase involvement in the non-canonical Wnt/PCP pathway.....	32
1.3.3	Main Rho GTPase regulators .....	34
1.4	Swap70, an atypical GEF for Rho GTPases.....	40
1.4.1	Structural features and variable intracellular localisation.....	40
1.4.2	Diverse biological functions.....	42
1.5	Preliminary investigation of Swap70 function in zebrafish embryogenesis ..	46
1.5.1	Identification of <i>def6</i> paralogues in zebrafish.....	47
1.5.2	Expression pattern of <i>swap70b</i> during zebrafish embryogenesis .....	50
1.5.3	Functional analysis of Swap70b during zebrafish development.....	54
1.6	Spleen tyrosine kinase (SYK), a direct upstream regulator of Swap70.....	62
1.6.1	Immune functions.....	64
1.6.2	SYK regulates B cell migration by phosphorylation of Swap70 .....	65
1.6.3	Function during development.....	65
1.7	Aims and objectives.....	66
<b>Chapter 2</b>	<b>Materials &amp; Methods.....</b>	<b>68</b>
2.1	Materials.....	68
2.1.1	Technical Equipment .....	68
2.1.2	Molecular biology .....	69
2.1.3	Zebrafish experiments .....	70

2.2 Methods .....	72
2.2.1 Molecular biology .....	72
2.2.2 Zebrafish techniques .....	75
<b>Chapter 3</b>	
<b>Swap70b is required for normal CE cell movements during gastrulation.....</b>	<b>80</b>
3.1 Introduction .....	80
3.2 Results .....	81
3.2.1 Swap70b loss-of-function results in aberrant gastrulation.....	81
3.2.2 Swap70b is required for normal CE cell movements in zebrafish.....	88
3.2.3 <i>Swap70b</i> knockdown does not affect cell fate specification .....	92
3.3 Discussion .....	94
<b>Chapter 4</b>	
<b>Swap70b regulates CE cell movements through the non-canonical Wnt/PCP pathway downstream of Wnt11 .....</b>	<b>96</b>
4.1 Introduction .....	96
4.2 Results .....	98
4.2.1 <i>Swap70b</i> MO induced-defects resemble those of <i>wnt5b</i> and <i>wnt11</i> morphants at late developmental stage .....	98
4.2.2 Swap70b modulates CE cell movements downstream of Wnt11 .....	101
.....	106
4.2.3 Swap70b enhances the <i>ppt/wnt5b</i> phenotype in <i>wnt5b</i> morphants ....	107
4.3 Discussion .....	112
4.3.1 <i>Swap70b</i> morphants share similar CE cell movements defects with both <i>wnt11</i> and <i>wnt5b</i> morphants.....	112
4.3.2 Swap70b functions downstream of Wnt11 in the non-canonical Wnt/PCP pathway.....	113
4.3.3 Swap70b and Wnt5b likely act in parallel pathways to regulate CE cell movements .....	114
<b>Chapter 5</b>	
<b>Swap70b showed no apparent effects on F-actin assembly.....</b>	<b>116</b>
5.1 Introduction .....	116

5.2 Results .....	118
5.3 Discussion .....	120
<b>Chapter 6</b>	
<b>Swap70b and Def6a perform overlapping and distinct function in the non-canonical Wnt/PCP pathway.....</b>	<b>121</b>
6.1 Introduction .....	121
6.2 Results .....	122
6.2.1 Swap70b and Def6a partially rescued each other when expressed ectopically.....	122
6.2.2 Swap70b and Def6a knockdown results in an additive effect on CE cell movements .....	133
6.3 Discussion .....	136
6.3.1 Swap70b and Def6a play partially redundant roles in the regulation of CE cell movements .....	136
6.3.2 Swap70b and Def6a execute distinct functions in the non-canonical Wnt/PCP pathway .....	137
<b>Chapter 7</b>	
<b>Essential role for SYK in zebrafish gastrulation via Swap70b ....</b>	<b>138</b>
7.1 Introduction .....	138
7.2 Results .....	139
7.2.1 <i>Syk</i> morphants display similar phenotypes to <i>swap70b</i> morphants .....	139
7.2.2 <i>Swap70b</i> enhances gastrulation defects in <i>syk</i> morphants .....	141
7.3 Discussion .....	144
<b>Chapter 8 Conclusions &amp; Prospects.....</b>	<b>145</b>
8.1 Conclusions .....	145
8.1.1 Swap70b is essential for normal CE cell movements during zebrafish gastrulation.....	145
8.1.2 Proposed model of Swap70b signalling in regulating CE cell movements .....	146
8.2 Prospects .....	149
8.2.1 Additional potential functions of Swap70b in zebrafish development..	149



8.2.2 In-depth analysis of mechanisms underlying Swap70b function .....	150
8.2.3 The potential role of SYK in the regulation of CE cell movements .....	152
<b>References .....</b>	<b>154</b>

# List of Figures

Figure 1.1 Structure and action mode of MO .....	4
Figure 1.2 Overview of zebrafish developmental stages.....	6
Figure 1.3 Gastrulation movements during zebrafish embryogenesis.....	11
Figure 1.4 Distinct cell behaviors along the D-V axis during CE cell movements.....	15
Figure 1.5 Overview of the Wnt signalling pathways.....	17
Figure 1.6 Schematic illustration of the non-canonical Wnt/PCP pathway..	19
Figure 1.7 Cell behaviours controlled by the non-canonical Wnt/PCP pathway in CE .....	27
Figure 1.8 Rho GTPases in the non-canonical Wnt/PCP pathway.....	33
Figure 1.9 The regulation of GTPase activity .....	35
Figure 1.10 Atypical domain arrangements of Def6 and Swap70 .....	38
Figure 1.11 A hypothetical model for the intracellular re-localisation of Swap70.....	41
Figure 1.12 Predicted domain structures of Def6 paralogues in Zebrafish...	48
Figure 1.13 Amino acid sequence comparison of Swap70b proteins in different species .....	49
Figure 1.14 Diverse developmental expressions of <i>def6</i> paralogues .....	50
Figure 1.15 <i>Swap70b</i> is ubiquitously expressed in zebrafish development.	52
Figure 1.16 Splice MOs affect <i>swap70b</i> pre-mRNA splicing. ....	56
Figure 1.17 Determination of the specificity of <i>swap70b</i> MOs .....	58
Figure 1.18 <i>Swap70b</i> loss-of-function resulted in underdeveloped, non-viable zebrafish embryos. ....	61
Figure 1.19 Schematic structures of SYK family tyrosine kinases .....	63
Figure 2.1 Fixation of phalloidin stained zebrafish embryos .....	79
Figure 3.1 <i>Swap70</i> morphants exhibiting reduced length of the body axis can be rescued by ectopic expression of GFP/ <i>Swap70b</i> fusion protein.....	83
Figure 3.2 <i>Swap70b</i> morphants display a shorter body axis that can be rescued by <i>swap70b</i> mRNA.....	86

Figure 3.3 CE cell movements are impaired in <i>swap70b</i> morphants. ....	89
Figure 4.1 <i>Swap70b</i> morphants phenocopy <i>wnt11</i> morphants and <i>wnt5b</i> morphants at 24hpf. ....	100
Figure 4.2 Wnt11-deficiency leads to aberrant CE cell movements that can be partially rescued by <i>GFP/swap70b</i> mRNA. ....	102
Figure 4.3 <i>GFP/swap70b</i> mRNA successfully rescued <i>wnt11</i> morphants at early developmental stage. ....	105
Figure 4.4 <i>Swap70b</i> mRNA failed to restore the <i>wnt5b</i> MO-induced CE movement defects. ....	108
Figure 4.5 Preliminary results suggest that Wnt5b/Swap70b double mutant embryos exhibit enhanced CE cell movement phenotype. ....	111
Figure 5.1 Organisation of the cytoskeleton in the zebrafish yolk cell during gastrulation ....	117
Figure 5.2 Preliminary results suggest that knockdown of Swap70b has no significant effects on actin rearrangements. ....	119
Figure 6.1 Ectopic expression of GFP/Swap70b fusion protein rescued <i>def6a</i> morphants. ....	124
Figure 6.2 <i>GFP/swap70b</i> mRNA successfully rescues <i>def6a</i> morphants at early developmental stage. ....	127
Figure 6.3 Ectopic expression of GFP/Def6a fusion protein rescues <i>swap70b</i> morphants. ....	129
Figure 6.4 <i>GFP/def6a</i> mRNA successfully rescues <i>swap70b</i> morphants at early developmental stage. ....	132
Figure 6.5 Def6a and Swap70b have partially redundant functions in CE cell movement. ....	134
Figure 6.6 Three dimensional structure predictions of Def6a and Swap70b ....	136
Figure 7.1 <i>Syk</i> morphants resemble <i>swap70b</i> morphants at 24hpf. ....	140
Figure 7.2 Swap70b worsens gastrulation defects in <i>syk</i> morphants. ....	142
Figure 8.1 A proposed model of Swap70b signalling ....	149

## List of Tables

Table 1.1 Major components of the non-canonical Wnt/PCP pathway .....	21
Table 1.2 Gene name and ID summary of <i>swap70</i> and <i>def6</i> paralogues in zebrafish.....	47
Table 2.1 Antisense riboprobes synthesised from listed genes for in situ hybridisations .....	74
Table 2.2 MOs used for specific gene knockdown in this thesis .....	76

# Chapter 1 Introduction

Activated by evolutionarily conserved Wnt ligands, Wnt signalling pathway is one of the most fundamental pathways essential for a wide range of developmental events, ranging from cell differentiation, proliferation, to cell migration and tissue patterning. Originally identified in *Drosophila melanogaster*, the non-canonical Wnt/PCP branch polarises cells in the plane of a tissue and equips cells with a specified orientation in numerous processes during vertebrate development. The convergence and extension cell movements (CE) during gastrulation are the first such process in which the critical role of the Wnt signalling pathway has been established.

## 1.1 Zebrafish as a model to investigate vertebrate development

In 1996, the publication of two large-scale forward genetic screens in the zebrafish (*Danio rerio*) marked the launch of zebrafish as a respectable vertebrate model system that could take a place next to the “big three” of *Xenopus*, chick, and mouse (Driever et al., 1996; Haffter et al., 1996). Over the past decades, the zebrafish has become a powerful tool for genetic dissection of early vertebrate development and organogenesis, and increasingly for studies in disease processes such as infection and cancer (Kari et al., 2007; Renshaw et al., 2012; Stern et al., 2003).

Both forward and reverse genetic approaches have been successfully used in zebrafish. The ease of maintenance, the high fecundity and the reasonably short generation time render performance of large-scale mutagenesis screens

to identify novel genetic pathways. In addition, the optically transparent embryos allow researchers to carry out *in vivo* imaging, allowing easy phenotypic analysis. Reverse genetic techniques applicable to the zebrafish model have been reviewed by Skromne et al. (2008), including pharmaceutical approaches, analysis of gene function by over-expression, antisense and transgenic approaches (Skromne et al., 2008). In particular, the establishment of morpholino oligonucleotide (MO)-mediated gene knockdown allowed easy loss-of-function analysis in zebrafish (Skromne et al., 2008).

### **1.1.1 The morpholino mediated gene knockdown technique**

Developed over 20 years ago, antisense technology has been a widely adopted approach used to inhibit the action of a gene of interest during development so as to learn its normal biological function (Izant et al., 1985). The conventional antisense mRNA technique proved successful in blocking the translation of endogenous mRNA in frog (Izant et al., 1985), and the use of antisense oligonucleotides allowed researchers to study the functions of maternally inherited transcripts in frog oocytes (Birsoy et al., 2006). Studies in *C. elegans* revealed that double-stranded RNAs interfere with endogenous gene function (Fire et al., 1998), which led to a Nobel Prize for the discovery of dsRNA mediated interference (Couzin, 2006). However, this approach failed to reveal the roles of zygotically expressed genes in the frog, and antisense RNA was shown to have widespread effects in the zebrafish, which prevented the use of this approach for the investigation of specific gene functions during development (Heasman, 2002; Oates et al., 2000). Early this century, it was shown that MOs can be used to knockdown specific genes in both frog and zebrafish (Egger, 2000; Heasman et al., 2000). The high efficacy of MOs to test gene function was thereafter quickly recognised and applied to a variety of

model organisms, such as the chick *Gallus gallus* (Kos et al., 2001) and oocytes of the mouse *Mus musculus* (Coonrod et al., 2001).

MOs are a synthetic derivative of DNA composed of chains of about 25 bases, which were first developed to inhibit the translation of RNA transcripts *in vivo* (Partridge et al., 1996; Stein et al., 1997; **Figure 1.1A, B**). Rapid advances in MO technology have accelerated discovery screening as well as individual gene function analysis (Eckfeldt et al., 2005; Lan et al., 2007; Pickart et al., 2006). Fluorescent MOs can be used to monitor the distribution of MOs within the developmental embryos (Rana et al., 2006). More recently, photoactivatable MO was reported to provide a measure of spatiotemporal control over gene knockdown, making it possible in principle to target gene in specific regions of the embryo, and at particularly relevant developmental stages as well (Shestopalov et al., 2007). Finally, MOs can also be used to inhibit the action of microRNAs by targeting either the mature microRNA or the microRNA precursor (Kloosterman et al., 2007). While some limitations such as reduced stability when stored in aqueous solution and off-target effects still exist, MOs remain the most common tool for gene-specific antisense knockdown in a wide range of model species (Victoria et al., 2011; Nasevicius et al., 2000).

There are two types of MO applications, translational blocking and splice blocking (Morcos et al., 2007; Summerton, 1999). The translation initiation blocking MOs (AUG MOs) have a sequence complementary to the region within the 5' untranslated region near the translational start site, hindering ribosome assembly (Summerton, 1999; **Figure 1.1C**). If an antibody to the protein of interest is available, the level of knockdown should be assessed through western blotting (Nasevicius et al., 2000). The splice-site blocking MOs (splice MOs) have a sequence complementary to an exon-intron boundary, and therefore interfere with pre-mRNA processing or even cause exon skipping (Draper et al., 2001; Gebiski et al., 2003; **Figure 1.1D**). The

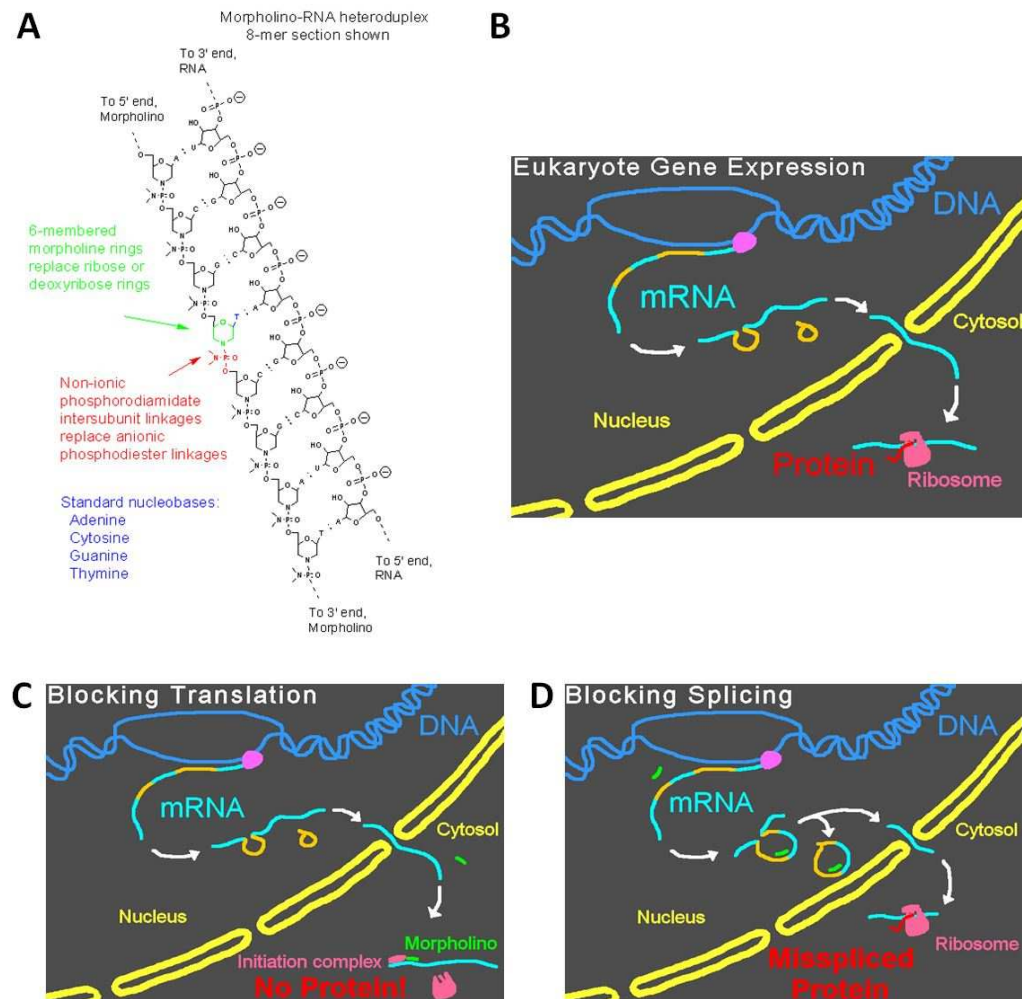


**Figure 1.1 Structure and action mode of MO**

(A) Morpholino antisense oligos are usually 25 bases in length, which bind to complementary sequences of RNA by standard nucleic acid base-pairing. (B) Normal gene expression in eukaryotes (C) AUG MO binds to the 5'-untranslated region of mRNA to interfere with progression of the ribosomal initiation complex from the 5' cap to the start codon, and thereby prevents translation of the coding region of the targeted transcript. (D) Splice MO binds to its target at the borders of introns on a strand of pre-mRNA to interfere with pre-mRNA processing steps, and thereby by prevent splice-directing small nuclear ribonucleoproteins (snRNP) complexes. All these images are adapted from <http://en.wikipedia.org/wiki/Morpholino#Structure>, which were made available under the GNU Free Documentation Licence.



quality and quantity of any new transcripts as well as knockdown of the original mRNA can be identified by RT-PCR (Morcos et al., 2007).

AUG MOs are particularly useful in model organisms whose genome sequence information is unavailable, since researchers don't need to know the intron-exon structure of the target gene. However, there is a shortcoming that it can be difficult to estimate the efficacy of MOs without an antibody of high quality (Eisen et al., 2008). Whereas splice MOs have an advantage when the gene of interest also has a maternal function, because they don't affect spliced maternal transcripts (Bennett et al., 2007; Gore et al., 2005). These two types of MOs are often used in combination to make the experimental results more trustworthy.

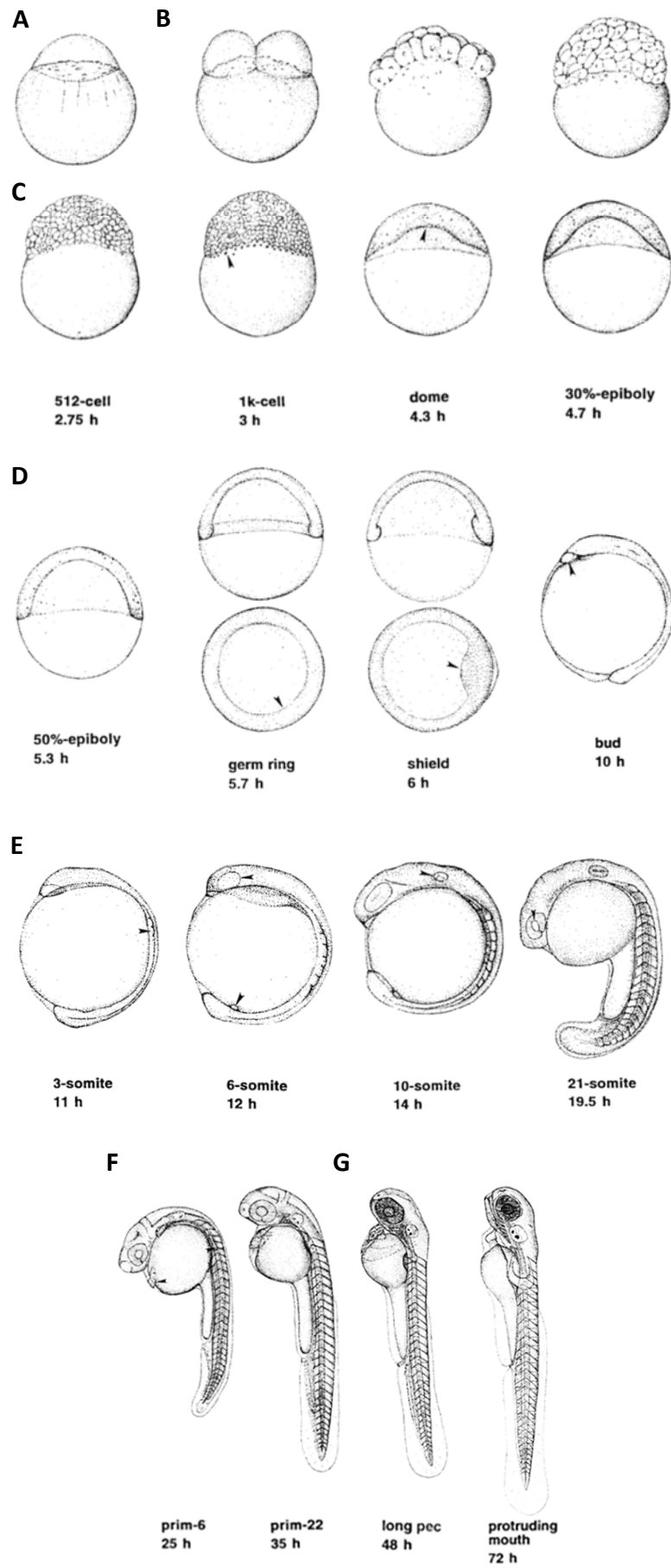
As mentioned above, there are some intrinsic problems with the MO technique despite its successes, such as the determination of the gene knockdown effectiveness and the off-target effects. In regard to these problems, Eisen et al. recommended several appropriate controls to researchers. One of them is to use at least two different MOs to target the same gene, with one designed to disrupt correct pre-mRNA splicing. The most reliable control Eisen et al. suggested is injecting the corresponding mRNA to attempt to 'rescue' the phenotype caused by the MO. This sort of rescue experiments can be straightforward for genes which are expressed ubiquitously or those without overexpression phenotype (Eisen et al., 2008).

### **1.1.2 Early developmental stages of zebrafish**

In 1995, Kimmel et al. published a staging series for the development of zebrafish embryo during the first three days after fertilization through reviewing and expanding earlier ones, which is widely accepted and applied in the developmental community (Kimmel et al., 1995, **Figure 1.2**).

## Figure 1.2 Overview of zebrafish developmental stages

Zebrafish embryos were sketched at selected stages. The anterior is to the top except for the two animal polar views shown below their lateral view counterparts for germ-ring and shield gastrulas. After shield stage, the ventral side is to the left and the dorsal side is to the right. **(A)** Zygote period; **(B)** Cleavage period; **(C)** Blastula period; **(D)** Gastrula period; **(E)** Segmentation period; **(F)** Pharyngula period; **(G)** Hatching period. Black arrows indicate the appearance of some characteristic features of the following stages: 1k-cell: YSL nuclei; dome: the doming yolk syncytium; germ ring: germ ring; shield: embryonic shield; bud: polster; 3-somite: third somite; 6-somite: eye primordium (upper arrow), Kupffer's vesicle (lower arrow); 10-somite: otic placode; 21-somite: lens primordium; prim-6: primordium of the posterior lateral line (arrow on the dorsal side), hatching gland (arrow on the yolk ball). Adapted from (Kimmel et al., 1995)



### Zygote period (0 - $\frac{3}{4}$ hours post fertilization (hpf))

Contact with water induces the chorion to swell and lift off the newly fertilized egg. Calcium waves trigger cytoplasmic streaming, during which process non-yolk cytoplasm streams towards the animal pole, resulting in a clear cytoplasmic part at the animal pole and a yolk granule-rich vegetal part (Leung et al., 1998; **Figure 1.2A**). This segregation continues throughout early cleavage stages.

### Cleavage period ( $\frac{3}{4}$ - $2\frac{1}{4}$ hpf)

After the first cleavage, the blastomeres divide regularly at approximately 15-minute intervals. The cleavages are incomplete, leaving the blastomeres, or a specific subset of them, to remain interconnected by cytoplasmic bridges (Kimmel et al., 1985). Cell cycles 2 through 7 occur rapidly and nearly synchronously (**Figure 1.2B**).

### Blastula period ( $2\frac{1}{4}$ - $5\frac{1}{4}$ hpf)

The blastula begins with the 128-cell stage embryo when the blastodisc looks ball-like, and ends with the onset of gastrulation (**Figure 1.2C**). This period includes the mid-blastula transition (MBT) at around the 512-cell stage, when rapid and metasyndronous cell cycles give way to lengthened and asynchronous ones. The yolk syncytial layer (YSL) forms at around the 1000-cell stage. Epiboly is a cell movement characterised by the simultaneous spreading and thinning of the blastodisc cell mound, as well as dispersal of the YSL nuclei over the yolk. It begins in late blastula and continues up until the end of the gastrulation period when the entire yolk is engulfed.

### Gastrula period ( $5\frac{1}{4}$ - 10 hpf)

The developing embryo undergoes gastrulation in parallel to epiboly (**Figure 1.2D**). During this process, morphogenetic cell movements of involution, convergence and extension generate the three primary germ layers and the embryonic axis. The onset of gastrulation is defined by the beginning of cell

involution at around 50% epiboly (5¼ hpf). Since there is no blastopore in zebrafish, the deep cell multi-layer (DEL) which involutes at the blastoderm margin plays the role instead. The blastoderm folds back on itself, giving rise to the germ ring. Subsequently convergence cell movements in this region generate a local thickening – the embryonic shield. This shield becomes progressively less distinctive as epiboly proceeds. Approximately 10-15 minutes after epiboly is complete, the embryo develops a prominent thickening at its caudal end, the tail bud, indicating the end of gastrulation. The majority of cells in the tail bud will contribute to the developing tail and, in a smaller proportion, to the trunk. At the end of gastrulation, the neural plate is already visible as a distinct thickening at the dorsal side within the anterior-most area.

#### Segmentation period (10 - 24 hpf)

The embryo elongates along the Anterior-Posterior (A-P) axis, the tail bud develops more prominently and the rudiments of the primary organs become discernible, such as the brain and eye (**Figure 1.2E**). Additionally, somites form in this period, and on the cellular level, the adaxial cells are the first cells that differentiate into muscle fibres. Like the somites, the notochord differentiates from anterior to posterior. Towards the end of this period, the first cells terminally differentiate, and earliest body movements appear.

#### Pharyngula period (24 - 48 hpf)

Ballard coined the term “pharyngula” to refer to the embryo that has entered the phylotypic stage (Ballard, 1981; **Figure 1.2F**). This term focuses attention on the primordial of the pharyngeal arches which give rise to the jaw and the gills. They appear at the start of this period, but at early times are difficult to discriminate individually. Other prominent structures that develop during this period include the hatching gland, pigment cells, fins, and the cardiovascular system etc. Moreover, traits such as circulation and pigmentation begin to develop.

### Hatching period (48 - 72 hpf)

The development of the jaw, the gill arches, and the pectoral fins are characteristic features of this period (**Figure 1.2G**). Most organ rudiments have more or less completed morphogenesis, and their development slows down. Zebrafish embryos from a single clutch hatch sporadically over the entire third day, and the time of hatching has no influence on the developmental progression. Therefore, developing zebrafish are arbitrarily termed as embryos up until the end of day three and as larvae thereafter, whether they have hatched or not.

### **1.1.3 Cell movements during gastrulation**

Gastrulation is a fundamental process that creates the internal organisation as well as the external form of developing animals (Solnica-Krezel, 2006). During this process, the seemingly unstructured early embryo is transformed into a gastrula with three germ layers: the endoderm, mesoderm and ectoderm. Moreover, these germ layers are molded into a body rudiment with clear dorsal-ventral (D-V) and anterior-posterior (A-P) axes, which will eventually give rise to all tissues and organs formed in the adult (Schier et al., 2005; Solnica-Krezel, 2005; Warga et al., 1990). These changes are achieved by a set of evolutionarily conserved morphogenetic cell movements: epiboly, internalisation, and convergence and extension (Solnica-Krezel, 2006; **Figure 1.3**).

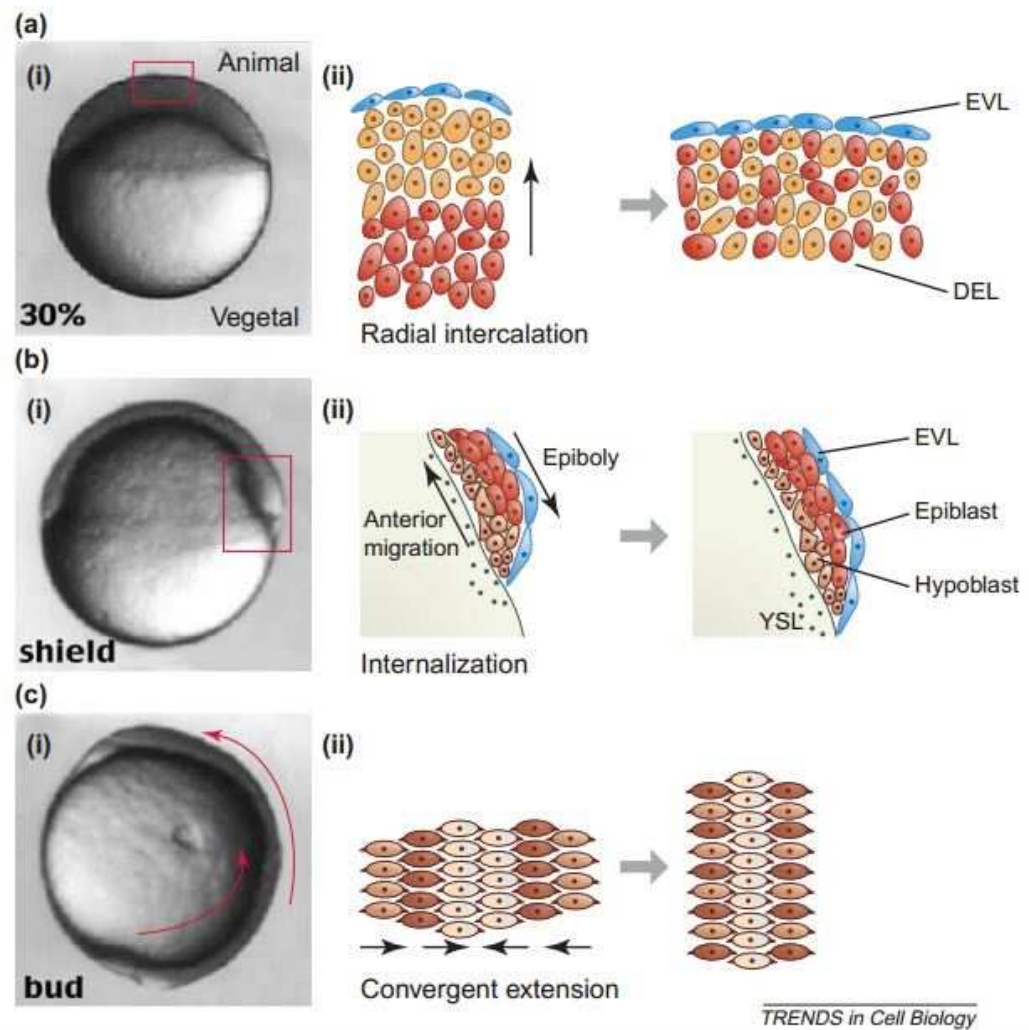


**Figure 1.3 Gastrulation movements during zebrafish embryogenesis**

(a) Epiboly driven by radial cell intercalations at the onset of gastrulation (a 30% epiboly stage embryo is shown). The cellular movements in the boxed area of (i) are illustrated schematically in (ii). (b) Internalisation of mesendodermal progenitor cells at shield-stage. The cellular movements in the boxed area of (i) are illustrated schematically in (ii). (c) Convergent extension movements of mesendodermal cells during gastrulation. Arrows in (a) (ii), (b) (ii) and (c) (i, ii) demarcate the directions of cell or tissue movements. EVL: enveloping layer; DEL: deep cell multilayer. Adapted from (Montero et al., 2004)

### 1.1.3.1 Epiboly cell movements

At the beginning of gastrulation, the blastula consists of a mass of cells, the blastoderm, piled atop the syncytial yolk cell (Kimmel et al., 1995). The blastoderm can be subdivided into a superficial epithelium of enveloping layer (EVL) cells covering the non-epithelial deep layer (DEL) cells (Montero et al., 2004). Epiboly is the first gastrulation cell movement during zebrafish embryogenesis, which starts at 4 hpf when the flat yolk cells begin to dome into the blastoderm (Warga et al., 1990). In the DEL, epiboly is triggered by a radial intercalation of cells deep within the blastula moving to more superficial layers to displace neighbours, thereby thinning the DEL and extending its margin over the yolk (**Figure 1.3a**). In contrast, the EVL connects at its margin to the yolk cell membrane and moves over the yolk cell towards the vegetal pole of the embryo (Kane et al., 2005; Montero et al., 2004; Warga et al., 1990).

Microfilament and microtubules networks in the yolk are implicated to contribute to epiboly (Cheng et al., 2004; Solnica-Krezel et al., 1994; Strahle et al., 1993; Topczewski et al., 1999). They are two components of the cytoskeleton both found in the cytoplasm of eukaryotic cells. Microfilaments are linear polymers of actin subunits functioning to give shape to the cell and support its internal components. Microtubules are tubular polymers of tubulin that also help define cell structure and movement. The latest publication implicated that the spreading of the EVL over the yolk cell in zebrafish epiboly is driven by a contractile actomyosin ring (Behrndt et al., 2012).

E-cadherin has been demonstrated to play essential roles during epiboly, possibly through mediating adhesion between the deep cells and the EVL (Babb et al., 2004; Kane et al., 1996; Kane et al., 2005). In addition, a number of transcription factors have been reported to be necessary for epiboly, such as the Eomes T-box transcription factor (Bruce et al., 2005).



### **1.1.3.2 Internalisation**

Internalisation or emboly begins with the accumulation of mesendodermal progenitors at the blastoderm margin, which gives rise to the germ ring. In the germ ring, mesendodermal progenitor cells internalise to form the inner hypoblast layer, which will develop into the mesodermal and endodermal germ layers. The ectodermal progenitor cells positioned above the hypoblast, known as the epiblast, will form the ectodermal germ layer (**Figure 1.3b**). Recently, high-resolution microscopy revealed that, in the dorsal region, the internalisation is driven by ingression, the inward movement of individual cells, and in the ventral and lateral regions, it occurs mainly by involution, the inward flow of a sheet of cells (Carmany et al., 2001; Keller et al., 2008; Montero et al., 2005).

The molecular basis of internalisation is still poorly understood. However, complete absence of Nodal signalling inhibits all internalisation cell movements (Carmany et al., 2001; Schier et al., 2005).

### **1.1.3.3 Convergence and extension movements**

Convergence and extension (CE) cell movements are defined as the narrowing of embryonic tissues medio-laterally (convergence) and their lengthening anterior–posteriorly (extension) at the same time (Concha et al., 1998; Keller et al., 2000; Sepich et al., 2005; Warga et al., 1990). It begins at the same time as the germ ring forming and mesendodermal cell internalisation starting (Montero et al., 2004). Convergence cell movements first become obvious in the germ ring by a local thickening at the dorsal side, which will generate the embryonic organiser termed the ‘shield’ (**Figure 1.3c**). The epiblast and hypoblast converge towards the dorsal side through medio-lateral cell intercalations, resulting in an elongation of the forming body axis along the A-P axis (Montero et al., 2004; **Figure 1.3c**).

CE cell movements are regulated spatiotemporally in a dynamic manner. Indeed, distinct cell behaviours and molecular mechanisms underlie CE cell

movements, depending on the cell's localisation along the D-V and A-P embryonic axes (Roszko et al., 2009; Sepich et al., 2000).

The ventral blastopore region is known as the “*no convergence, no extension zone*”, where cells spread over the yolk and later migrate towards the tailbud region instead of CE (Myers et al., 2002). In the lateral region, cells undergo dorsally directed migration, which is initially slow, but increases as cell groups move dorsally (Pezeron et al., 2008; Sepich et al., 2005; **Figure 1.4**), resulting in a narrowing and thickening of tissue without extension.

On the dorsal side, where the most intense CE cell movements occur, hypoblast cells move away from the margin immediately after internalisation. The prechordal plate (anterior axial mesoderm) precursors engage in directed migration towards the animal pole (Schier et al., 2005). The posterior axial mesoderm undergoes a dramatic extension accompanied by limited convergence, eventually forming midline embryonic tissues. In this domain, medio-lateral intercalation is the predominant cell behaviour, where medio-laterally elongated cells employ bipolar protrusion to intercalate between their medial and lateral neighbours (Myers et al., 2002). Polarised radial intercalation is also reported to be involved (Yin et al., 2008; **Figure 1.4**).

The non-canonical Wnt/PCP pathway has been demonstrated to play a central role in regulating CE cell movements, which will be detailed in the following section (Schier et al., 2005).

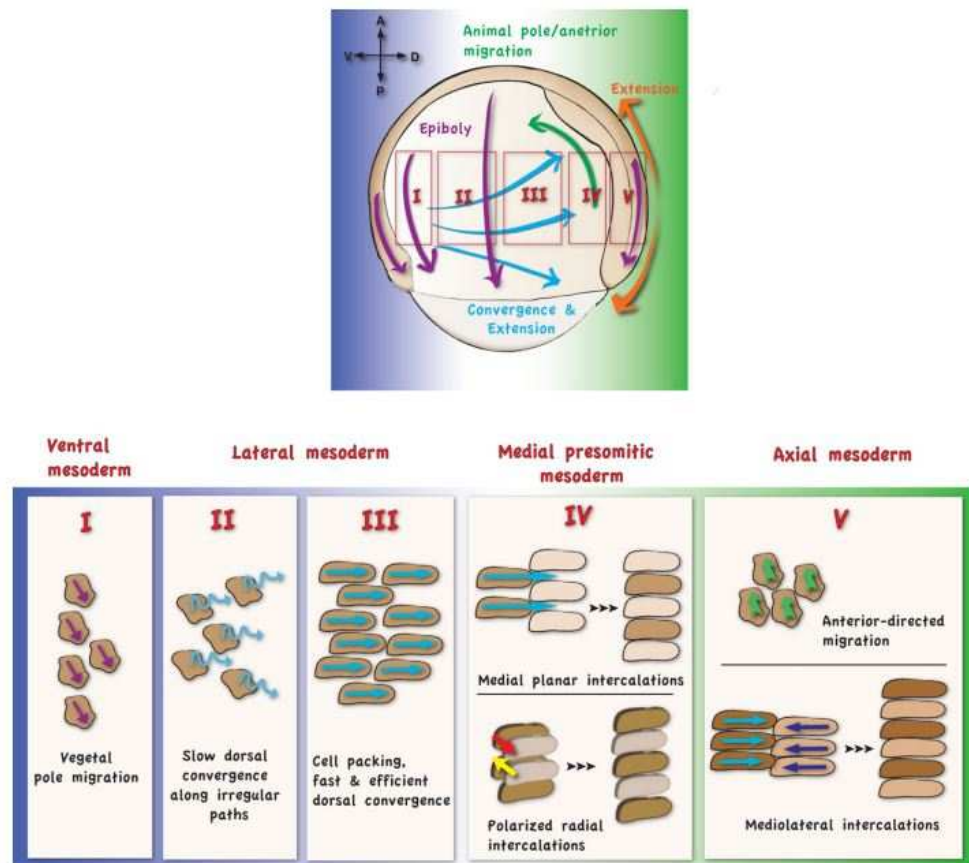


**Figure 1.4 Distinct cell behaviors along the D-V axis during CE cell movements**

Five distinct domains are distinguished along the D-V axis according to the type of mesodermal cell behaviors. In the most ventral region (I), cells migrate towards the vegetal pole. In the ventral-lateral domain (II), the cells undergo slow convergence cell movements along irregular paths, and extend along the A-P axis. In the lateral domain (III), the cells engage in fast convergence cell movements along straight migration paths. In the lateral-dorsal domain (IV), migration is increased and the cells undergo polarised medio-lateral and radial intercalation movements that drive modest CE. In the dorsal domain (V), the most anterior cells migrate anteriorly, while posterior cells undergo massive cell intercalation movements that contribute to fast extension and modest convergence. Adapted from (Roszko et al., 2009)

## 1.2 The non-canonical Wnt/PCP pathway in CE regulation

The Wnt signalling pathway is an ancient and evolutionarily conserved pathway that has been implicated in multiple developmental events during embryogenesis (Logan et al., 2004; Rao et al., 2010). It is historically divided into two categories: canonical or non-canonical, between which the difference is that a canonical Wnt pathway involves the protein  $\beta$ -catenin whereas a non-canonical Wnt pathway is independent of it (Rao et al., 2010; **Figure 1.5**). According to the major intracellular mediators used, the latter is further divided into the non-canonical Wnt/planar cell polarity (PCP) pathway and the non-canonical Wnt/ $\text{Ca}^{2+}$  pathway (Rao et al., 2010; **Figure 1.5**).

Planar cell polarity (PCP) refers to the coordinated polarisation of cells within the plane of a cell sheet (Goodrich et al., 2011). The non-canonical Wnt/PCP pathway was initially discovered to mediate the establishment of cell polarity in the plane of epithelia in *Drosophila melanogaster* (Adler, 2002; Klein et al., 2005; Wallingford et al., 2002). Increasing evidence from mutant studies and molecular analyses in vertebrates have demonstrated its essential role in regulating several polarised cell behaviours in CE cell movements (Roszko et al., 2009; Wang et al., 2006; Ybot-Gonzalez et al., 2007; Yen et al., 2009).

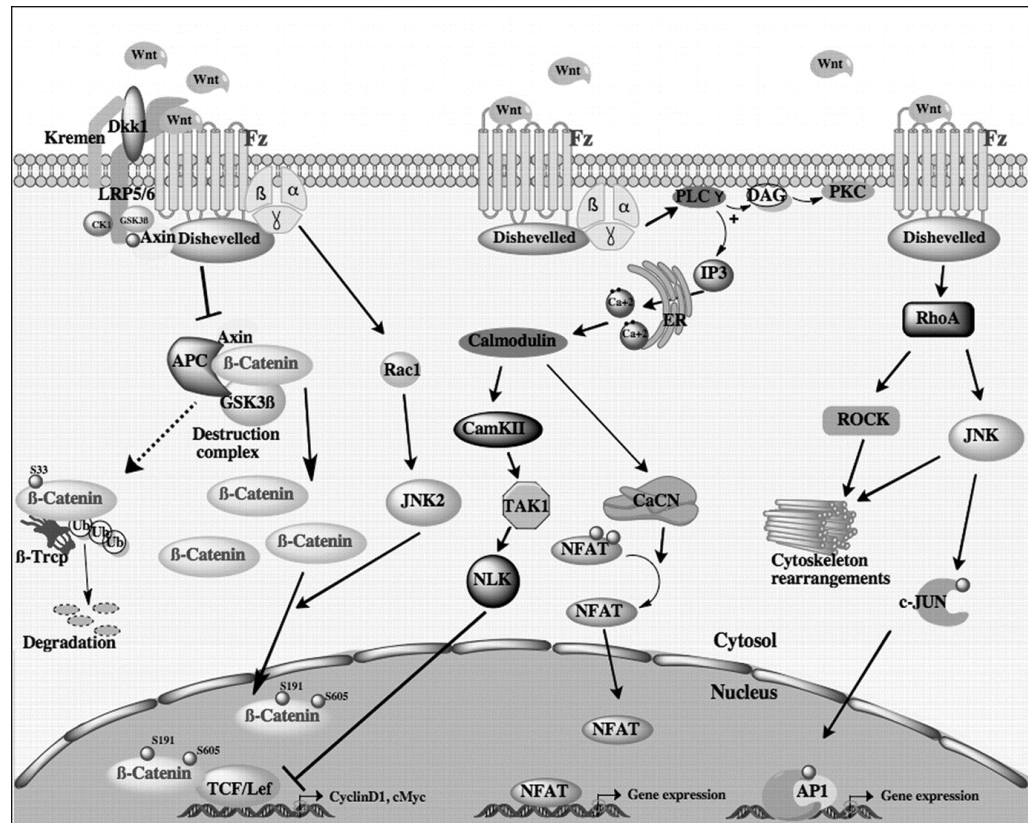


**Figure 1.5 Overview of the Wnt signalling pathways**

In the canonical Wnt pathway (left), Wnt ligands bind Frizzled (Fz) to initiate a cascade of events, leading to the disassembly of the destruction complex consisting of axin, adenomatous polyposis coli (APC), and glycogen synthase kinase 3β (GSK 3β). Therefore β-catenin is accumulated in the cytoplasm, and is eventually translocated into the nucleus to act as a transcriptional co-activator of transcription factors. In the non-canonical Wnt/Ca<sup>2+</sup> pathway (middle), activates Ca<sup>2+</sup> and calmodulin-dependent kinase II (CamKII), protein kinase C (PKC) and calcineurin. Calcineurin activates nuclear factor of activated T cells (NFAT), which regulates the transcription of genes controlling cell fate and cell migration. The non-canonical Wnt/PCP pathways (right) Planar cell polarity (PCP) signalling triggers activation of the small GTPases RhoA and Rac1, which in turn activate Rho kinase (ROCK) and JUN-N-terminal kinase (JNK), respectively, leading to actin polymerization and microtubule stabilization. This pathway is prominently involved in the regulation of cell polarity, cell motility and morphogenetic movements. CaCN indicates calcineurin. Adapted from (Rao et al., 2010)

## 1.2.1 Structure of the non-canonical Wnt/PCP pathway

Wnt proteins are a group of secreted glycoproteins carrying a conserved pattern of 23-24 cysteine residues, usually with a length of 350–400 amino acids, which have been involved in a myriad of developmental processes (Cadigan et al., 1997). As shown in **Figure 1.6**, they initiate the non-canonical Wnt/PCP pathway by binding the N-terminal cysteine-rich domain of Frizzled (Fz), which is a kind of G protein-coupled receptor spanning the plasma membrane seven times (Malbon et al., 2004). Subsequently, this signal is transmitted to the cytoplasmic phosphoprotein Dishevelled (Dvl), which is an adaptor protein containing a DEP (Dsh, Egl-10, Pleckstrin) domain and a PDZ (Postsynaptic density 95, Discs Large, Zonula occludens-1) domain, via a direct interaction between Fz and Dvl. Downstream of Dvl, a variety of signalling branches modulate different aspects of cytoskeleton reorganization in cell movements and polarity (Wang, 2009).

Besides, other core proteins in the non-canonical Wnt/PCP pathway have been identified in various model animals, including Prickle (Pk), Vangl/Strabismus (Vangl/Stbm), Celsr/Flamingo (Celsr/Fmi) and Diego (Dgo) that will be described in details below (Djiane et al., 2000; Habas et al., 2001; Karni et al., 2009; Tree et al., 2002; Wallingford et al., 2005; **Table 1.1**). Rac1 and RhoA are small GTPases acting as key downstream effectors in this pathway and will be described separately in section **1.3**.

### 1.2.1.1 Model of the non-canonical Wnt/PCP pathway

As shown in **Figure 1.6**, after Wnt ligands binding to Fz, two protein complexes are assembled at the cell membrane, with the Vangl/Stbm-Pk complex localised proximal to the cell membrane, and the Fz–Dvl–Dgo complex localised distally, which leads to planar polarisation (Veeman et al.,

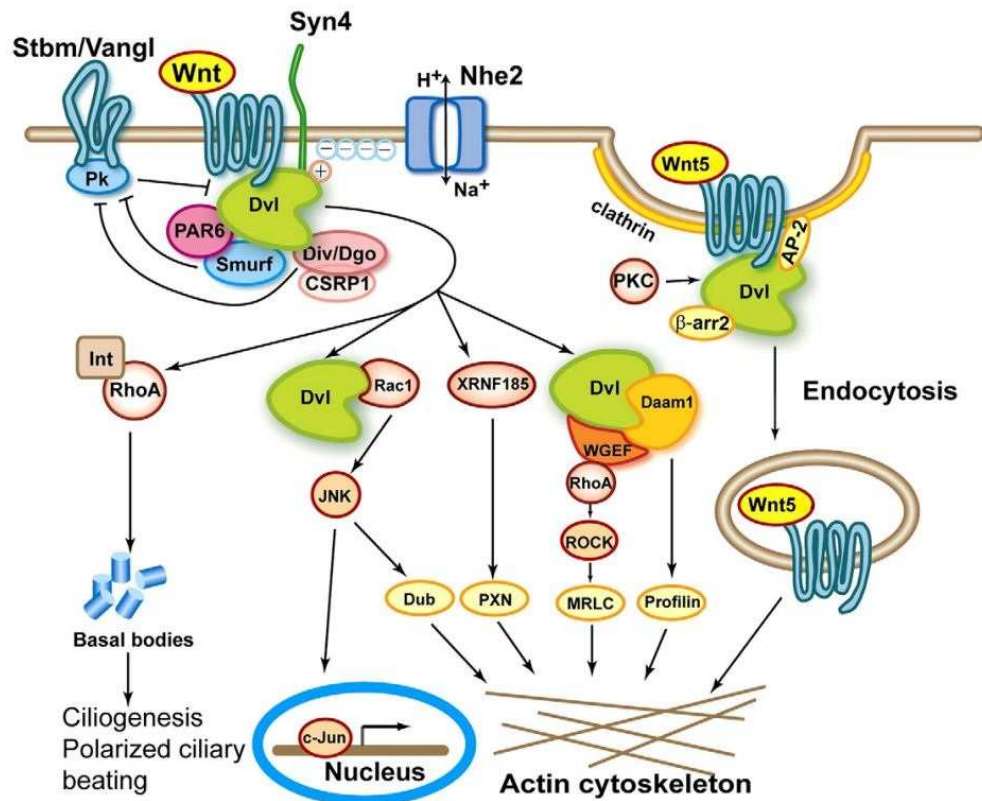


**Figure 1.6 Schematic illustration of the non-canonical Wnt/PCP pathway**

Non-canonical Wnt ligands trigger the non-canonical Wnt/PCP pathway through binding to seven-transmembrane Frizzled receptors, resulting in the assembly of two complexes that are located dissymmetrically in each cell. The distal location of the Fz–Dvl–Dgo complex and the proximal location of the Vangl/Stbm–Pk complex to the cell membrane lead to planar polarisation. The non-canonical Wnt/PCP pathway diverges through the interaction of Dvl with multiple downstream effectors, such as the Dvl–Daam1–RhoA complex, Dvl–Rac1 complex and *Xenopus* ring finger protein 185 (XRN185), to modulate actin cytoskeleton and gene transcription. During *Xenopus* gastrulation, the actin-binding protein Profilin1 acts downstream of Daam1 to control blastopore closure, and the weak-similarity Rho guanine nucleotide exchange factor (WGEF) mediates Wnt signalling to regulate CE cell movements. This pathway does not involve the nuclear translocation of  $\beta$ -catenin. In addition, Dvl acts together with its effector protein Inturned (Int) to govern activation of RhoA at the apical surface of ciliated epithelial cells, and thereby regulate the docking and/or maintenance of basal bodies in multi-ciliated cells. Adapted from (Gao et al., 2010)

2003). Dgo promotes the activation of Dvl and competes with Pk for Dvl binding. Pk inhibits Dvl activity by hindering its membrane localisation, whereas Dvl also antagonizes Pk by recruiting Smurf, an E3 ubiquitin ligase, to the Fz-Dvl complex with Partition defective protein 6 (PAR6), which results in the degradation of Pk (Gao et al., 2010; **Figure 1.6**). Taken together, this antagonistic interaction between the two complexes plays a crucial role in PCP establishment.

Multiple molecular pathways downstream of the core Wnt/PCP components mediate different cell behaviours, including gene transcription, ciliogenesis and actin cytoskeleton rearrangement (Gao et al., 2010; **Figure 1.6**). Rho GTPases have been found to be important downstream effectors of the Wnt signalling pathway. In addition, a RING finger protein XRN185 can mediate Wnt/Dvl signalling to regulate cell migration during *Xenopus* gastrulation. Interestingly, Dvl-PCP function is also modulated by the endocytosis of Fz receptor (Gao et al., 2010; **Figure 1.6**).



Protein Family	Gene Manipulation	Process/Tissue Dymorphogenesis
Wnt	<i>pipetail/wnt5</i> mutant zebrafish	Convergence and extension; axial elongation
-	<i>wnt5a</i> manipulations in <i>Xenopus</i>	Convergence and extension; axial elongation
-	<i>silberblick/wnt11</i> mutant zebrafish	Convergence and extension; axial elongation
Celsr	<i>Spin</i> and <i>Crash/Celsr1</i> mutant mice	Craniorachischisis; polarity of hair follicles
-	<i>Celsr 2; Celsr2/3</i> mutant mice	Polarity of ependymal basal body
-	<i>fmi/celsr</i> overexpression of mutant forms in zebrafish	Convergence and extension defect
Vangl	<i>stbm/vangl2</i> loss of function	Gastrulation/convergence and extension
-	<i>Looptail/Vangl2</i> double mutant mice; electroporation of GFP- <i>Vangl</i> <sup>LP</sup>	Craniorachischisis; translation polarity of the basal body
-	<i>trilobite/vangl2</i> zebrafish mutants	Convergence and extension/axial elongation; translation polarity of cilia in Kupffer's vesicle
Prickle	Pk1 gain of function; loss of function in zebrafish	Convergence and extension
-	Pk2 gain of function/mutations in zebrafish	Convergence and extension
Frizzled	Fz 8	Convergence and extension; axial Elongation
-	Fz3, 6 double mouse mutants	Craniorachischisis
-	Fz6 mouse mutants	Coat hair polarity defect; polarity of hair follicles
-	<i>fz7a; fz7b</i> zebrafish maternal zygotic double mutants	Convergence and extension; defects in the orientation of cell division
Dishevelled	<i>Dvl</i> gain of function; loss of function in <i>Xenopus</i>	Convergence and extension of neural plate and lateral plate mesoderm
-	<i>Dvl1</i> , 2 mouse double mutants	Craniorachischisis
-	<i>Dvl2</i> , 3 mouse double mutants	Craniorachischisis
Diego/Inversin	Inversin loss of function	Axial elongation, convergence and extension

**Table 1.1 Major components of the non-canonical Wnt/PCP pathway**

The expanded number of vertebrate core non-canonical Wnt/PCP homologs makes it challenging to deciphering vertebrate non-canonical Wnt/PCP signalling. For example, in the mouse, there are ten annotated Frizzled (Fzd1-10), two Vangl (Vangl1-2), and three Dvl homologs (Dvl1-3). Despite these genetic redundancies, single and compound mutants in some core PCP genes manifest CE defects in *Xenopus* and zebrafish and/or craniorachischisis in the mouse. Adapted from (Gray et al., 2011)

### 1.2.1.2 Principle components

#### Non-canonical Wnt ligands

Wnt ligands were primarily divided into the canonical Wnt1/Wg class and the non-canonical Wnt5a class, based on their supposed biological functions in activating the canonical Wnt/ $\beta$ -catenin pathway and the non-canonical Wnt/PCP pathway respectively (Uysal-Onganer et al., 2012). Four genes (*wnt4*, *wnt5a/5b* and *wnt11*) have been identified to encode ligands for the non-canonical Wnt/PCP signalling in zebrafish (Ciruna et al., 2006; Heisenberg et al., 2000; Rauch et al., 1997; Tada et al., 2000; **Table 1.1**).

The non-canonical Wnt protein Wnt11 is encoded by *silberblick* (*slb*) in zebrafish. Its loss-of-function results in cyclopia and head defects essentially caused by a reduced elongation of the body axis during gastrulation (Heisenberg et al., 1996; Heisenberg et al., 1997). Cell line studies have provided evidence for roles of Wnt11 in cell adhesion, which promotes cohesion of mesodermal and endodermal progenitor cells by mediating E-cadherin internalisation through the small GTPase Rab5c (Ulrich et al., 2005).

Similarly, Wnt5b that is encoded by *pipetail* (*ppt*) also influences CE through the non-canonical Wnt/PCP pathway (Du et al., 1995; Moon et al., 1993; Rauch et al., 1997; Wallingford et al., 2001). Because *wnt5b* and *wnt11* mRNAs rescue the *wnt11* mutant (Heisenberg et al., 2000; Kilian et al., 2003), non-canonical Wnts are speculated to perform a permissive role in CE without providing positional signals (Rohde et al., 2007; Simons et al., 2008). However, CE defects caused by zygotic loss of *wnt5b* cannot be rescued by exogenous *wnt5b* mRNA (Kilian et al., 2003; Westfall et al., 2003), suggesting that localised Wnt5b may be able to provide essential spatial information (Lin et al., 2010). Recently, Wnt5b has been demonstrated to modulate directional cell migration via Ryk-mediated signalling during zebrafish gastrulation (Lin et al., 2010).

### Frizzled (Fz) receptors

Frizzled is a family of G protein-coupled receptors consisting of 10 members, each containing an N-terminal signal peptide, an extracellular cysteine-rich domain, a seven-pass transmembrane domain, and an intracellular C-terminal PDZ (Postsynaptic density 95, Discs Large, Zonula occludens-1) domain (Schulte, 2010; **Table 1.1**).

Fz proteins function as receptors in the Wnt signalling pathway, and each member of this family interacts with more than one of the 19 Wnt isoforms to trigger downstream Wnt signalling via the cysteine-rich domain (Malbon, 2004; King et al., 2012). Among them, Fz2 and Fz7 serve as receptors for Wnt5 and Wnt11 during CE cell movements in zebrafish (Kilian et al., 2003) and *Xenopus* (Djiane et al., 2000; **Table 1.1**). In zebrafish embryos, Wnt11 induces the accumulation of Fz7 at the plasma membrane, thereby increasing cell contact persistence through plasma membrane interactions among Wnt11, Fz7 and the atypical cadherin Flamingo (Uysal-Onganer et al. 2012; Witzel et al. 2006). Moreover, Wnt11 signals through Fz5 to promote formation of the eye field during zebrafish development, although it remains unknown if Wnt11 binds to Fz5 (Cavodeassi et al. 2005; Uysal-Onganer et al. 2012).

### Dishevelled (Dsh/Dvl)

Dsh is an adaptor protein that functions downstream of the Frizzled receptor. It was originally identified based on the phenotype of disorientation in body and wing hairs in *Drosophila*. Dsh proteins possess three conserved domains, an N-terminal DIX (Dishevelled, Axin) domain, a C-terminal DEP domain, and a central PDZ domain, which enables Dsh to transduce signals from Fz to downstream components by direct interaction with Fz (Boutros et al., 1999; Schulte et al., 2010). The overexpression of Fz7 promotes membrane accumulation of Dsh (Carreira-Barbosa et al., 2003; Kinoshita et al., 2003).

Since Dsh regulates and channels the Wnt signal into every branch, it is considered to be the hub of Wnt signalling. In the non-canonical Wnt/PCP

branch, Dsh associates with the small GTPase RhoA via Daam1 (Dsh associated activator of morphogenesis 1), which is a Formin homology adaptor protein (Habas et al., 2001). As shown in **Figure 1.6**, Dsh can activate small GTPase Rac1, leading to the stimulation of c-Jun N-terminal kinase (JNK), to regulate cell polarity and movements during *Xenopus* gastrulation (Habas et al., 2003).

### Vangl/Strabismus (Vangl/Stbm) and Prickle(Pk)

Vangl/Strabismus (Vangl/Stbm) and Prickle (Pk) are also known as key members in the non-canonical Wnt/PCP pathway. Vangl/Stbm is a membrane protein that was firstly identified in *Drosophila*, by which Pk is recruited to the cell surface membrane (Bastock et al., 2003). The loss-of-function as well as the overexpression of Vangl2/Trilobite (Tri) resulted in defects of CE cell movements in *Xenopus* and zebrafish (Goto et al., 2002; Jessen et al., 2002; Park et al., 2002; **Table 1.1**). Recently, Vangl2 was reported to modulate the endocytosis and cell surface level of membrane type-1 matrix metalloproteinase (MMP14), which functions downstream of zebrafish Vangl2 to influence both extracellular matrix remodelling and gastrulation cell movements (Williams et al., 2012).

Similarly, both gain- and loss-of-function of Pk lead to CE defects in zebrafish (Carreira-Barbosa et al., 2003; Takeuchi et al., 2003; Veeman et al., 2003). Pk1 blocks the Fz7-dependent membrane translocation of Dsh, likely through accelerating the degradation of Dsh in zebrafish, indicating its role as an inhibitor of Dsh which establishes cell polarity by negatively regulating the non-canonical Wnt/PCP pathway (Carreira-Barbosa et al., 2003). Furthermore, *pk1* interacts genetically with *tri/strabismus* to mediate the posteriorly directed migration of cranial motor neurons and CE (Carreira-Barbosa et al., 2003).

Taken together, Vangl and Pk are both essential members of the non-canonical Wnt/PCP pathway, but neither of them is simply a linear component of this pathway (Roszko et al., 2009).

### Flamingo/Celsr (Fmi/Celsr) and Diego (Dgo)

Flamingo (Fmi) is an evolutionary conserved non-classical cadherin, containing nine cadherin repeats and a seven trans-membrane domain discovered in *Drosophila* (Elvis et al., 2013). Celsr is its vertebrate homologue implicated in several biological processes, including CE cell movements and neuronal migration (**Table 1.1**). Fmi/Celsr is well known for regulating the establishment of planar cell polarity, through functioning together with PCP members, such as Fz and Dsh (Carreira-Barbosa et al., 2009).

Three Celsr paralogs have been identified in zebrafish and mammals, among which Celsr1a and Celsr1b were revealed to cooperatively regulate CE cell movements in collaboration with the non-canonical Wnt/PCP pathway during zebrafish gastrulation (Formstone et al., 2005; **Table 1.1**). Celsr2 was discovered to modulate CE cell movements by indirectly influencing Dsh localisation at the cell membrane (Carreira-Barbosa et al., 2009). Furthermore, the Wnt11-mediated local accumulation of Fz7 at cell–cell contacts is dependent on Fmi/Celsr proteins in both zebrafish and *Drosophila* (Witzel et al., 2006).

Diego (Dgo) is an ankyrin-repeat protein originally identified in *Drosophila* and co-localises with Fmi at proximal/distal cell boundaries (**Table 1.1**). Fz acts through Dgo to promote polarised accumulation of Fmi (Fabian et al., 2001). Dgo promotes Fz signalling and can bind directly to Dsh, whereas the Fz-PCP antagonist Pk can also bind Dsh. Thus Dgo and Pk were supposed to compete for Dsh binding, and thereby modulate Fz/Dsh activity and ensure precise control over Fz initiated PCP signalling (Jenny et al., 2005).

### Other components

It is known that glypican4, a member of the heparan sulfate proteoglycans family, is also involved in the Wnt signalling pathway in zebrafish and *Xenopus*. Zebrafish Glypican4/Knypek (Kny) is proposed to act as a co-receptor along with Fz for Wnt ligands in the non-canonical Wnt/PCP pathway, and

potentiate this pathway to establish polarised cell behaviours underlying CE cell movements during vertebrate gastrulation (Topczewski et al., 2001).

Previous studies have demonstrated that the core PCP proteins form asymmetric PCP domains at apical junctions of epithelial cells (Bastock et al., 2003). Recently, VhaPRR, an accessory subunit of the proton pump V-ATPase, is proved to be required for stable PCP domains, and therefore is identified as a novel PCP core protein. Particularly, VhaPRR physically interacts with Fmi via its extracellular domain and Loss of VhaPRR causes PCP defects as well as PCP core protein mislocalisation (Hermle et al., 2013).

## **1.2.2 Specific CE cell behaviours regulated by the non-canonical Wnt/PCP pathway**

As described in section 1.1.3.3, there are various cell behaviours driving CE cell movements, depending on the cell's position along the embryonic axes. Cell motility analyses have illustrated that some of them are modulated by the non-canonical Wnt/PCP pathway (Roszko et al., 2009; **Figure 1.7**).

### **1.2.2.1 Directional migration**

As mentioned in section 1.1.3.3, after internalisation, cells at the anterior edge of the prechordal mesoderm actively migrate from the marginal region along trajectories directed anteriorly (Heisenberg et al., 2002; Rohde et al., 2007; **Figure 1.7A**). The non-canonical Wnt/PCP pathway has been revealed to regulate this cell movement. In *slb/wnt11* mutants, not only the average

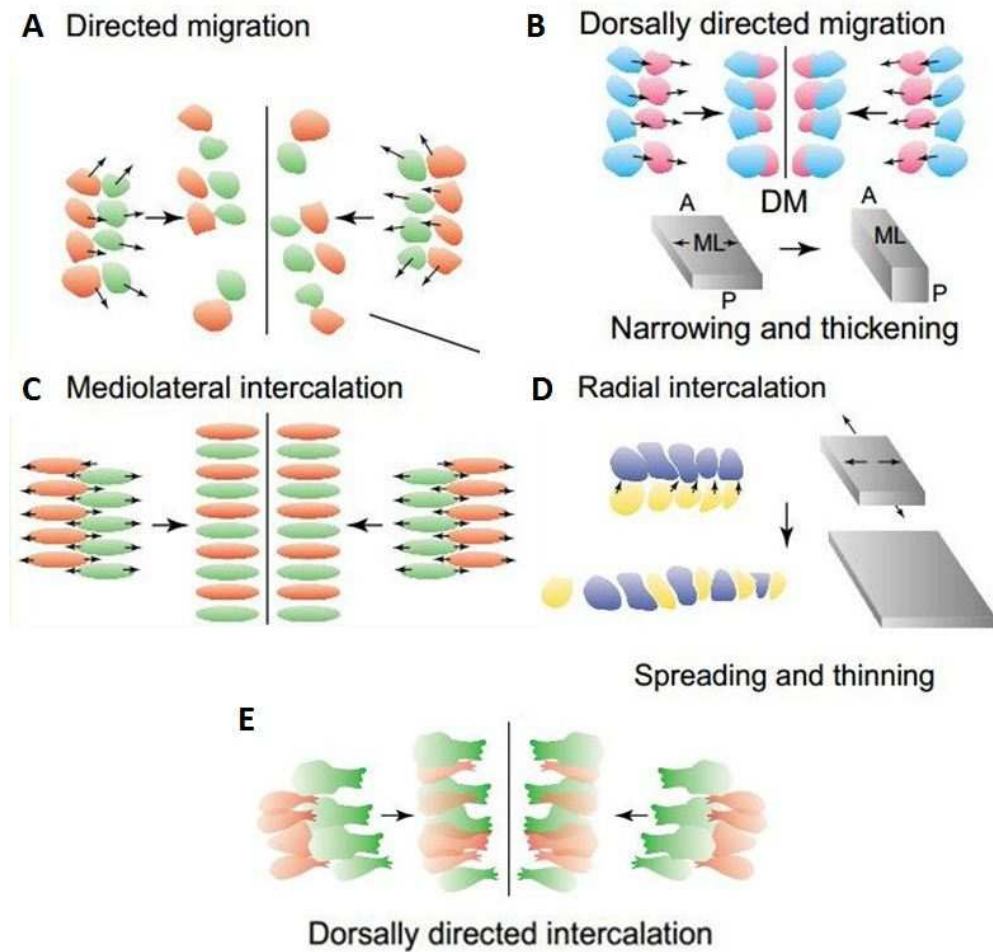


**Figure 1.7 Cell behaviours controlled by the non-canonical Wnt/PCP pathway in CE**

The non-canonical Wnt/PCP pathway regulates a variety of cell behaviours during CE. **(A)** Directed migration lengthens and narrows embryonic tissues. **(B)** Dorsally directed migration leads to narrowing and thickening of tissue. **(C)** Mediolateral intercalation in mesoderm contributes to CE. **(D)** Radial intercalation results in the spreading and thinning of tissue. **(E)** In *Xenopus*, dorsally directed intercalation drives convergent extension. The unbroken black line indicates the dorsal margin (DM). A: anterior. ML: mediolateral. P: posterior. Adapted from (Myers et al., 2002)

velocity and persistence of the anterior migration of the prechordal mesoderm cells are reduced significantly, the direction of the pseudopod-like process also becomes randomised (Ulrich et al., 2003; Ulrich et al., 2005). These defects can be rescued by the ubiquitous expression of *wnt11*, suggesting that non-canonical Wnt/PCP acts as a permissive cue (Roszko et al., 2009; Ulrich et al., 2003).

At early gastrulation, lateral cell populations migrate slowly towards the animal pole with amoeboid morphology, but subsequently change their trajectories to approach the dorsal midline with increasing speed and along more direct paths at midgastrulation (Myers et al., 2002; **Figure 1.7B**). During late gastrula or early segmentation stages, these cells exhibit medio-laterally elongated shape. However, in *knypek (kny)* and *vangl2 (tri)* mutant embryos, not only the migration velocity is greatly decreased, the cells also display rounder shape, indicating a reduced polarity (Roszko et al., 2009).

### **1.2.2.2 Medio-lateral and polarised radial intercalation**

Within the axial domain, CE is driven by medio-lateral intercalation, whereas in the paraxial domain, a cooperation of medio-lateral intercalation and polarised radial intercalation contribute to CE (Glickman et al., 2003; Yin et al., 2008; **Figure 1.7C, D**). In the chordamesoderm, medio-lateral intercalation is supposed to be the main cell behaviour for CE (Roszko et al., 2009). However, when medio-lateral intercalation is destroyed in *no tail* mutants, the notochord extends without convergence, indicating that there exist cell behaviours contributing to axis extension other than medio-lateral intercalation (Glickman et al., 2003; Roszko et al., 2009).

Radial intercalation was reported to drive CE in the middle layer of presomitic mesoderm by separating the anterior and posterior rather than medial and lateral neighbouring cells and thus leading to the extension of presomitic mesoderm (Yin et al., 2008; **Figure 1.7D**). On the contrary, in *tri;kny* double



mutants, the AP intercalations are weakened and the medio-lateral intercalations are strengthened (Roszko et al., 2009; Yin et al., 2008).

By late gastrulation, the dorsal mesodermal and ectodermal cells become elongated with their axes oriented perpendicular to the dorsal midline (Concha et al., 1998; Roszko et al., 2009; Topczewski et al., 2001; **Figure 1.7E**). In contrast, the knock-down of *kny* or *tri* caused defectiveness in this medio-lateral elongation and the notochord become wider, indicating that medio-lateral polarity are reduced in these cells and that medio-lateral intercalations are disrupted (Jessen et al., 2002; Roszko et al., 2009; Topczewski et al., 2001).

### **1.2.2.3 Oriented cell division**

As a common feature during the vertebrate developmental process, oriented cell division plays an important function in tissue elongation (Gong et al., 2004; Wei et al., 2000). During zebrafish gastrulation, cells in dorsal tissues preferentially divide along the animal-vegetal axis of the embryo, which is a driving force for axis extension (Gong et al., 2004). The non-canonical Wnt/PCP pathway components Wnt11, Dishevelled and Strabismus are all required for the establishment of this animal-vegetal polarity (Gong et al., 2004).

## **1.3 Rho GTPases, downstream effectors of the non-canonical Wnt/PCP pathway**

Rho (Ras homologous) small GTPases are a subfamily of the Ras superfamily (Wennerberg et al. 2005), which can be further divided into three subgroups: Rho, Rac and Cdc42 (cell division cycle 42) (Charest et al. 2007). Rho GTPases play a fundamental role in a vast array of biological activities, ranging from the rearrangement of the actin cytoskeleton to the regulation of cell proliferation.

As described earlier, the polarised reorganisation of cytoskeleton, which results in changes in cell movement, is a key feature of non-canonical Wnt/PCP signalling (Schlessinger et al., 2009). Rho GTPases mediate these specific cell behaviours acting downstream of the non-canonical Wnt/PCP pathway.

### **1.3.1 Rho GTPases in the reorganisation of cytoskeleton**

#### **1.3.1.1 Actin cytoskeleton**

RhoA was found to regulate the assembly of contractile actin:myosin filaments, while Rac and Cdc42 facilitate the polymerisation of actin at the cell periphery to produce protrusive forces in the form of lamellipodia and filopodia, respectively. These effects on the actin cytoskeleton are achieved through the formation (actin polymerisation) and organisation (filament bundling) of actin filaments, which are both precisely modulated by Rho GTPases (Jaffe et al., 2005).

There are two major modes of actin polymerisation regulated by Rho GTPases. RhoA promotes linear elongation of filaments at barbed ends by activating formin proteins, whereas Rac and Cdc42 trigger a branched filament network by activating the Arp2/3 complex. In particular, Rho induces actin polymerisation in mammalian cells through mDia, a diaphanous-related formin that is a direct target of Rho (Jaffe et al., 2005).

In addition, Rho GTPases are also required for the correct spatial organisation of filaments, which has been best characterised for Rho-induced assembly of contractile actin:myosin filaments (Jaffe et al., 2005). Rho-associated protein kinase (ROCK), a serine/ threonine kinase and one of the major downstream effectors of RhoA, plays a pivotal role in this process (Coque et al., 2014; Riento et al., 2003). Because it can phosphorylate and thereby inactivate

myosin light chain (MLC) phosphatase, the phosphorylation of MLC is increased, which promotes the actin filament cross-linking activity of myosin II (Riento et al., 2003). It has been found that Wiskott–Aldrich syndrome protein (WASP) verprolin homologous (WAVE) activates the heptameric actin-polymerizing complex actin-related protein 2/3 (Arp2/3), leading to the meshwork of peripheral F-actin induced by Rac1 (Chen et al., 2010; Eden et al., 2002; Hall, 2012). Cdc42 activates Arp2/3 through a direct interaction with another Arp2/3 activator, neuronal WASP (N-WASP) (Hall, 2012). It has also been shown to interact biochemically and genetically with Par proteins in regulating the actin cytoskeleton through a Cdc42-PAR6-aPKC pathway (Georgiou et al., 2008; Harris et al., 2008; Leibfried et al., 2008). In particular, a recent study in *Drosophila* revealed a mutual dependence between PAR proteins and Cdc42 for their localization and control of the actin cytoskeleton (Leibfried et al., 2013). Furthermore, pleomorphic adenoma gene like-2 (PLAGL2) was found to modulate actin cytoskeleton remodelling through the regulation of the activity of RhoA and Rac1 (Sekiya et al., 2014).

### **1.3.1.2 Microtubule cytoskeleton**

Microtubule dynamics are profoundly influenced by microtubule plus end-binding proteins, which can be regulated by Rho GTPases. For example, Rac and Cdc42 mediate the phosphorylation of Op18/stathmin, which leads to its inactivation and thereby resulting in net elongation of microtubule ends.

The effects of Rho on microtubule dynamics appear to be context dependent. Particularly, Rho facilitates the formation of stabilised microtubules in migrating fibroblasts, which appears to be mediated by mDia without changes to the actin cytoskeleton (Jaffe et al., 2005). Another downstream effector of RhoA, Rho-associated protein kinase (ROCK), has been demonstrated to play an important role in the remodelling of microtubules (Chen et al., 2013; Schofield et al., 2013). ROCK and cyclin-dependent kinase 1 (Cdk1) inhibit microtubule dynamics by phosphorylating tubulin polymerization promoting protein 1 (TPPP1) (Schofield et al., 2013).

In addition, increasing evidences show that microtubules also serve as signalling platforms coupling microtubules dynamics to Rho GTPase activation in a variety of cellular conditions (Birkenfeld et al., 2007; Birkenfeld et al., 2008; Nalbant et al., 2009; Wojnacki et al., 2014). Particularly, GEF-H1, a member of the Dbl family of guanine nucleotide exchange factors (GEFs) that activate Rho GTPases, is uniquely regulated by its localisation to the microtubules. Microtubules depolymerization results in GEF-H1 activation, while relocalisation to microtubule inhibits its activity (Birkenfeld et al., 2007; Birkenfeld et al., 2008; Nalbant et al., 2009).

### **1.3.2 Rho GTPase involvement in the non-canonical Wnt/PCP pathway**

Rho GTPases have emerged as key mediators of Wnt signals in the non-canonical Wnt/PCP pathway, due to their pivotal functions in the establishment of cell polarity and the regulation of cell motility (**Figure 1.8**).

Rho and Rac have been proposed to be regulated by independent and parallel branches in the non-canonical Wnt/PCP pathway during CE cell movements. Wnt/PCP signalling stimulates formation of a complex consisting of Rho, Dvl and Daam1. As mentioned earlier, Daam1 binds the PDZ domain of Dvl and mediates Rho activation, which in turn promotes activity of ROCK and mediates cytoskeletal reorganisation (Marlow et al., 2002). In contrast, Rac binds to the DEP domain of Dvl independently of Rho, triggering Wnt/Fz activation of Jun-N-terminal kinase (JNK) (Habas, et al., 2003). In *Xenopus*, the Wnt11/Fz/Dsh signalling results in co-activation of Rac1 and RhoA, which perform both distinct and overlapping functions in CE regulation (Habas et al., 2003; Tahinci et al., 2003). It was shown the RhoA/Rok2 pathway determine cell elongation to a great extent, whereas Rac1 predominantly control filopodia activity (Tahinci et al., 2003). Results from zebrafish studies also

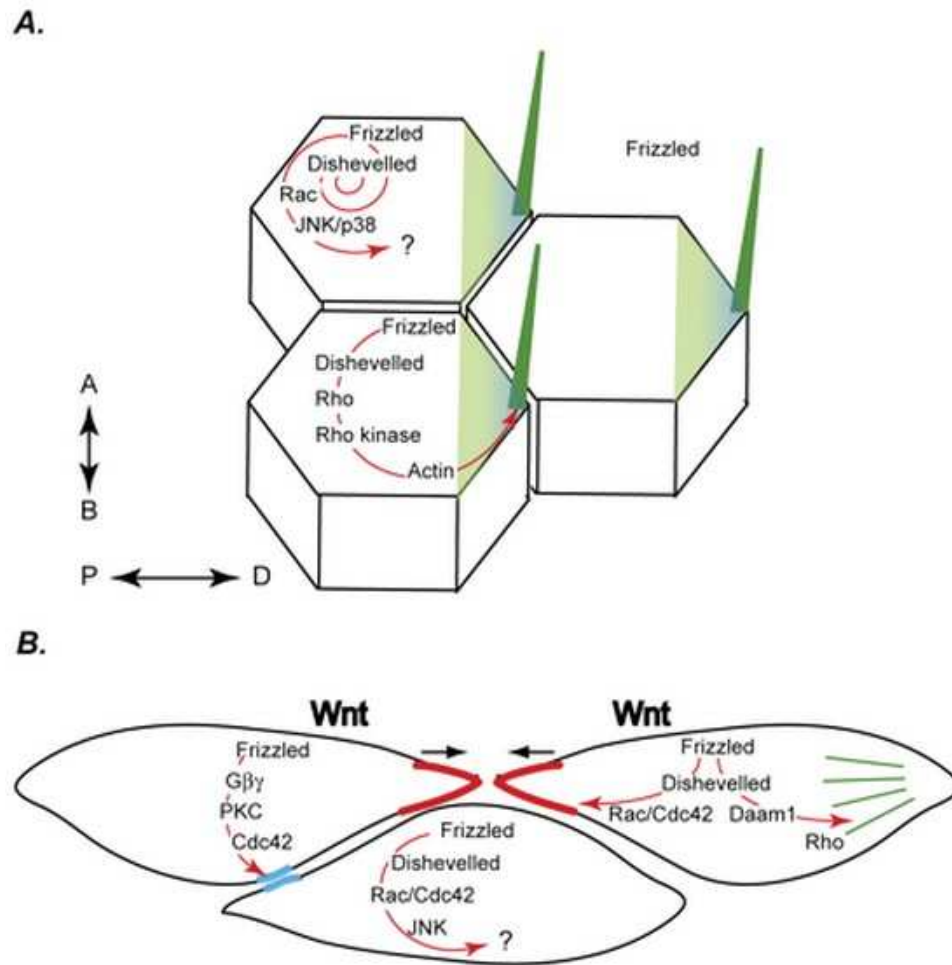


**Figure 1.8 Rho GTPases in the non-canonical Wnt/PCP pathway**

(A) During PCP signalling in the wing of *Drosophila*, activation of Frizzled in the distal region of each hair cell (green shading) stimulates the activation of localised Rho, which is necessary for actin-rich hair formation. Meanwhile, Frizzled/Dishevelled induce Rac activation that results in activation of JNK/p38 MAP kinases, which ultimately causes gene expression alterations in the fly eye. A: apical; B: basal; P: proximal; D: distal. (B) During vertebrate CE cell movements, cells elongate and intercalate at the embryonic midline. Frizzled activation facilitates downstream Rho GTPase activation. Rac and Cdc42 activation are necessary for polarised protrusive activity (red) and cell elongation, which are also required for JNK activation. Rho activation is required for actin:myosin contractility. Finally, Cdc42 regulates cell–cell contacts (blue) in a Dishevelled-independent manner. Adapted from (Schlessinger et al., 2009)

indicate Rac1 and RhoA are core downstream effectors of Dsh in the non-canonical Wnt/PCP pathway (Matsui et al., 2005; Moeller et al., 2006).

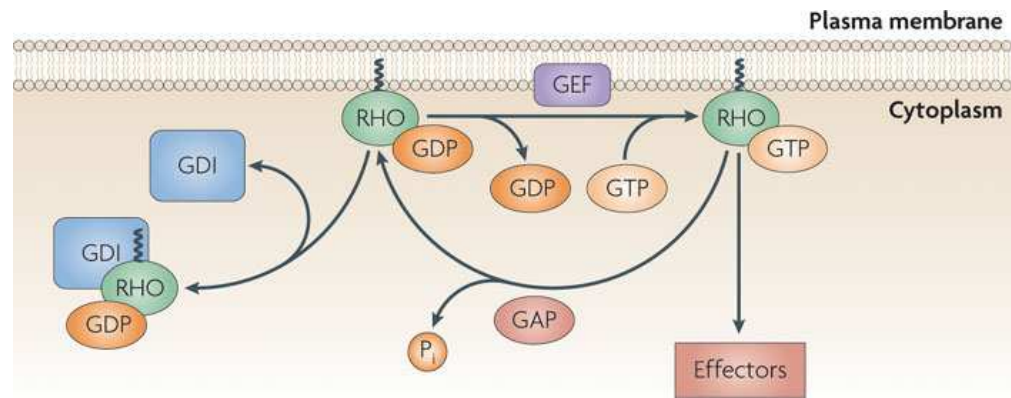
During *Xenopus* gastrulation, Wnt11 functionally and biochemically interact with its Fz7 receptor, leading to the activation of Cdc42 (Djiane et al., 2000; Penzo-Mendez et al., 2003). Cdc42, in turn, is thought to regulate CE through the protein kinase C (PKC- $\alpha$ )-mediated Wnt/Ca<sup>2+</sup> pathway (Choi et al., 2002).

### 1.3.3 Main Rho GTPase regulators

Rho GTPases function as a binary molecular switch cycling between two conformation states: an active GTP-bound state and an inactive GDP-bound state (**Figure 1.9**). This cycle is precisely regulated by guanine nucleotide exchange factors (GEFs), GTPase activating proteins (GAPs), and guanine nucleotide dissociation inhibitors (GDIs).

GEFs catalyse exchange of GDP for GTP to activate Rho GTPases, whereas GAPs stimulate GTP hydrolysis to inactivate the Rho GTPases. The third set of regulatory proteins, i.e. GDIs block spontaneous activation through extracting the inactive Rho GTPases from membranes (Jaffe et al., 2005; **Figure 1.9**). In particular, GDIs primarily bind the switch regions and the C-terminal isoprenyl moiety of Rho GTPases to sequester them in the cytosol (**Figure 1.9**). The mechanism of release of Rho GTPases from GDIs still needs to be fully elucidated, but this process is necessary before the engagement of GEFs that also bind the switch regions (Wennerberg et al., 2005).

Currently, there are 83 identified GEFs for Rho GTPases in the mammalian genome, which will be detailed later (Vigil et al., 2010). And there are 65 GAPs for Rho GTPases known in mice, all of which contain a conserved Rho GAP domain, as well as other protein–protein interaction domains and catalytically active domains. Some GEFs and GAPs are specific for only one or a few Rho GTPases, whereas others have a much wider specificity. This diversity of regulators acts to relay signals from a broad variety of receptors to their



Nature Reviews | Immunology

**Figure 1.9 The regulation of GTPase activity**

Rho GTPases are active when they are GTP-bound and non-functional when GDP-bound. These two states are tightly regulated by three classes of proteins: GEFs, GAPs and GDIs. Active GTPases interact with their various effectors to mediate a host of cellular responses that usually influence the organisation of cytoskeleton or the expression levels of multiple genes. Adapted from (Tybulewicz et al., 2009)

downstream Rho GTPases, making these Rho proteins focal points for crosstalk between different signalling pathways. Finally, there are only three GDIs for Rho proteins: GDI  $\alpha$ , GDI  $\beta$  and GDI  $\gamma$  (Tybulewicz et al., 2009).

In addition, Rho GTPases can be modulated through phosphorylation or ubiquitination.

RhoA can be directly phosphorylated by cAMP-dependent protein kinase A (PKA) and cGMP-dependent protein kinase G (PKG) at serine-188, triggering tight association of its GTP-bound form with Rho GDI, and extraction of RhoA from membranes (Ellerbroek et al., 2003; Lang et al., 1996; Liu et al., 2012; Sauzeau et al., 2000). Phosphorylation of serine-71 on Rac1 by serine/threonine kinase Akt inhibits the GTP-binding activity of Rac1,

whereas phosphorylation of tyrosine-64 on Cdc42 by Src tyrosine kinase increases its association with GDIs (Kwon et al., 2000; Tu et al., 2003).

Rho GTPases are also subject to regulation by the ubiquitin–proteasome system (UPS) in a balancing act with constitutive activation (Doye et al., 2002; Flatau et al., 1997; Liu et al., 2012). The HECT domain-containing E3-ubiquitin-ligase tumor suppressor (HACE1) preferentially binds to GTP-bound Rac1 for ubiquitination. RhoA is directly targeted for UPS-mediated degradation by the E3 ligase Smurf1, which regulates Smad protein stability. Furthermore, cytotoxic necrotizing factor 1 (CNF1)-activated Cdc42 is also subject to UPS-mediated degradation (Liu et al., 2012).

### **1.3.3.1 Guanine nucleotide exchange factors (GEFs)**

As mentioned above, GEFs are responsible for transiting Rho GTPases from their inactive GDP-bound to their active GTP-bound states. They respond to diverse extracellular stimuli and ultimately regulate numerous cellular activities such as proliferation, differentiation and motility via Rho GTPases (Wennerberg et al., 2005).

GEF proteins can be classified into three families, the largest of which is the Dbl family (Wennerberg et al., 2005). Up to now, 72 distinct members of this family have been identified in humans, sharing a Dbl homology (DH) domain and an adjacent C-terminal pleckstrin homology (PH) domain. A large amount of structural data has led to crucial insights into the molecular mechanism employed by Dbl family GEFs to facilitate the exchange of GDP for GTP. Essentially, they implement this function by promoting GTPase intermediates that are devoid of nucleotide and  $Mg^{2+}$  through their DH domains (Wennerberg et al., 2005). Compared with DH domains, their associated PH domains are found to be diverse in conformation, which contribute to binding to Rho GTPases and localise Dbl proteins to plasma membranes. Swap70 seems to be the only Rac-GEF for which the PH domain



is sufficient for conferring membrane binding. PH domains are also shown to regulate the GEF activity through allosteric mechanisms by binding lipids. Outside the DH–PH domains, Dbl proteins exhibit significant divergence and typically include other protein domains that are responsible for the specific functions of various family members (Wennerberg et al., 2005).

A second family is the Dock family, which are characterised by two regions with high sequence conservation designated Dock-homology region-1 and -2 (DHR1 and DHR2). In some GEFs, the DHR2 alone is sufficient for promoting guanine nucleotide exchange. Dock GEFs have been reported to activate Rac and Cdc42 in cell migration, morphogenesis, and phagocytosis. In humans, there are 11 Dock proteins that are clustered into four subfamilies, according to their primary sequence conservation and different specificities for Rho GTPases (Yang et al., 2009).

In contrast to typical GEF proteins, Swap70 and Def6 both feature an unusual combination of amino acid motifs and domains, including a putative N-terminal EF-hand motif, a central PH domain, and a C-terminal DH-like (DHL) domain, which displays limited sequence homology to the DH domain of classical GEFs (Biswas et al., 2010; **Figure 1.10**). The region between the EF-hand motif and the PH domain, which is highly conserved between Def6 and Swap70, is referred to as Def6/Swap70 Homology (DSH) domain (Mavrikakis et al., 2004; **Figure 1.10**). There is a controversy about which GEF family they belong to. Some scientists regard them as atypical members of the Dbl family, because their catalytic DH-like domain is fully functional (Heerema et al., 2004). However, some others consider that they should be classified into a third family, the Def6/Swap70 family, which contains Def6 (differentially expressed in FDCP 6; Hotfilder et al., 1999) and Swap70 (switch-associated protein 70; Hotfilder et al., 1999) only (Biswas et al., 2012; Goudevenou et al., 2011).

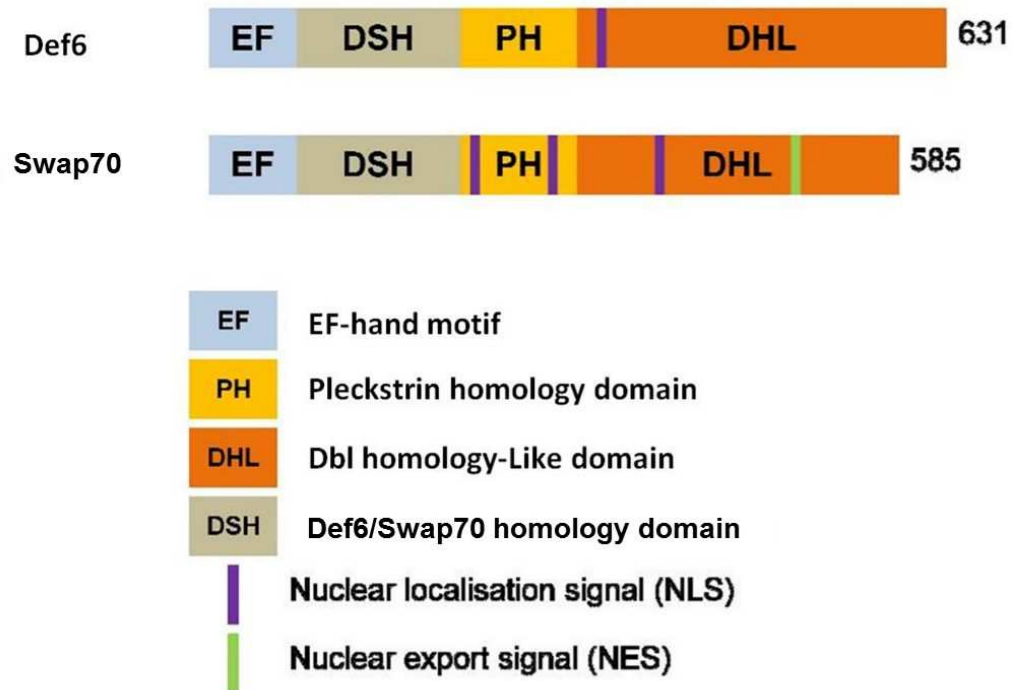


**Figure 1.10 Atypical domain arrangements of Def6 and Swap70**

Both proteins have a putative N-terminal EF-hand motif followed by a DSH domain and a DHL domain to the C-terminus of the PH domain. Moreover, Swap70 has three NLS and one NES whereas Def6 has only one NLS. Adapted from (Shuen, MRes thesis, 2010)

### 1.3.3.2 Rho GEFs involved in CE cell movements

Up to now, a number of GEFs have been suggested as upstream regulators in CE cell movements, but little is known whether they exert this function through their target Rho proteins.

For example, Quattro (Quo) was defined as a novel GEF for Rho GTPases in zebrafish due to its strong Rho-GEF domain homology to Dbl family GEFs (Daggett et al., 2004; Debant et al., 1996). The expression of *quo* gene is restricted to the anterior mesendoderm, cells that possess coordinated cell motility behaviours (Daggett et al., 2004). In *quo* morphants, a lack of

extension behaviour in prechordal plate mesoderm was observed, indicative of CE defects during late gastrulation (Daggett et al., 2004). It can be presumed that Quo is required for normal CE cell movements, but whether it executes its function through the non-canonical Wnt/PCP pathway is unknown.

A subsequent study identified a microtubule-binding Rho-GEF in *Xenopus*, XLfc (Krendel et al., 2002; Kwan et al., 2005). Its nucleotide exchange activity was proved to be essential for microtubule depolymerisation that can inhibit CE cell movements. A follow-up XLfc loss-of-function experiment confirmed it as a major endogenous effector of microtubule depolymerisation during CE cell movements (Kwan et al., 2005). Also in *Xenopus*, the weak similarity GEF (WGEF) was the first identified GEF protein to be involved in the non-canonical Wnt/PCP-mediated CE cell movements (Tanegashima et al., 2008). Overexpression of WGEF activated RhoA and rescued the impaired CE cell movements induced by dominant negative Wnt11, whereas WGEF loss-of-function led to disruption of CE cell movements that could be rescued by RhoA or Rho-associated kinase activation. Hence, it was proposed that WGEF forms a complex with Dsh, Daam-1 and RhoA upon Fz-7 activation. Taken together, WGEF is an upstream member of the non-canonical Wnt/PCP pathway connecting Dsh to Rho activation (Tanegashima et al., 2008).

Similarly, a recent study in zebrafish uncovered that a RhoA GEF, the synectin-binding RhoA exchange factor (Syx), is essential for normal gastrulation (Goh et al., 2010). Furthermore, the only close homolog of Swap70, Def6 was the first zebrafish GEF protein that was revealed to play a central role in the control of CE cell movements through the non-canonical Wnt/PCP pathway (Goudevenou et al., 2011).

## **1.4 Swap70, an atypical GEF for Rho GTPases**

Swap70 is a 70 kDa protein originally isolated as part of a DNA recombination complex in mouse B lymphocytes, which promotes heavy chain immunoglobulin class switching by DNA recombination (Borggreve et al., 1998). Subsequently, Swap70 was found in mast cells and in various organs as well (Gross et al., 2002; Hilpela et al., 2003; Shinohara et al., 2002).

### **1.4.1 Structural features and variable intracellular localisation**

As depicted in **Figure 1.10**, Swap70 has within it three nuclear localisation signals (NLSs) and a nuclear exit signal (NES), through which it can occupy various cellular compartments.

The phosphoinositide-binding site and NLS within the Swap70 PH domain localise Swap70 to the plasma membrane and nucleus respectively, indicating that this PH domain plays a critical role in functional intracellular location of Swap70. Indeed, a recent study found that the conformation of the Swap70 PH domain can be altered at the lipid bilayer surface, suggesting a regulatory mechanism of Swap70 function associated with its intracellular location (Tokuda et al., 2012).

Furthermore, it has been reported that the specific binding of the C-terminus of Swap70 to non-muscle F-actin is required to induce membrane ruffling (Ihara et al., 2006). In an un-stimulated state, this interaction is masked. In growth factor stimulated cells, the conformational alteration of the Swap70 PH domain at the membrane surface mediates exposure of the F-actin-binding site, and thereby triggers co-localisation of Swap70 and F-actin (Tokuda et al., 2012).

In resting B lymphocytes, Swap70 is predominantly found in the cytoplasm. Upon B cell activation, it is recruited to the plasma membrane and then translocates to the nucleus (**Figure 1.11**). In the nucleus, it is involved in heavy-chain class switch recombination. When transported to the cell membrane, it is associated with the B cell receptor complex and function in signal transduction. In mast cell, Swap70 stays cytoplasmic or localised to the plasma membrane (Gross et al., 2002). A recent study in zebrafish also reported that, in developing neural cells, Swap70 localises to the cytoplasm in most cells but the nucleus of cells associated with the proliferative zone of the medial spinal cord (Takada et al., 2011).

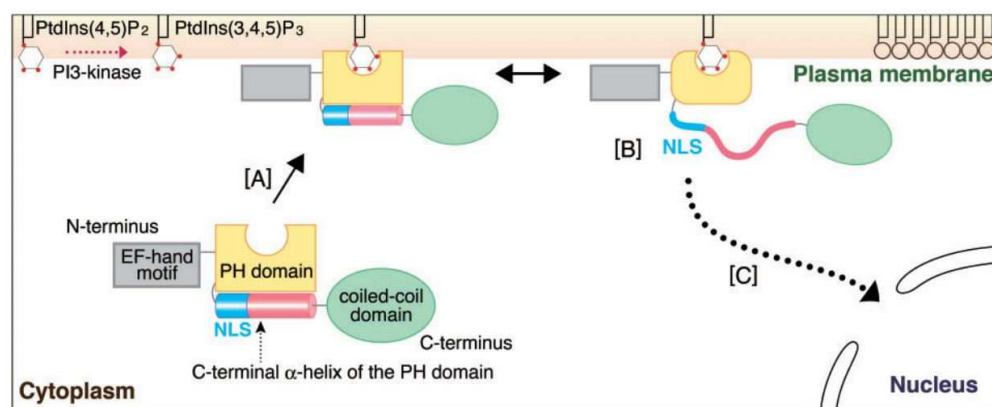


**Figure 1.11 A hypothetical model for the intracellular re-localisation of Swap70**

**[A]** After PtdIns(3,4,5)P<sub>3</sub> is produced in the plasma membrane in response to cell stimulation, Swap70 is recruited to the plasma membrane from the cytoplasm. **[B]** The interaction between the plasma membrane and the PH domain, which is anchored by the head group of phosphoinositide to the membrane, induces conformational transition of the C-terminal α-helix within the PH domain. As a result, the NLS adopts a water-exposed extended conformation recognizable by a nuclear import receptor, importin-α. **[C]** Swap70 is translocated into the nucleus through binding to importin-α. Adapted from (Tokuda et al., 2012)

## 1.4.2 Diverse biological functions

The unique domain arrangement and variable intracellular localisation of Swap70 predict its multiple functions through numerous signalling activities.

### 1.4.2.1 Function as a Rho GEF

#### Mediating membrane ruffling

Membrane ruffling induced by growth factors, such as epidermal growth factor (EGF) and platelet-derived growth factor (PDGF), is essentially caused by actin remodelling. Among the signalling molecules activated by these growth factors, Phosphoinositide-3-OH kinase (PI3K) is required for membrane ruffling by producing a lipid second messenger, phosphatidylinositol-3, 4, 5-triphosphate (PIP<sub>3</sub>). Swap70 was identified as a PIP<sub>3</sub>-binding protein via its PH domain, and it mediates membrane ruffling through acting as a Rho GEF for Rac (Shinohara et al, 2002).

In mammalian cells, cytoplasmic Swap70 is recruited to cell membrane upon stimulation by growth factors. In this process, Swap70 catalyses PI3K-dependent guanine nucleotide exchange to Rac. In contrast, mutant Swap70 lacking the ability to bind PI3K blocked membrane ruffling induced by EGF or PDGF. Swap70-deficient fibroblasts showed disrupted membrane ruffling after stimulation with EGF, and failed to activate Rac completely. Hence, during membrane ruffling, Swap70 transduces signals from tyrosine kinase receptors to Rac (Shinohara et al, 2002).

Subsequent research showed that Swap70 also directly binds to non-muscle F-actin in this process, whereas the binding to muscle F-actin appears much weaker. A truncated mutant of Swap70, Swap70 (448-585), which contains only the C-terminal region readily co-localises with F-actin. In contrast, full-length Swap70 does not co-localise with F-actin unless cells are stimulated with growth factors, indicating a stimuli-dependent regulatory mechanism underlying the actin-binding activity of Swap70 *in vivo*. It was found that the

C-terminal Moreover, the overexpression of a Swap70 mutant, Swap70 (1-564), which is depleted of this binding domain blocks the membrane ruffling, implying that the binding activity of Swap70 to non-muscle F-actin is required for membrane ruffling (Ihara et al, 2006).

### Regulation of mast cell activation, cell-cell adhesion, and migration

As described earlier, in mast cells, Swap70 stays cytoplasmic or localises to the cell membrane, which is consistent with its PH domain present in the centre region. Through its PH domain Swap70 binds the PI3K product phosphatidylinositol-3, 4, 5-triphosphate (PIP<sub>3</sub>), and this binding is necessary for its localisation to membrane ruffles. As a GEF for Rac, Swap70 promotes formation of the GTP-bound, activated form of Rac, which is a central molecular switch in a wide range of signalling pathways, including signalling from immunoglobulin superfamily receptors such as FcεRI, and from growth factor receptors such as c-kit (Mani et al., 2009).

C-kit signalling is a key proliferation and differentiation pathway in mast cell development. A number of proteins become activated upon c-kit stimulation, such as PI3K and small Rho GTPases, through which actin rearrangements and the release of Ca<sup>2+</sup> are initiated (Linnekin, 1999; Sivalenka et al., 2004).

Cultured bone marrow mast cells (BMMC) from Swap70<sup>-/-</sup> mice show reduced FcεRI-triggered degranulation, abnormal actin reorganisation and defective migration both *in vitro* and *in vivo*. Moreover, Swap70<sup>-/-</sup> BMMC are impaired in calcium flux, and in translocation of Rac1 and Rac2 upon c-kit activation. Adhesion to fibronectin is also inhibited, whereas c-kit induced homotypic cell association is largely increased in Swap70<sup>-/-</sup> BMMC, which requires extracellular Ca<sup>2+</sup>. Together, Swap70 plays a crucial role in regulating specific effector cascade pathways in c-kit mediated mast cell activation, migration, and cell adhesion (Sivalenka et al, 2004).

### Association with endocytosis in dendritic cells

Macropinocytosis is a specialised form of endocytosis through which cells accomplish the non-selective uptake of extracellular fluids, antigens and pathogens (Swanson et al., 1995). Studies in dendritic cells (DCs) and NIH/3T3 fibroblasts established a sequential association of Rac-GTP, Swap70 and Rab5 with macropinosomes. In particular, the N-terminal region, the PH domain and the C-terminal region of Swap70 contribute in a combinatorial manner to the transient association with newly formed macropinosomes in the cell periphery, suggesting Swap70 as a transient component of early macropinosomes (Oberbanscheidt et al., 2007).

The phospholipid mediator sphingosine 1-phosphate (S1P) stimulates motility and endocytosis of mature dendritic cells (DCs). However, in response to S1P and S1P-induced up-regulation of endocytosis, *in vitro* migration of Swap70<sup>-/-</sup> bone marrow-derived DCs (BMDCs) is significantly reduced. In addition, these observations correlate with delayed entry into lymphatic vessels as well as migration to lymph nodes of skin DCs in Swap70<sup>-/-</sup> mice. Although expression of S1P receptors by Swap70<sup>-/-</sup> BMDCs is similar to that in wild type, Swap70<sup>-/-</sup> BMDCs can neither activate RhoA nor localise Rac1 and RhoA into areas of actin polymerisation after S1P stimulus. Collectively, Swap70 contributes to proper and stable activation of RhoA in S1P signalling affecting motility and endocytosis in DCs (Ocana-Morgner et al., 2011).

### **1.4.2.2 Association with B cells**

In addition to blast formation and differentiation into plasma or memory cells, B cell activation leads to heavy chain class switching. As mentioned above, in naive resting B cells, Swap70 is localised mainly in the cytoplasm. Upon stimulation either by the B cell receptor (BCR) or the CD40 pathway, it is transported to the cell membrane and then translocates to the nucleus. After class switching has occurred, Swap70 is recruited to the plasma membrane again. Therefore, Swap70 was proposed to act as a link between the activated BCR on the cell surface, and activation or inactivation of the switch



recombinase in the nucleus, where it was found linked only to IgG, but not IgM. This association may allow previously memory B cells to signal faster and stronger, and reduce the frequency of further switch recombination (Masat et al., 2000).

Swap70 has been shown to regulate processes essential for B cell entry into lymph node (LN), such as reorganisation of the actin cytoskeleton, integrin-mediated attachment, and polarization (Pearce et al., 2006). Moreover, it was demonstrated to be necessary for proper germinal center formation and function, and memory response, possibly through Rho GTPases on F-actin cytoskeletal rearrangements (Quemeneur et al., 2008). Swap70 also acts as a regulator of the adhesion process of marginal zone B cells (MZB), particularly important for differentiation control of B cell precursors and their contribution to splenic tissue formation (Chopin et al., 2010).

Swap70<sup>-/-</sup> mice are phenotypically healthy, but their B lymphocytes are two- to threefold more sensitive to gamma-irradiation. The CD40 signalling pathway is compromised, and CD40-dependent switching to the IgE isotype is largely reduced (Borggreffe et al., 2001; Shinohara et al., 2002). In addition, Swap70<sup>-/-</sup> mice developed autoantibodies at a much higher frequency, and mouse embryo fibroblasts (MEFs) show impaired membrane ruffling and fail to grow in soft agar after transformation by v-Src. (Murugan et al., 2008; Shu et al., 2013).

### **1.4.2.3 Emerging role in zebrafish neural cell development**

Recently, Swap70 was reported to regulate the transition of dividing neural precursors to specified oligodendrocyte progenitor cell (OPC) during zebrafish neural development (Takada et al., 2011). This was the first time Swap70 was investigated in zebrafish and implicated in vertebrate development.

During vertebrate development, multipotent neural precursors produce oligodendrocyte lineage cells, which then migrate to become dispersed

throughout the neural tube and extend long membrane processes, leading to successful myelination. These dynamic cellular behaviours imply dynamic regulation of the cytoskeleton (Kirby et al., 2006; Rowitch et al., 2010).

Swap70 is expressed by oligodendrocyte lineage cells. Given the highly dynamic nature of OPC membrane processes during migration and axon wrapping, coupled with Swap70 promoting cell motility through its GEF function, Swap70 was initially supposed to regulate oligodendrocyte lineage cell behaviour. However, utilising morpholino as the tool for gene knockdown, Swap70 loss-of-function experiments carried out in zebrafish did not provide evidence for this hypothesis. Instead, Swap70-deficient larvae were found to have excess neural precursors and a deficit of OPCs, indicating a novel role for Swap70 in regulating the transition of dividing neural progenitors to specified OPCs (Takada et al., 2011).

## **1.5 Preliminary investigation of Swap70 function in zebrafish embryogenesis**

Def6 is necessary for normal CE cell movements during zebrafish gastrulation (Goudevenou et al., 2011). The high sequence homology shared by Swap70 and Def6 raised an intriguing possibility that Swap70 also plays a vital role in the regulation of CE.

In this section, preliminary studies carried out by Wai Ho Shuen and Katerina Goudevenou, who are previous members of our lab, are summarised, including the identification of *def6* paralogues within the zebrafish genome, the expression pattern and functional analysis of Swap70b during zebrafish embryogenesis.

### 1.5.1 Identification of *def6* paralogues in zebrafish

According to the Ensembl database (<http://www.ensembl.org/>) Ensembl release version 58 (May 2010), five *swap70/def6* paralogues were identified in the zebrafish genome, belonging to the Swap70 family (protein family ID ENSFM00250000001889). The details of these five genes along with different IDs in various databases are shown in **Table 1.2**. Phylogenetic analysis revealed that *def6a* represents the zebrafish orthologue of human and mouse *def6*, whereas *defb* and *def6c* are both *def6* co-orthologues (Goudevenou et al., 2011). Similarly, *swap70b* is the orthologue closest to human and mouse *swap70*, and *swap70a* is a co-orthologue.

Name	Ensembl Gene ID	Chr:	NCBI symbol	NCBI Gene ID	ZFIN Gene ID	UniProt ID
<i>swap70a</i>	ENSDARG000000051819	7	<i>zgc:63599</i>	393645	ZDB-GENE-040426-1182	Q6PEH7
<i>swap70b</i> *	ENSDARG000000057286	18	<i>si:dkey-8l13.4</i>	562490	ZDB-GENE-030131-3587	Q1LYE0
<i>def6a</i> *	ENSDARG000000012247	8	<i>zgc:63721</i>	394015	ZDB-GENE-040426-1246	Q7SYB5
<i>def6b</i>	ENSDARG000000044524	22	<i>LOC570940</i>	570940	ZDB-GENE-110408-59	-
<i>def6c</i>	ENSDARG000000034717	4	<i>si:dkeyp-15g12.1</i>	563690	ZDB-GENE-060503-87	Q1L978

**Table 1.2 Gene name and ID summary of *swap70* and *def6* paralogues in zebrafish**

\* Zebrafish orthologues of *swap70* and *def6* are shown in bold, co-orthologues in regular font.

Adapted from (Shuen, MRes thesis, 2010)

Domain structure comparison of these five *swap70* and *def6* paralogues was carried out by Wai Ho Shuen using three domain prediction programmes (Pfam 24.0, SMART and JCoil), indicating that they share highly similar domain structures (Shuen, MRes thesis, 2010; **Figure 1.12**).

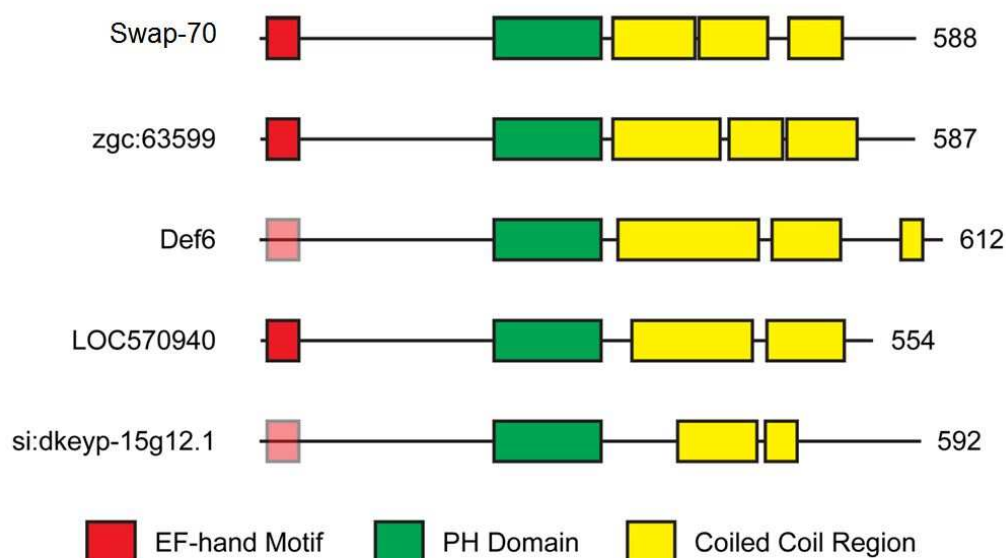


**Figure 1.12 Predicted domain structures of Def6 paralogues in Zebrafish**

Pfam and SMART were used to predict EF-hand motif and PH domain, JCoils and 2Zip were used to predict Coiled coil regions. In Def6 and si:dkeyp-15g12.1, EF-hand motifs were proposed based on the highly conserved N-terminal end among Def6 paralogues. The lengths of the amino acid sequences are indicated next to C-terminus. Adapted from (Shuen, MRes thesis, 2010)

Accordingly, the predicted amino acid sequence of Swap70b shares high sequence identity and similarity with its human, mouse and frog counterparts (**Figure 1.13B**), and exhibits N-terminal EF hand motifs, a central PH domain and C-terminal DHL domain containing a coiled coil motif (**Figure 1.13A**).

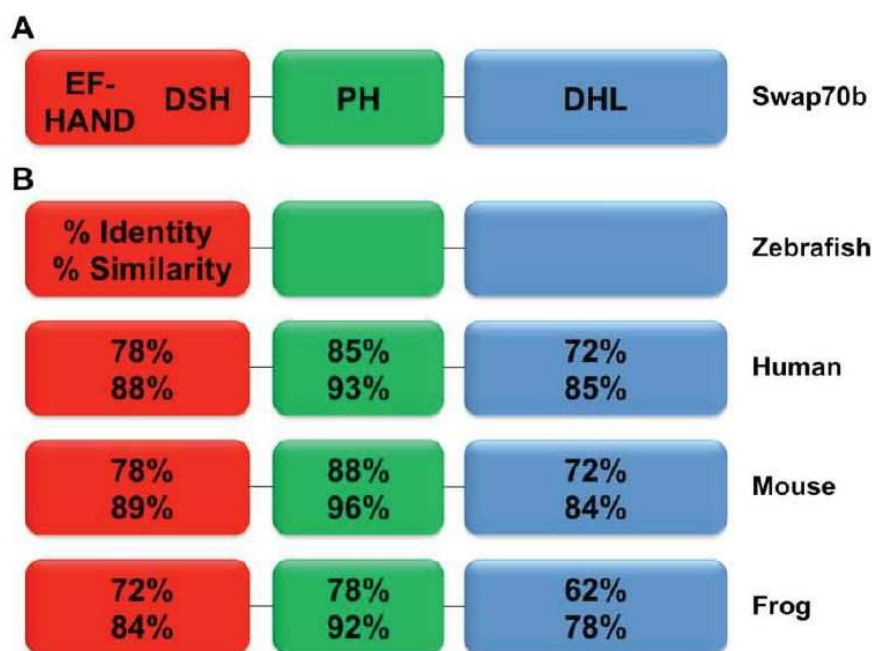


**Figure 1.13 Amino acid sequence comparison of Swap70b proteins in different species**

**(A)** Schematic representation of zebrafish Swap70b with putative  $\text{Ca}^{2+}$ -binding EF-hand motifs at the N-terminus followed by a Def6/Swap70 homology (DSH) domain, a pleckstrin-homology (PH) domain at the centre, and a Dbl-homology-like (DHL) domain that contains a coiled coil motif at the C-terminus. **(B)** The numbers refer to amino acid identities and similarities between the different orthologous. Adapted from (Shuen, MRes thesis, 2010)

RT-PCR analysis showed that all five genes are expressed differentially during early zebrafish development (**Figure 1.14**). While *swap70a* and *def6c* were not or weakly expressed at early stage of development, expression of both was readily detectable at 24, 48, and 72 hpf. Expression of *def6b* was barely detectable until 72 hpf. In contrast, *swap70b* and *def6a* were both ubiquitously expressed from 1 hpf until 72 hpf, indicating that they are both maternally expressed. Zygotic expression of *swap70b* and *def6a* is strong during gastrulation and segmentation (**Figure 1.14**).

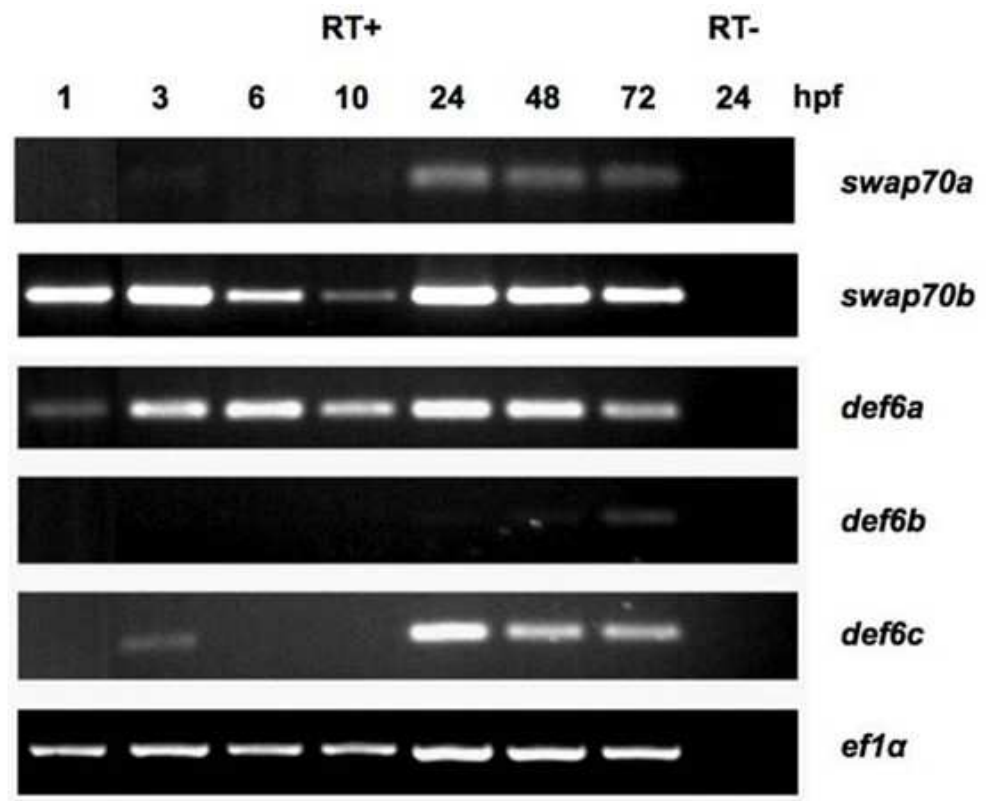


**Figure 1.14 Diverse developmental expressions of *def6* paralogues**

RT-PCR was performed to indicate the expression patterns of five *def6* paralogues at various stages. hpf: hours post-fertilisation. PCR reactions without reverse transcription (RT-) served as a negative control, and *ef1α* which is a housekeeping gene was amplified as a positive control. Adapted from (Shuen, MRes thesis, 2010)

### **1.5.2 Expression pattern of *swap70b* during zebrafish embryogenesis**

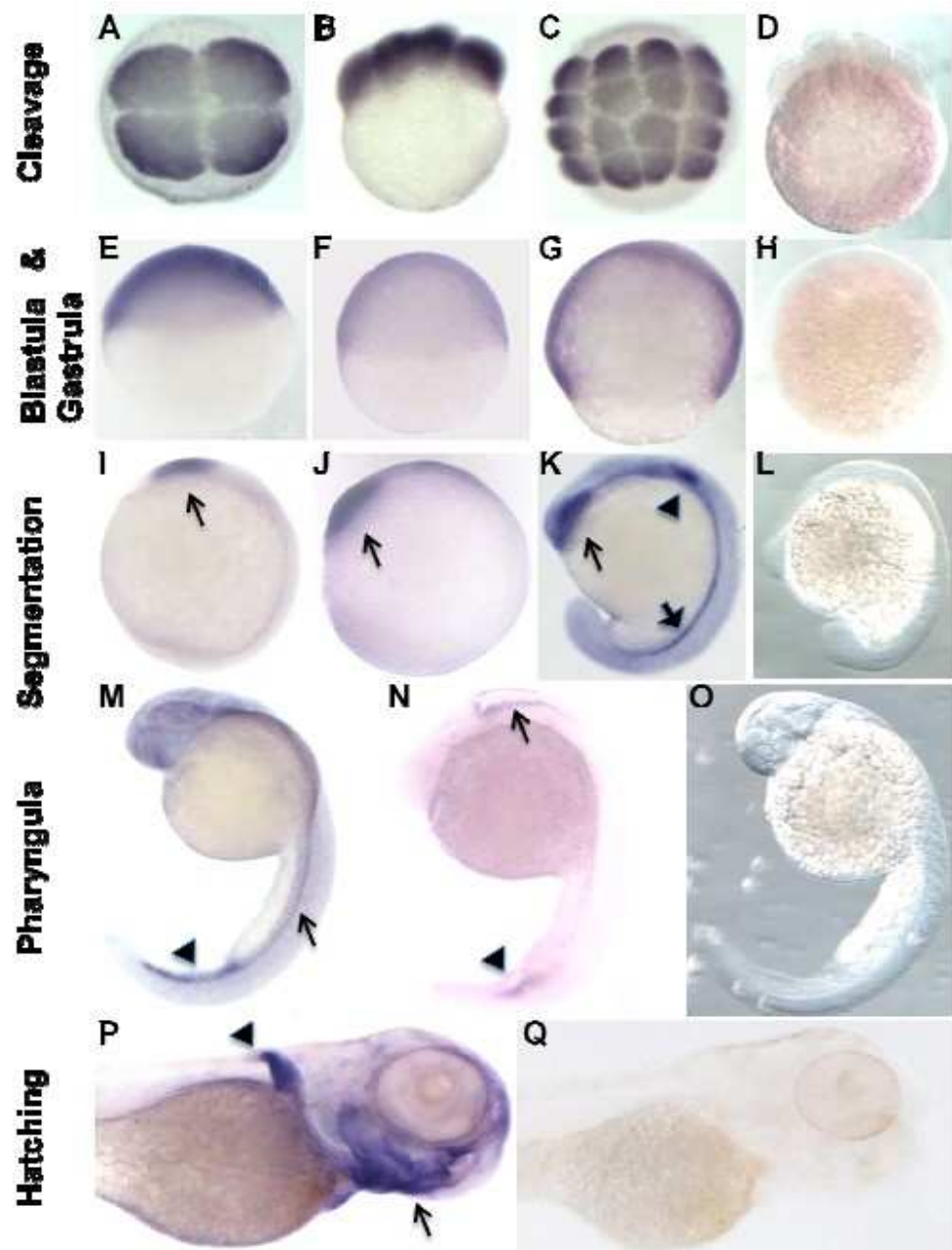
Whole-mount *in situ* hybridisation using a *swap70b* antisense probe confirmed maternal expression of *swap70b* (Figure 1.15A, B), and indicated that it was ubiquitously expressed throughout early zebrafish embryogenesis. During the cleavage stage, the embryos exhibited signals that appeared to

distribute in the cytoplasm (**Figure 1.15A-D**). At blastula and gastrula stages, wide expression of *swap70b* was detected at the dorsal organiser and prospective dorsal midline (**Figure 1.15E-H**). Then at tail bud stage, *swap70b* expression was restricted to optic primordium (**Figure 1.15I**), and at late segmentation stage, *swap70b* expression was detectable in optic primordium, otic vesicle, and ventral mesoderm (**Figure 1.15J-L**). At pharyngula stage, *swap70b* showed preferential expression in caudal vein (**Figure 1.15M-O**), and finally at hatching stage, *swap70b* transcripts were mainly observed in pectoral fins as well as pharyngeal arches (**Figure 1.15P-Q**). The dynamic expression pattern of *swap70b* implies that it is precisely regulated during zebrafish embryogenesis (Shuen, MRes thesis, 2010).

**Figure 1.15 *Swap70b* is ubiquitously expressed in zebrafish development.**

Whole-mount *in situ* hybridisation with a *swap70b*-specific antisense probe at various developmental stages: **(A)** 4-cell; **(B)** 8-cell; **(C)** 16-cell stage; **(E)** 30% epiboly; **(F)** 50% epiboly; **(G)** 70% epiboly; **(I)** bud; **(J)** 4 somites; **(K)** 15 somites; **(M)** primordium 6; **(N)** primordium 16; **(P)** high pectoral. Embryos in **(A-C)**, **(E-G)**, **(I-K)**, **(M-N)**, and **(P)** were probed with anti-sense *swap70b*. Sense *swap70b* probe was used as negative controls in **(D)**, **(H)**, **(L)**, **(O)**, and **(Q)**, representing cleavage, blastula & gastrula, segmentation, and hatching stages respectively. Adapted from (Shuen, MRes thesis, 2010)





### 1.5.3 Functional analysis of Swap70b during zebrafish development

The broad expression pattern of *swap70b* throughout early zebrafish development prompted further investigation of its possible role during this process. Therefore, a loss-of-function strategy using the morpholino gene knockdown technique, which has been introduced in section 1.1.1, was employed to determine the consequences of lost Swap70b function in developing embryos.

#### 1.5.3.1 Swap70b loss-of-function analysis

In Wai Ho Shuen's research, three different MOs were designed to reduce the level of endogenous Swap70b protein, aiming at dissecting its normal function. Splice MO1 was designed to bind to the exon1-intron1 junction inducing the inclusion of intron1, splice MO2 was designed to delete exon6 from transcripts, and AUG MO targets the initial translation codon of *swap70b* (Shuen, MRes thesis, 2010).

#### Evaluation of MO efficiencies

As mentioned in section 1.1.1, the efficiencies of splice MO1 and splice MO2 need to be evaluated by RT-PCR. Embryos were co-injected with 1.5ng splice MO1 and splice MO2. For splice MO1 which was supposed to induce the inclusion of intron1, primers e1 and i1 were designed to amplify mRNA with altered splicing, whereas primers e1 and e2 were designed to amplify mRNA with both normal and altered splicing. In terms of splice MO2 expected to delete exon6, primer e5 and e8 were designed to amplify both wild type and altered transcripts, whereas primer e6 and e8 were designed to amplify wild type transcripts only. As shown in **Figure 1.16**, both MOs achieved the desired results. Splice MO1 injection enhanced e1i1 amplification and reduced e1e2 amplification. In the case of splice MO2, two bands were detected after e5e8 amplification, the larger one representing the wild type transcript and the

other one representing the altered mRNA. Both bands were gel extracted and sequenced to confirm the removal of exon 6. The e6e8 amplification indicated a decreased amount of normal transcript containing exon (Shuen, MRes thesis, 2010).

Due to the lack of good antibody against endogenous Swap70b protein, the effectiveness of AUG MO could not be assessed. Thus, the majority of the results presented in this thesis were generated from experiments using splice MO only.

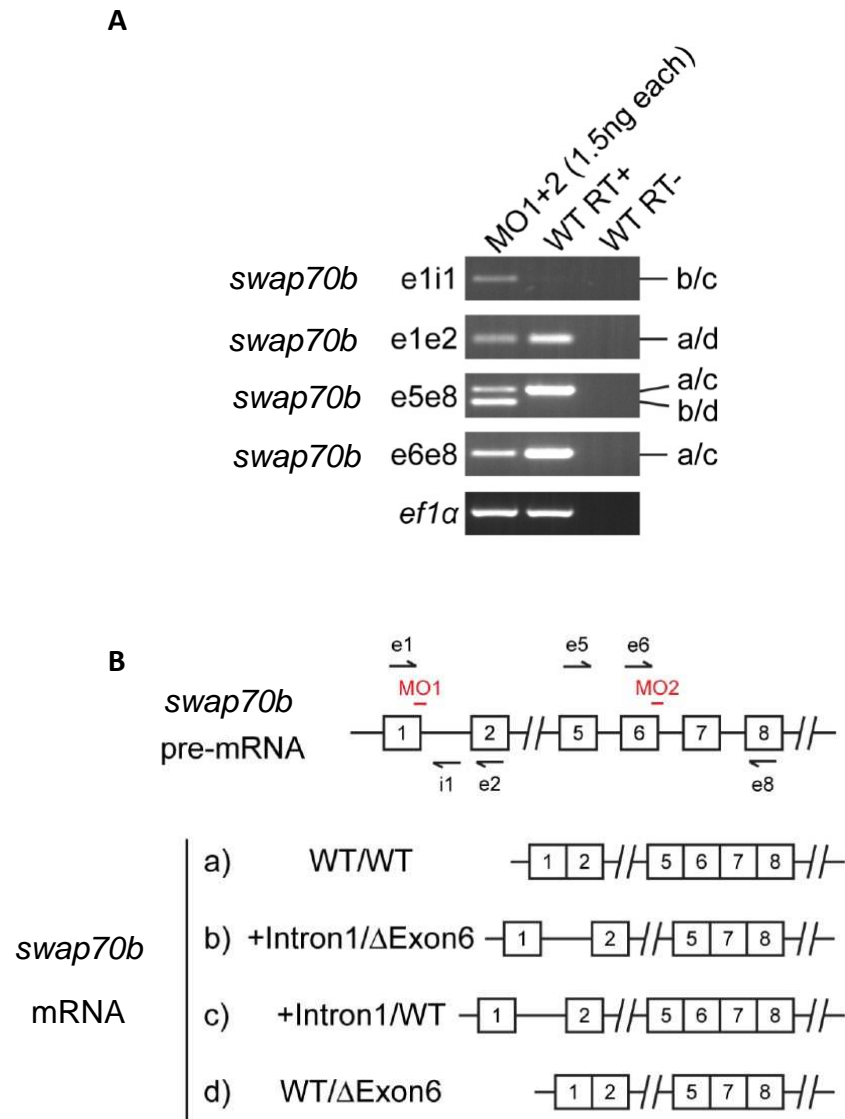


**Figure 1.16 Splice MOs affect *swap70b* pre-mRNA splicing.**

(A) RT-PCR analysis was carried out using mRNA isolated from zebrafish embryos co-injected with splice MO1 and MO2 (1.5ng each). PCR reaction using mRNA from un-injected embryos either with reverse transcription (RT+) or without reverse transcription (RT-) served as positive and negative control, respectively. The housekeeping gene *ef1α* served as internal control. (B) Sequence analysis of the PCR products confirmed the four possible outcomes of *swap70b* mRNA after co-injection of *swap70b* splice MO1 and MO2. Adapted from (Shuen, MRes thesis, 2010)

### Evaluation of MO specificity






















As described in section **1.1.1**, a potentially confounding variable of MOs are the off-target effects, which can be minimized by the use of multiple non-overlapping MOs targeting the same gene. These MOs should be injected independently to ensure that they yield similar phenotypes, and also simultaneously in a low amount which give no phenotype to test for synergism. In addition, RNA rescue is another popular approach to provide strong evidence for the specificity of MOs (Amsterdam et al., 2006; Eisen et al., 2008).

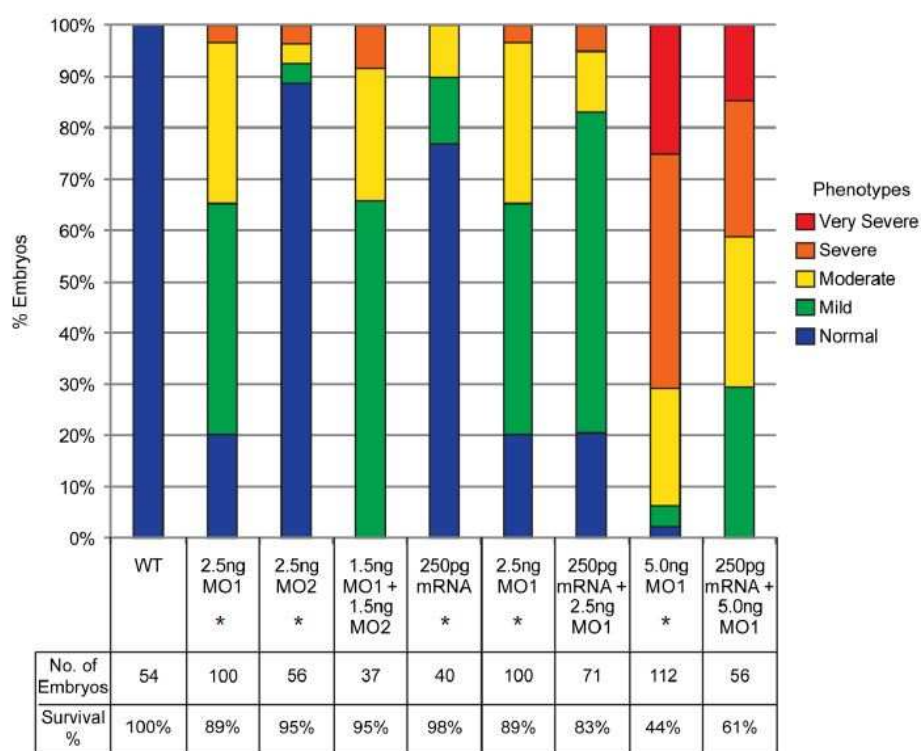
Initial experiments injecting different amounts of splice MO1 or splice MO2, respectively, revealed a similar range of phenotypes in *swap70b* morphants at 24 hpf (**Figure 1.17A**), suggesting that they target the same *swap70b* transcript. *Swap70b* morphants exhibited morphological alterations in brain, eyes, yolk extension, and tail. In addition, the body axis of *swap70b* morphants appeared shorter compared to wild type embryos (**Figure 1.17A**). With increasing amounts of MO injected, the phenotype became more severe, and embryonic lethality went up as well (**Figure 1.17A**). Images of representative embryos with various degrees of defects were shown, which are also used as the classification reference in following experiments in this thesis. Given that severity including embryonic death was much higher when splice MO1 was injected compared to splice MO2, we assume splice MO2 injection resulted in a truncated Swap70b protein with residual function and milder phenotype, whereas injection of splice MO1 resulted in a non-functional truncated protein (Shuen, MRes thesis, 2010). This is in line with recent data by (Takada et al., 2011), showing that the targeting splice donor site of exon 5 induced a milder phenotype affecting neural precursor proliferation and differentiation. Therefore, MO1 was selected for further experiments, and *swap70b* MO mentioned in the following chapters refers to splice MO1 only.

**Figure 1.17 Determination of the specificity of *swap70b* MOs**

(A) 2.5ng, 5.0ng of *swap70b* splice MO1 and splice MO2 were injected independently into 2-4 cell stage embryos. At 24hpf, injected embryos were grouped into normal (blue), mild (green), moderate (yellow), severe (orange), and very severe (red) according to the phenotypes. Un-injected embryos were used as control. The percentages of embryos in each group are indicated. The body axes of embryos were measured by microscopy with 10X magnification and were presented as mean  $\pm$  standard derivation, or just the mean in case of less than 3 embryos found in the group with unit, mm. Modified from (Shuen, MRes thesis, 2010). (B) Co-injection of *swap70b* splice MO1 and splice MO2 (1.5ng each), co-injection of 250pg *swap70b* mRNA and 2.5ng or 5.0ng *swap70b* splice MO1 were performed. Embryos were classified according to the same criteria in (A). Number of surviving embryos is given in %. Adapted from (Shuen, MRes thesis, 2010)

**A**

	Un-injected Wild Type Embryos	Morpholino (MO) Injected Embryo Phenotypes				
	Normal	Normal	Mild	Moderate	Severe	Very Severe
2.5ng Splice MO1	 100% 20.4±0.84	 20.2% 19.6±0.92	 44.9% 19.1±0.68	 31.5% 16.0±0.92	 3.4% 10.3±1.53	0%
5.0ng Splice MO1	 100% 18.3±1.02	 2.0% 19.0	 4.1% 13.0	 22.4% 10.2±1.25	 44.9% 9.5±0.67	 24.5% 9.7±0.65
2.5ng Splice MO2	 100% 20.0±1.08	 88.7% 18.8±0.96	 3.8% 17.0	 3.8% 20.0	 3.8% 13.0	
5.0ng Splice MO2	 100%	 53.7%	 43.3%	 1.5%	 1.5%	

**B**



















Subsequently, synergism tests of splice MOs and RNA rescue experiments were carried out and the statistic results are shown in **Figure 1.17B**. The simultaneous injection of two splice MOs in low amounts showed clear synergistic effects. Moreover, after the addition of synthetic *swap70b* mRNA, the population of normal embryos and those with mild defects increased, whereas those with severe or very severe phenotype decreased, indicating that the defects induced by splice MO1 were successfully restored by the corresponding RNA (Shuen, MRes thesis, 2010).

### Preliminary Swap70b loss-of-function analysis



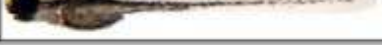

Subsequently, Swap70b loss-of-function analysis was carried out using splice MO1 and AUG MO. 2.5ng splice MO1 or 20ng AUG MO were injected into 2-4 cell stage embryos respectively, un-injected embryos served as control, and comparison was made regarding embryos in specific developmental stages (**Figure 1.18**).

Embryos injected with splice MO1 or AUG MO both developed normally through the blastula stage (3 hpf) in comparison to wild type embryos. As mentioned in section 1.1.1, the beginning of cell involution at around 50% epiboly (5¼ hpf) marks the onset of gastrulation. At this stage (6 hpf), the shield was formed correctly in all three groups of embryos and no significant differences were observed. However, when gastrulation proceeded to the bud stage (10 hpf), embryos injected with splice MO1 exhibited a reduced extension of the body axis, suggesting impaired gastrulation movements, and embryos injected with AUG MO displayed more severe phenotypes. The differences between the un-injected embryos and the injected ones became apparent thereafter. During the segmentation period from 10 hpf to 24 hpf, the formation of eyes, somites, tail were largely delayed and disrupted in both MO injected groups, and the mortality rates were much higher than the wild type control. Survived embryos showed typical gastrulation deficiency, such as reduced embryonic axis and curved tails (Myers et al., 2002). In embryos with severe phenotypes, the development of important organs such as eyes and



	WT n=33	2.5ng Splice MO n=29	20ng AUG MO n=37
3hpf	 100%	 100%	 100%
6hpf	 100%	 100%	 100%
10hpf	 97%	 79%	 95%
13hpf	 97%	 69%	 41%
18hpf	 97%	 62%	 3%
24hpf	 97%	 62%	 3%

	WT	2.5ng Splice MO	20ng AUG MO
48hpf	 97%	 31%	0%
72hpf	 97%	 21%	0%

**Figure 1.18 Swap70b loss-of-function resulted in underdeveloped, non-viable zebrafish embryos.**

2.5ng splice MO1 and 20ng AUG MO were separately injected into 2-4 cell stage embryos and then monitored under microscopy at specific intervals during development process. Un-injected embryos served as experimental control. Images of representative embryos were shown. The percentages indicate the survival rates of embryos at different stages. Adapted from (Shuen, MRes thesis, 2010)

brains were even stopped completely. This was especially obvious in the embryos injected with 20 ng AUG MO, all of which died by the end of the pharyngula period (48 hpf). At 48 hpf, one third of splice MO1 injected embryos survived with curly trunk and shortened body length. At 72 hpf, no red blood cells were formed in 7% of embryos within this group (**Figure 1.18**).

The similarity shared by phenotypes mediated by splice MO1 and AUG MO further suggested the specificity of *swap70b* MO, making it a reliable tool in subsequent research work.

## **1.6 Spleen tyrosine kinase (SYK), a direct upstream regulator of Swap70**

Spleen tyrosine kinase (SYK) was first characterised as a 72 kDa non-receptor cytoplasmic tyrosine kinase (Taniguchi et al., 1991), consisting of two tandem Src Homology 2 (SH2) domain separated by a linker domain, and a C-terminal kinase domain (**Figure 1.19A**). SYK-B is an alternatively spliced form of SYK which lacks 23 amino acids within interdomain B (**Figure 1.19B**). In addition,  $\zeta$ -chain-associated protein kinase of 70 kDa (ZAP70) is a homologue of SYK expressed in mammals (**Figure 1.19C**; Mocsai et al., 2010).

SYK is highly expressed by all haematopoietic cells, and therefore was initially thought to be specific for haematopoietic cells. However, later studies found its expression and novel functions in a vast range of tissues (Shigeru et al., 2001), which will be detailed in the following sections. The mechanism underlying the generation of the SYK-B isoform is still poorly understood. ZAP70 is mostly confined to the T and natural killer cells in mammals and other SYK-related kinases are discovered in invertebrates (Mocsai et al., 2010).

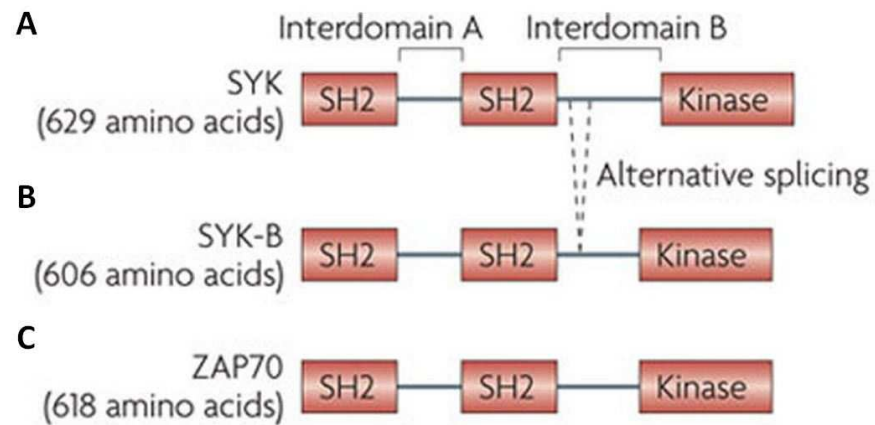


**Figure 1.19 Schematic structures of SYK family tyrosine kinases**

**(A)** The two SH2 domains within SYK are linked by interdomain A, whereas the C-terminal SH2 domain and the tyrosine kinase domain are linked by interdomain B. **(B)** In comparison with the alternatively spliced isoform SYK-B, SYK contains an insert of 23 amino acids within interdomain B, including a nuclear localisation signal (Mocsai et al., 2010; Turner et al., 2000). **(C)** ZAP70 is a cytosolic tyrosine kinase structurally related to SYK. Adapted from (Mocsai et al., 2010)

To date, 64 and 23 direct substrates of SYK have been identified specific to B cells and breast cancer cells, respectively, such as breast cancer anti-estrogen resistance 1 (BCAR1) and signal transducer and activator of transcription 3 (STAT3) (Kim et al., 2011; Uckun et al., 2010; Xue et al., 2012). One of the natural substrates for ZAP70 is the zeta-chain (Chan et al., 1994). The Src homology 2 (SH2) domain-containing leukocyte protein of 76 kDa (SLP-76) and linker for activation of T cells (LAT) are both principle substrates of ZAP70 (Bubeck et al., 1996; Zhang et al., 1998).

### 1.6.1 Immune functions

SYK was originally found to contribute to the signalling responses of immunoreceptors in the adaptive immune response. Classical immunoreceptors, including B cell receptors, T cell receptors and Fc receptors, signal by a conceptually similar mechanism. In the classical model of immune cell signalling, all these receptors either contain or associate with transmembrane proteins containing one or more immunoreceptor tyrosine-based activation motifs (ITAMs), which are short peptide sequences with two tyrosine residues separated by 6–12 amino acids. ITAMs are either present in receptor-associated adaptors or in the cytoplasmic tail of the receptor chain itself. Following receptor engagement, two tyrosine residues, either in a single ITAM or in two hemITAMs on two separate receptor peptide chains, are phosphorylated by SRC family kinases. Next SYK or ZAP70 are recruited to plasma membrane through binding of their tandem SH2 domains to the dually-phosphorylated ITAMs in the receptor complex. This triggers activation of SYK or ZAP70 leading to diverse downstream cellular responses including proliferation, differentiation, and phagocytosis (Mocsai et al., 2010).

The above SYK signalling pathway was initially considered to be restricted to immunoreceptors of the adaptive immune response. However, glycoprotein VI, which is a collagen receptor expressed by platelets, was found to signal by a similar mechanism (Poole et al., 1997). A recently identified ITAM-based signalling in *Drosophila melanogaster* also indicated a role for such pathways beyond adaptive immunity (Ziegenfuss et al., 2008).

### **1.6.2 SYK regulates B cell migration by phosphorylation of Swap70**

Recently, a study demonstrated that Swap70 is post-translationally modified and becomes tyrosine phosphorylated by SYK upon B cell activation, which inhibits binding of Swap70 to F-actin (Pearce et al., 2011).

The transduction of signals from cell surface receptors to the actin cytoskeleton, which controls cell adhesion and migration, requires Rho GTPases. As an upstream regulator of Rho proteins, Swap70 has been demonstrated to be essential for efficient B cell migration and homing to lymph nodes *in vivo* (Pearce et al., 2006). With the aim to determine whether and how Swap70 is posttranslationally modified in this process, Pearce et al. identified SYK as the kinase that phosphorylates Swap70. After CXCL12 stimulation of B cells, SYK becomes activated and directly phosphorylates Swap70. This event blocks the interaction between Swap70 and F-actin, suggesting an important role for Swap70 phosphorylation and hence regulation of its F-actin binding activity by SYK (Pearce et al., 2011).

Interestingly, the addition of the Swap70 N-terminal region to kinase reactions *in vitro* stimulates SYK autophosphorylation. Taking into account that an ITAM like sequence is present in the N-terminal domain of Swap70, it is possible that other than being phosphorylated by SYK, Swap70 may in turn promote recruitment of SYK to the leading edge of the cell via its ITAM motif, and thereby form a positive feedback mechanism (Pearce et al., 2011).

### **1.6.3 Function during development**

Additional studies have revealed the widespread expression of SYK in a variety of cell types other than haemocytes and a large number of non-immune functions of SYK have been identified, especially a role during vascular development (Mocsai et al., 2010).

SYK<sup>-/-</sup> mice die during embryonic development around midgestation and exhibit severe defects in the development of the lymphatic system. Normally, lymphatic endothelium differentiates from veins and forms an independent vascular tree with only few connections to the general circulation. However, in mice deficient of SYK, the lymphatics and the blood vessels form abnormal shunts, leading to leakage of blood into the lymphatic system. To identify the underlying mechanism, a genetic fate mapping approach was employed. SYK was absent from the lymphatic endothelium, but SYK expression was detected in myeloid cells, which produce chemokines and growth factors and thereby orchestrate the proper separation of lymphatics and blood system during embryogenesis. Thus, SYK acts as an essential regulator of lymphatic system development in mice (Brenda et al., 2011).

## 1.7 Aims and objectives

Swap70 has been implicated in various signalling pathways regulating cell adhesion and motility, due to its Rho GEF function and key interaction with F-actin (Gross et al., 2002; Raja et al., 2004). The spatial and temporal expression pattern of its zebrafish orthologue, Swap70b, during zebrafish embryogenesis predicts its important role in this process. Therefore, the aims for this thesis are to understand the function of Swap70b in early zebrafish development, particularly CE cell movements, as well as the underlying molecular mechanism.

In the first part of this thesis, the antisense morpholino oligonucleotide (MO) mediated gene knockdown strategy was employed to analyse the functions of Swap70b during zebrafish embryogenesis. In particular, a combination of phenotypic analysis and *in situ* hybridisation, which used markers of cell fate and CE cell movements, was performed to test the effects of *swap70b* knockdown on zebrafish development. Subsequently, it was examined whether Swap70b is involved in the non-canonical Wnt/PCP pathway through using *swap70b* mRNA to rescue the defects induced by *wnt11* and

*wnt5b* MO. Next, rescue experiments were carried out to explore the possible interplay between Swap70b and Def6 in the non-canonical Wnt/PCP pathway. Finally, the possible role of SYK in modulating zebrafish gastrulation was studied preliminarily.

## Chapter 2 Materials & Methods

### 2.1 Materials

#### 2.1.1 Technical Equipment

Name	Company
Heating block DRI-BLOCK DB3	Jencons Techne
Dual-intensity UV transilluminator	UVP, LLC
Electrophoresis power supply EPS300	Pharmacia Biotech
Molecular Imager Gel Doc XR System	Bio-Rad
Nanodrop spectrophotometer ND1000	Nanodrop
Orbital incubator SI50	Stuart Scientific
Pipettes	Gibson
Horizon 58 electrophoresis apparatus	GIBCO
Minispin plus centrifuge	Eppendorf
Micromax RF 3593 centrifuge	IEC
Water bath	Jencons
<b>Injection apparatus and microscopes</b>	
Borosilicate glass capillaries 1mm O.D. x 0.58mm I.D.	Harward apparatus
Flamming/brown micropipette puller Model P-97	Sutter instrument
Incubator	LEEC



Picospritzer micro-injector	Intracel
Stereomicroscope Stemi SV 6	Zeiss
Stereomicroscope Stemi 2000-C	Zeiss
Eyepieces W-PI10x/23 Br. Foc	Zeiss
Cold Light Sources KL1500 LCD	Zeiss
Stereomicroscope SMZ1500	Nikon
Eyepieces C-W10X A/22	Nikon
Camera DS-5MC	Nikon
Digital sight DS-U1	Nikon
Mercury lamp	Nikon
Confocal laser scanning microscope	Leica microsystems

## 2.1.2 Molecular biology

### Reaction kits:

Name	Company
First-Strand cDNA Synthesis	Invitrogen
mMESSAGE mMACHINE T3 Kit	Ambion
G-50 columns	GE

### Reagents and chemicals:

Name	Company
10X DNaseI buffer	New England Biolabs
Chloroform	Fisher Scientific
Ethanol	Sigma-Aldrich

Isopropanol	Fisher Scientific
Phenol:chloroform:isoamylalcohol (25:24:1)	BDH

### Enzymes:

Name	Company
DNaseI	Roche
EcoRI	New England Biolabs
SfiI	New England Biolabs

## 2.1.3 Zebrafish experiments

### Zebrafish (*Danio rerio*)

Zebrafish were maintained and embryos were collected and raised according to standard laboratory conditions (Westerfield, 2000).

### Reagents and chemicals:

Name	Company
morpholino	Gene Tool
MS222 (ethyl-3-amino benzoate methanesulfonate salt)	Invitrogen
tRNA from Baker's yeast	Roche
Trypsin	Sigma-Aldrich
BM Purple	Roche
20X SSC (sodium sulphate saline)	Promega
blocking reagent	Roche

Nuclease-Free Water	Ambion
Alexa 488 phalloidin	Life technologies

## Solutions

Name	Ingredients
MS222	4 g MS222 to 1 litre with dH <sub>2</sub> O; pH 7.0
Phosphate Buffered Saline (PBS)	1.7 mM KH <sub>2</sub> PO <sub>4</sub> ; 5.2 mM Na <sub>2</sub> HPO <sub>4</sub> ; 150 mM NaCl
PBST	0.1% Tween20 in PBS
Paraformaldehyde (PFA)	4% PFA in PBS
Maleic acid Buffer (MAB)	0.1 M Maleic acid; 0.15 M NaCl; pH 7.5
MABT	0.1% Tween20 in MAB
DIG block	2% blocking reagent in MABT
Hybridisation Buffer (Hybe)	50% deionised formamide; 5X SSC; 50 mg/ml Heparin; 9.2 mM Citric acid; 0.1% Tween20 (Hybe <sup>+</sup> buffer also includes 0.5 mg/ml yeast tRNA)
BCL Buffer III	0.1 M Tris-HCl pH 9.5; 0.1 M NaCl; 50 mM MgCl <sub>2</sub> ; 0.1% Tween20

## 2.2 Methods

### 2.2.1 Molecular biology

#### 2.2.1.1 General techniques

##### Agarose gel electrophoresis

1%-1.5% gels were prepared by melting agarose powder in TBE buffer using a microwave oven, cooling down the gel, adding 5% v/v ethidium bromide and pouring the mixture into the gel tank fitted with a suitable comb. DNA or RNA samples were mixed with loading dye and loaded into the gel wells. After electrophoresis at 80V for 40-60 minutes, gel was examined under UV light.

##### Quantification of nucleic acid samples

A Nanodrop 3300 spectrophotometer was used to quantify DNA and RNA samples. The concentration was indicated by the UV absorption at 260nm. The purity was assessed by the 260nm/280nm and 260nm/230nm ratios.

#### 2.2.1.2 RNA manipulation

##### *In vitro* transcription of mRNA for embryo injections

An 80 µl reaction was set up to linearize the template DNA, consisting of 10 µg template DNA, 1 µl restriction enzyme, 8 µl 10X buffer, 0.8 µl 100X BSA, and nuclease-free water. The reaction was incubated at 37°C for 4 hours before being mixed with an equal volume of phenol: chloroform: isoamylalcohol (25:24:1), vortexed for 30 seconds and centrifuged at 13000 rpm for 3 minutes to allow phase separation. The lower phase containing proteins was discarded. These steps were repeated and the samples were re-extracted as above with 80µl chloroform. 8µl NaAc (3M) and 200µl 100% EtOH were added to the sample, which was then incubated at -20°C for at least 30 minutes and centrifuged at 13000 rpm at 4°C for 30 minutes. The

pellet was rinsed with 200µl ice cold 70% EtOH and centrifuged at 13000 rpm in 4°C for 5 minutes. Residual EtOH was removed using a pipette with small tip and the pellet was air dried for at least 10 minutes, prior to re-suspension in 10 µl nuclease-free water and being stored at -20°C.

The mMESSAGE mMACHINE High Yield Capped RNA Transcription Kit (Ambion) was used to prepare mRNA for micro-injection. A 20 µl reaction was set up, consisting of 1µg linear template DNA, 10 µl 2x NTP/CAP analogue buffer, 2 µl 10X reaction buffer, 2 µl enzyme mix and nuclease-free water. According to the manufacturer's instructions, the reaction was incubated at 37°C for 2 hours. Following transcription, 1 µl DNaseI was added to the reaction which was then incubated for 20 minutes at 37°C. 1 µl product was run on agarose gel to check whether an intact transcript had been made. To stop the transcription reaction, 115 µl nuclease-free water and 15 µl ammonium acetate STOP solution were added to bring the final volume to 150 µl. mRNA was extracted by an equal volume of phenol/chloroform, using the same method for DNA which was described above. An equal volume of isopropanol was added to the sample, which was then incubated at -20°C for at least 30 minutes and centrifuged at 13000 rpm in 4°C for 15 minutes. Residual isopropanol was removed using a pipette with small tip and the pellet was air dried for at least 10 minutes, prior to re-suspension in 20 µl nuclease-free water. The RNA product was quantified by Nanodrop, and aliquots were stored at -80°C.

### *In vitro* transcription of mRNA for whole mount *in situ* hybridisation

A 20 µl reaction was set up, consisting of 1µg linear template DNA, 0.5 µl RNase inhibitor, 1 µl RNA polymerase, 4 µl 5X transcription buffer, 2 µl DIG-UTP NTP mix and nuclease-free water. The reaction was incubated at 37°C for 2 hours or room temperature overnight, and 1 µl was taken to run on agarose gel to verify whether full length transcript has been produced. 1 µl DNaseI was added to the reaction which was then incubated for 20 minutes at 37°C to

remove residual DNA. Probes were purified with G-50 columns (GE) according to manufacturer's instructions, followed by being re-suspended in hybridisation mix at a 1:1 volume and stored at -80°C.

When used for *in situ* hybridisation, probes were diluted 1:200 in hybridisation buffer. These probes were re-used and stored at -20°C.

**Table 2.1** shows the genes, restriction enzymes and RNA polymerases used to produce antisense probes for whole-mount *in situ* hybridisation in this thesis.

Gene	Restriction enzyme	Source	References
<i>hgg1</i>	XhoI/T3	Steve Wilson <sup>1</sup>	(Thisse et al., 1994)
<i>ntl</i>	XhoI/T7	Martin Gering <sup>2</sup>	(Schulte-Merker et al., 1992)
<i>dlx3b</i>	EcoRV/T7	Steve Wilson <sup>1</sup>	(Ekker et al., 1992)
<i>myoD</i>	BamHI/T7	Simon Hughes <sup>3</sup>	(Weinberg et al., 1996)
<i>chd</i>	NotI/T7	Martin Gering <sup>2</sup>	(Miller-Bertoglio et al., 1997)
<i>gsc</i>	SmaI/T7	Paul Scotting <sup>2</sup>	(Schulte-Merker et al., 1994)
<i>bmp2b</i>	EcoRI/T3	Paul Scotting <sup>2</sup>	(Kishimoto et al., 1997)
<i>cdx4</i>	BamHI/T7	Martin Gering <sup>2</sup>	(Davidson et al., 2003)
<i>pax2</i>	BamHI/T7	Martin Gering <sup>2</sup>	(Krauss et al., 1991)

**Table 2.1 Antisense riboprobes synthesised from listed genes for *in situ* hybridisations**

\*Affiliations: <sup>1</sup>Department of Cell and Developmental Biology, University College London, United Kingdom, <sup>2</sup>Molecular Cell and Developmental Biology, School of Life Sciences, The University of Nottingham, United Kingdom, <sup>3</sup>Randall Division of Cell and Molecular Biophysics, King's College London, United Kingdom.

## **2.2.2 Zebrafish techniques**

### **2.2.2.1 Embryos maintenance and staging**

Embryos were raised at 28.5°C in system water containing methylene blue as a fungicide, following standard procedures (Westerfield, 2000). The staging was carried out according to morphological criteria shown in **Figure 1.1** (Kimmel et al., 1995).

### **2.2.2.2 mRNA and morpholino microinjections**

In this thesis, mock injections were done using DNA loading dye while practicing the technique of microinjection, which caused no phenotypic alterations in zebrafish embryos.

#### mRNA injection

Stock mRNA solutions were thawed on ice and diluted to the concentration required for the experiment with nuclease-free water. After the mRNA sample was loaded into the injection needle, the needle was locked tightly in the injection apparatus. Embryos at 2-4 cell stage were aligned along the edge of a slide placed on a Petri-dish lid and then rotated to make their yolk face the slide edge. The head of the needle was opened by using fine forceps (World Precision Instrument) while viewing under a Nikon SMZ1500 microscope with the highest magnification. The pulse duration was changed to calibrate the bubble size to 500pl and the sample was injected into the animal pole of each embryo. After completion of the injections, embryos were transferred to a Petri-dish containing fresh aquarium water containing methyl blue and incubated at 28.5°C for further investigation.

#### MO injections

MOs were designed and synthesised by GeneTools. Stocks were prepared at a 50ng/nl concentration with nuclease-free water and stored at -20°C. Prior to use, stocks were heated at 65°C for 5 minutes, spun at 13000 *g* for 1

minute, and diluted to the required concentration with nuclease-free water. These working solutions were stored at 4°C. MOs used in this thesis were shown in **Table 2.2**.

Name	MO sequence (5' to 3')
<i>swap70b</i> MO ( <i>swap70b</i> splice MO1)	AGAGCAAAACGACAAACCTTCAGCT
<i>wnt11</i> MO	GAAAGTTCCTGTATTCTGTCATGTC
<i>wnt5b</i> MO	GTCCTTGGTTCATTCTCACATCCAT
<i>def6a</i> MO	AAAGAGAGCATACCTTGTCCAGGAT
<i>syk</i> MO	AGTGAAGAAGACTTACAGAAATTTG

**Table 2.2** MOs used for specific gene knockdown in this thesis

### 2.2.2.3 Whole mount *in situ* hybridisation

#### Fixation of embryos

Embryos younger than 24hpf were fixed in 4% PFA overnight at 4°C or for 3 hours at room temperature before being dechorinated by using fine forceps. In the case of 24hpf embryos, dechorination was done before fixation. Embryos were then rinsed three times with PBST, 5 minutes per time, and dehydrated through 25%, 50%, 75% methanol in PBST into 100% methanol, 5 minutes each wash. 100% methanol was replaced once, and embryos were stored at -20°C for a minimum overnight period.

#### Hybridisation

Embryos were rehydrated through 75%, 50%, 25% methanol in PBST, with a final twice wash in 100% PBST, 5 minutes each. In order to increase probe penetration, embryos older than 25 somites were treated with proteinase K



(10 µg/ml in PBST) for 10 minutes or longer at room temperature. This reaction was stopped by two washes in 2mg/ml glycine in PBST of 5 minutes each. Embryos were re-fixed in 4% PFA for 20 minutes at room temperature and then washed five times in PBST at room temperature, with 5 minutes per wash. They were then washed in 50% Hybe buffer in PBST for 5 minutes before being pre-hybridised in pre-warmed Hybe<sup>+</sup> buffer for at least 1h at 65°C.

Hybe<sup>+</sup> buffer was replaced with prepared probe(s) which were typically diluted 1:200 in Hybe buffer, and the samples were incubated overnight at 65°C.

### Probe removal

After the completion of hybridisation, the probe(s) was removed and stored at -20°C for reuse in the future. Embryos were washed in a 65°C hot block successively with Hybe buffer, 75%, 50%, 25% Hybe buffer in 2xSSC, and 2xSSC, for 10 minutes each, with two final washes with 0.2x SSC for 15 minutes each. Embryos were then washed successively with 75%, 50%, and 25% 0.2 x SSC in MABT buffer, and finally in MABT buffer, for 5 minutes each at room temperature.

### Detection

Embryos were blocked with MAB buffer containing 2% Boehringer Blocking reagent (Roche) for at least 1 hour at room temperature with gentle agitation. The blocking solution was then replaced with anti-digoxigenin antibody fragments conjugated to alkaline phosphatase (Roche) diluted 1:5000 in 2% Boehringer Blocking reagent in MAB buffer, followed by incubation for three hours at room temperature with gentle agitation or overnight at 4°C.

### Colour development

Excess antibody was removed, and embryos were washed with MABT eight times at room temperature with gentle shaking for 15 minutes each.

Embryos were equilibrated with BCL buffer III three times at room temperature for 5 minutes each. The BCL buffer III was replaced by 50% BM Purple (Roche) in BCL buffer III, and the embryos were incubated at 37°C with protection from light until colour appeared.

To permanently stop the reaction, embryos were fixed in 4% PFA for 20 minutes at room temperature, washed in PBST 5 times for 5 minutes each, and dehydrated through 50% methanol in PBST into 100% methanol. Embryos were rehydrated through 50% methanol in PBST into 100% PBST, and taken through 30% and 50% glycerol in PBST before being transferred to 80% glycerol and stored at -20°C.

### Image acquisition and data quantification

Live and *in situ* hybridised embryos were visualized under a Nikon SMZ1500 microscope, and images were captured with a Nikon-DS-5M camera, a NIKON DS-1 control unit and Nikon ACT-2U 1.40 software. Fluorescent pictures were taken on a Leica MZ16F fluorescence stereomicroscope using a Leica DFC 300Fx camera and Leica software. Angles were measured and ratios were calculated from the lengths measured under the same magnification. Two-tailed Student's *t*-tests were then used to analyse the statistical significance.

### **2.2.2.4 Phalloidin (actin) staining of embryos**

75% epiboly (8hpf) stage embryos were fixed in 4% PFA in PBS at 4 °C overnight, followed by two washes in PBST, 5 min each, and incubation in 0.1% Triton X-100 in PBS for 5 minutes for permeabilization. Embryos were then washed twice by PBST for 5 min each. The Alexa 488 phalloidin stock was diluted 1:20 in PBST in which embryos were incubated for 1.5 h at RT and kept from light from then on. Embryos were washed 6 times in PBST for 10 min each, transferred through a glycerol series (25%, 50%, 80% in PBS), and incubated for 30 min. Next, embryos were mounted in 80% glycerol, fixed on double sided sticky tape with the position shown in **Figure 2.1A**, and covered

by a cover slip as shown in **Figure 2.1B**. Finally the whole system was sealed with nail polish for confocal microscopy observation.

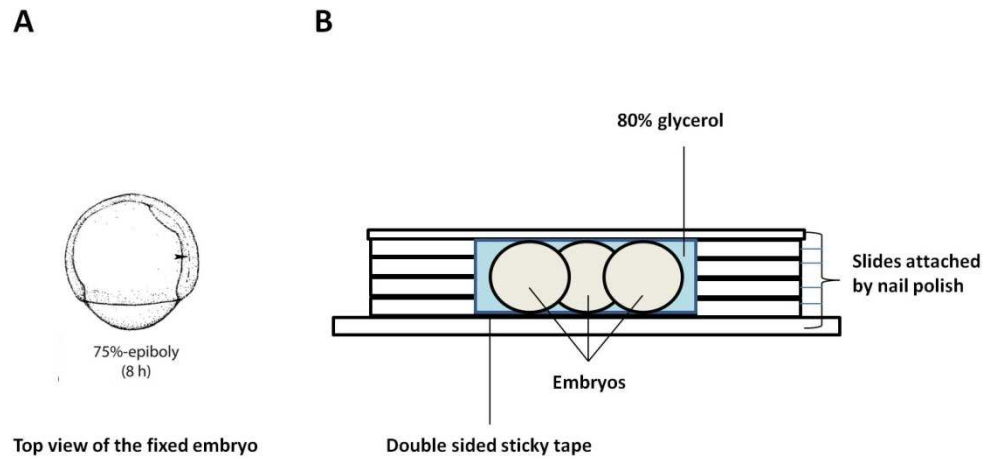


**Figure 2.1 Fixation of phalloidin stained zebrafish embryos**

(A) Embryos were positioned on double sided sticky tape with the lateral side upwards, ventral side to the left and dorsal side to the right. (B) A system was set up to fix phalloidin stained embryos. Embryos were fixed by double sided sticky tape on a glass slide, mounted using 80% glycerol, covered by a cover slip, and the whole system was sealed with nail polish for observation.

## Chapter 3

# Swap70b is required for normal CE cell movements during gastrulation

### 3.1 Introduction

Previous work by Wai Ho Shuen in our lab has shown that Swap70b loss-of-function leads to obvious deficiencies in zebrafish development, which may be caused by impaired CE cell movements during gastrulation (Shuen, MRes thesis, 2010). Therefore, we hypothesised that Swap70b is essential for normal CE cell movements. To assess this hypothesis, MO-induced Swap70b loss-of-function was carried out using a combination of phenotypic analysis and *in situ* hybridisation. In addition, cell fates of different germ layers were examined in *swap70b* morphant embryos to clarify whether the gastrulation-associated defects were due to aberrant CE cell movements or cell fate alterations.

In general, embryos with CE defects display some common phenotypes including shorter A-P body axis, wider dorsal structures like the notochord or somites, and malformed eyes (Roszko et al., 2009). Particularly, the non-canonical Wnt/PCP mutants undergo normal epiboly and internalisation without affecting cell fates, suggesting that Wnt/PCP signalling is required selectively for CE during gastrulation (Habas et al., 2001; Roszko et al., 2009).

## 3.2 Results

### 3.2.1 Swap70b loss-of-function results in aberrant gastrulation

In order to repeat Wai Ho Shuen's previous research (Shuen, MRes thesis, 2010), two amounts (2.5 ng to 5 ng) of *swap70b* MO were injected into 2-4 cell stage embryos that were allowed to grow to 24 hpf for observation. In addition, because morpholinos generally can produce non-specific side effects (Nasevicius et al., 2000), rescue of the *swap70b* MO mediated phenotype was attempted by co-injection of *swap70b* MO and *GFP/swap70b* mRNA.

As mentioned in section 1.5.3.2, *swap70b* MO (named splice MO1 in section 1.5.3.2) was designed to bind to the exon1-intron1 junction, inducing the inclusion of intron1 to the *swap70b* pre-mRNA. Therefore it does not interact with the co-injected *GFP/swap70b* mRNA, which is used to compensate for the loss of endogenous mRNA. According to Wai Ho Shuen's work (Shuen, MRes thesis, 2010), the injection of 250 pg of *GFP/swap70b* mRNA already resulted in abnormal gastrulation movements. Thus *GFP/swap70b* mRNA was injected into zebrafish embryos at a variety of amounts less than 250 pg (data not shown).

Based on the morphological analysis displayed in **Figure 3.1A**, the injection of 150 pg of *GFP/swap70b* mRNA by itself didn't generate any obvious defects in comparison to un-injected control embryos. Therefore this amount was chosen for further investigation. On the contrary, embryos injected with both 2.5 ng and 5 ng of *swap70b* MO exhibited a range of phenotypes associated with defective gastrulation (**Figure 3.1A**), which was consistent with Wai Ho Shuen's data (Shuen, MRes thesis, 2010).

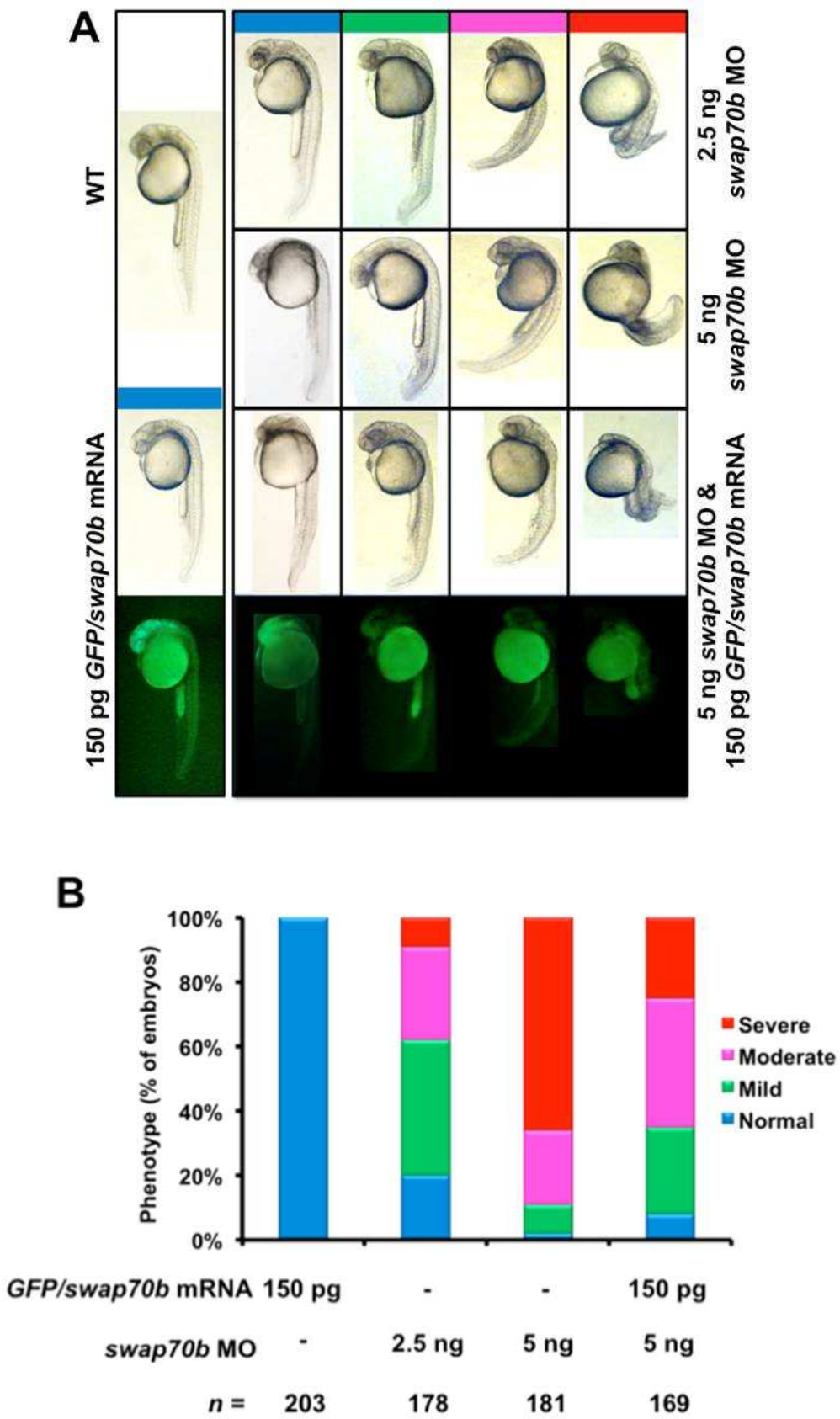
Using the same quantification method described in Wai Ho Shuen's thesis (Shuen, MRes thesis, 2010), including the classification criteria, all embryos injected with 150 pg *GFP/swap70b* mRNA or 2.5 ng, 5 ng *swap70b* MO alone,

or co-injected with 150 pg *GFP/swap70b* mRNA and 5 ng *swap70b* MO, were divided into four groups except that the severe and very severe groups were combined (**Figure 3.1A**). The un-injected wild type embryos served as the standard-of-normal group. The mild, moderate and severe groups were judged according to the severity extent of gastrulation defectiveness. In the mild group, embryos exhibit a curved tail and slightly disorganised somites only. The moderate group embryos exhibit apparently shortened body length, highly curved tail, disordered somite pattern and slightly underdeveloped head structure. The embryos in severe group are even more misshapen, with greatly reduced body length, twisted trunk, and extremely malformed eyes and brain (**Figure 3.1A**).

As shown in **Figure 3.1**, compared with embryos injected with 2.5 ng *swap70b* MO, the percentage of embryos with normal and mild phenotypes decreased from 19.1% (n=34) and 42.1% (n=75) to 2.2% (n=4) and 7.7% (n=14) in the 5 ng *swap70b* MO injected group respectively. Whereas the population with moderate phenotype decreased from 30.9% (n=55) to 21.0% (n=38), the one with severe phenotype increased dramatically from 7.9% (n=14) to 69.1% (n=125) (**Figure 3.1B**). However, after the addition of 150 pg *GFP/swap70b* mRNA, this trend was reversed. In the co-injection group, the population with severe phenotype fell to 7.7% (n=13), whereas the percentage of embryos with mild and moderate phenotype rose to 27.2% (n=46) and 40.2% (n=68) (**Figure 3.1B**). Although co-injection resulted in a partial rescue, these data strongly suggested that the defects induced by *swap70b* MO were specific to *swap70b* knockdown.

**Figure 3.1 *Swap70* morphants exhibiting reduced length of the body axis can be rescued by ectopic expression of GFP/*Swap70b* fusion protein.**

(A) Zebrafish embryos were either un-injected (WT) or injected with *GFP/swap70b* mRNA (150 pg), *swap70b* MO (2.5 ng, 5 ng) or co-injected with *GFP/swap70b* mRNA (150 pg) and *swap70b* MO (5 ng). All embryos at 24 hpf were grouped according to the severity of their morphological phenotypes into normal (blue), mild (green), moderate (pink) and severe (red). Images of representative embryos are shown. Each panel of the bottom two rows depict identical embryos. Green fluorescence in yolk and yolk extension is due to auto-fluorescence (data not shown). (B) Quantification of the phenotypic analysis. Bar graphs show the percentage of embryos with normal, mild, moderate and severe phenotypes. Wild type control embryos did not show any phenotypic alterations (data not shown). n: total number of embryos derived from at least three independent experiments.

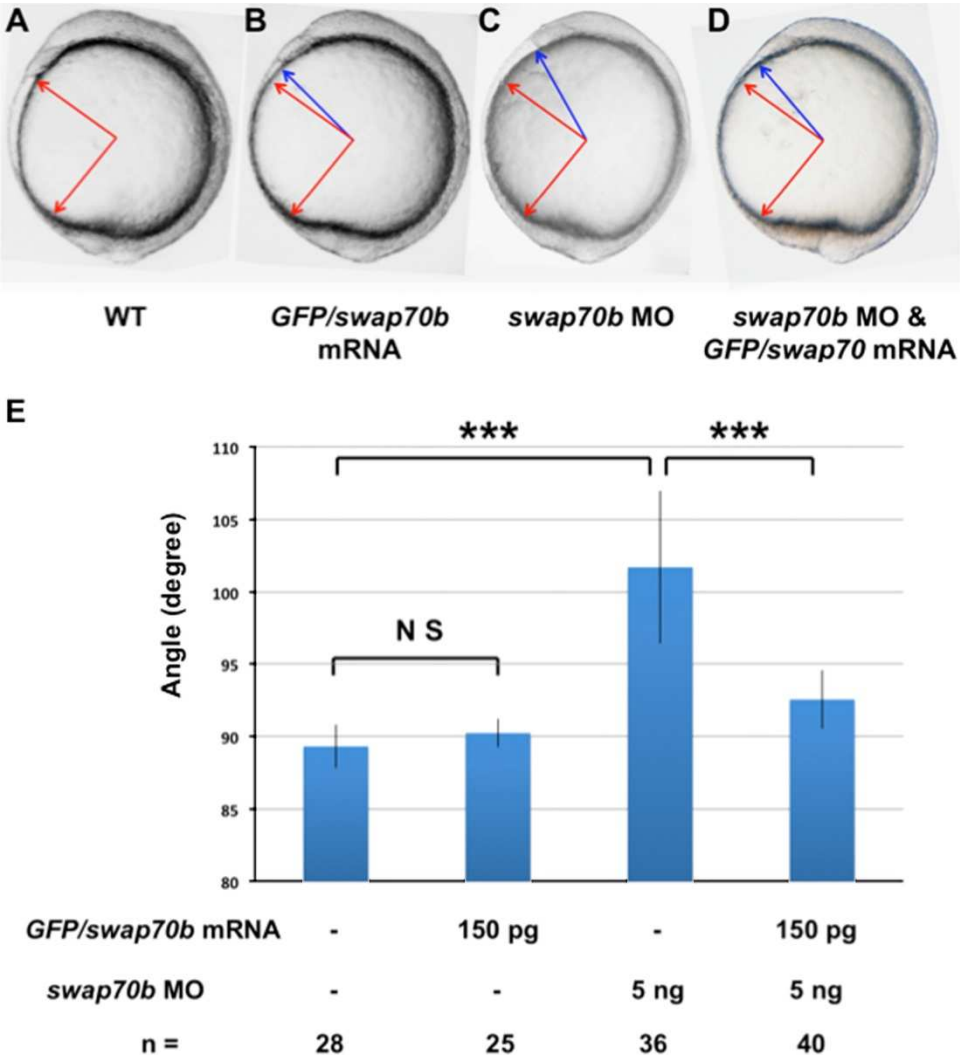




Subsequently, one somite stage at 10½ hpf embryos were analysed. Embryos injected with 150 pg of *GFP/swap70b* mRNA retained a wild type phenotype (**Figure 3.2A, B**). By contrast, embryos injected with 5 ng *swap70b* MO failed to extend properly around the yolk, and thus their body axis was visibly shorter than that of un-injected controls (**Figure 3.2C**), which was largely reversed after the co-injection of *GFP/swap70b* mRNA (**Figure 3.2D**). This was further quantified by measuring the angle between the anterior- and posterior- most structures (Jopling et al., 2005). Consistent with results obtained from 24 hpf embryos, two-tailed Student's *t*-tests indicate a non-significant change in the angle after the injection of 150 pg *GFP/swap70b* mRNA. In contrast, *swap70b* MO led to a significant ( $p<0.001$ ) increase in the angle due to shortening of the body axis, whereas co-injection of 150 pg *GFP/swap70b* mRNA and 5 ng *swap70b* MO decreased the angle significantly ( $p<0.001$ ) (**Figure 3.2E**). Together, 150 pg of *GFP/swap70b* mRNA partially rescued the gastrulation deficiency induced by 5 ng *swap70b* MO, without giving rise to any phenotype of defective gastrulation on its own.

**Figure 3.2** *Swap70b* morphants display a shorter body axis that can be rescued by *swap70b* mRNA.

Zebrafish embryos either un-injected (WT; **A**) or injected with *GFP/swap70b* mRNA (150 pg) (**B**), with *swap70b* MO (5 ng) alone (**C**), or co-injected with *GFP/swap70b* mRNA (150 pg) and *swap70b* MO (5 ng) (**D**) are shown at 10  $\frac{1}{3}$  hpf. (**E**) To assess the length of the body axis, the angle between anterior and posterior ends was measured in wild type (WT; red arrows) and compared to the angle in morphant embryos (blue arrows). Standard deviation (error bars) is shown. Two-tailed Student's *t*-test was performed to establish significance. \*\*\*:  $P < 0.001$ . N.S.: not significantly different.



### 3.2.2 Swap70b is required for normal CE cell movements in zebrafish

Given that shortened body axis can be caused by impaired CE cell movements, as observed for mutants in the non-canonical Wnt/PCP pathway, embryos were un-injected or injected with 5 ng *swap70b* MO, followed by fixation at bud stage and *in situ* hybridisation to evaluate CE cell movements, especially in the dorsal region where the most active CE takes place (Roszko et al., 2009).

Subsequently, two quantification analyses were performed, using the probes for *dlx3b* (*distal-less homeobox gene 3b*) that labels the borders of neural and non-neural ectoderm, *hgg1* (*hatching gland 1*) that marks the anterior-most end of the prechordal plate, and *ntl* (*no-tail*) that is specific for the notochord. Firstly, CE phenotypes were assessed by measuring the widening of the *dlx3b* staining in un-injected and *swap70b* MO injected embryos (**Figure 3.3A, B**). The average lengths were then plotted as a ratio of the embryo width, which is directly proportional to convergence as impaired convergence causes widening of the neural plate edges. Two-tailed Student's *t*-tests were carried out to compare control and *swap70b* MO injected embryos, which showed a significant increase in the ratio of neural plate width to embryo diameter (**Figure 3.3G**). Given that the body length can be indicated by the distance between the anterior-most end of the prechordal plate labelled by *hgg1* (green arrows, **Figure 3.3C, D**) and the tail bud labelled by *ntl* (blue arrows, **Figure 3.3C, D**), it can be seen that the body length was apparently shortened in *swap70b* MO injected embryos.

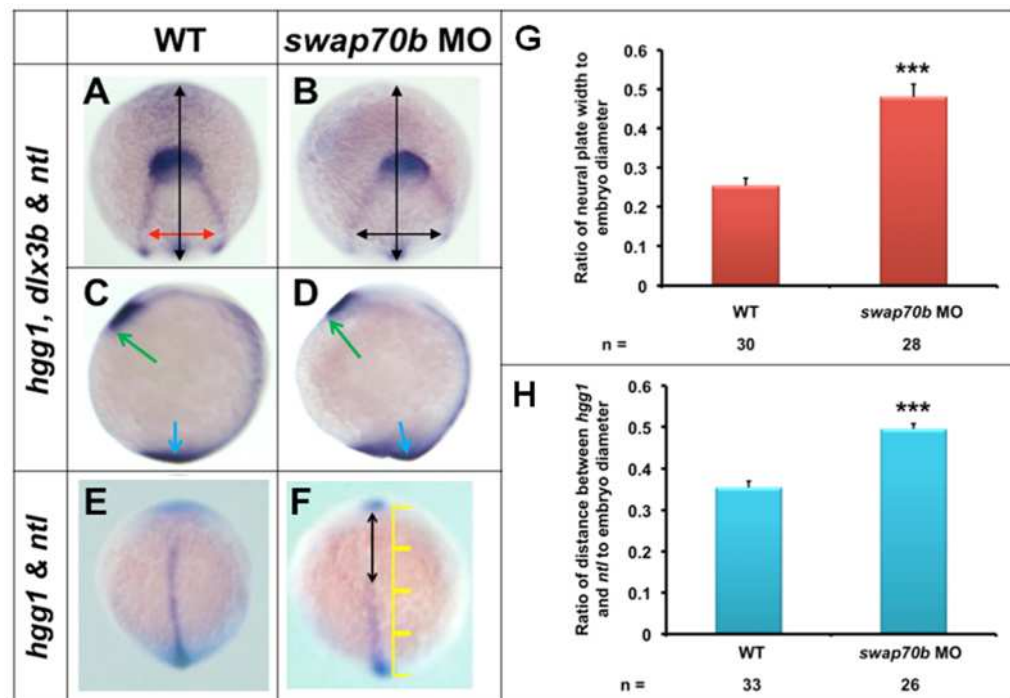


**Figure 3.3 CE cell movements are impaired in *swap70b* morphants.**

*In situ* hybridisation of un-injected embryos (A, C, E) and embryos injected with 5 ng *swap70b* MO (B, D, F) were performed at tail-bud stage with *hgg1* (marker of the polster/prechordal plate), *ntl* (marker of the notochord) and *dlx3b* (marker of the edges of the neural plate). Medio-lateral narrowing (convergence) was quantified by measuring the ratio (G) of width of the *dlx3b* staining (red/black double-headed arrow) at a distance (1/4 of the embryo diameter) from the *dlx3b* arc to the embryo width (vertical black arrow). Images C, D show the lateral views, in which green arrows indicate the anterior-most end of the prechordal plate labelled by *hgg1*, and blue arrows indicate the tail bud labelled by *ntl*. The extent of anterior-posterior lengthening (extension) was quantified by measuring the ratio (H) of the distance between *hgg1* and *ntl* (double-headed arrow) to the embryo width (yellow scale). Two-tailed Student's *t*-tests were performed to determine statistical significance. \*\*\*: P<0.001.

Secondly, the posterior axial domain was tested by the *in situ* hybridisation of *hgg1/ntl* in control and *swap70b* MO injected embryos (**Figure 3.3E, F**). The presumptive notochord marked by *ntl* displayed apparent deficiency in extension along the A-P axis. It is noteworthy that Two-tailed Student's *t*-tests revealed this change is statistically significant (**Figure 3.3H**).

Next, both bud stage (**Figure 3.4A, B, C, and D**) and 10-somite stage embryos (**Figure 3.4E, F**) were tested in the paraxial mesoderm using *myoD* (*myogenic differentiation*) as a marker. As reported by Weinberg et al. (1996), in wild type embryos, the first phase of *myoD* expression begins in the adaxial cells, and then extends from mid-gastrula to just before somite formation, when *myoD* is expressed by cells adjacent to the axial mesoderm (Weinberg et al., 1996; **Figure 3.4A, C**). By contrast, the adaxial cells expressing *myoD* failed to extend properly along the A-P axis or converge dorsally towards the midline in *swap70b* morphants, resulting in a shorter and wider *myoD* expression pattern (**Figure 3.4B, D**). At 10-somite stage, wild type embryos express *myoD* in the posterior region of each somite (Weinberg et al., 1996; **Figure 3.4E**). In *swap70b* morphants, *myoD* staining revealed largely thinner and wider somites, and additional phenotypes are the slight down-regulation of *myoD* expression and relatively disorganised somites (**Figure 3.4F**). Although these data were not quantified, it seemed apparent that CE cell movements in the paraxial mesoderm of *swap70b* morphants were disrupted.

To sum up, it can be firmly established that Swap70b plays an essential role in regulating CE cell movements during zebrafish gastrulation.

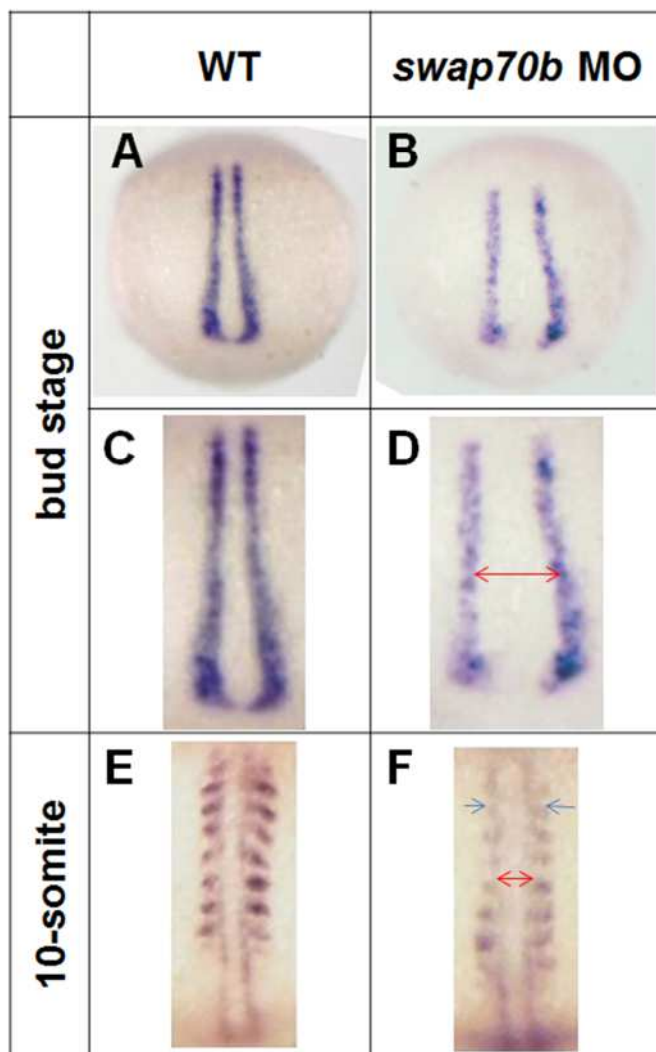


**Figure 3.4** *Swap70b* knockdown induced CE defects in dorsal structures.

Embryos un-injected or injected with 5 ng *swap70b* MO were stained for *myoD* expression. Dorsal views of tail-bud stage (**A**, **B**, **C**, and **D**) and 10-somite stage (**E**, **F**) embryos are depicted with anterior to the top. Images **A**, **B** show the whole embryos at bud stage, whereas **C** and **D** show the enlargement of dorsal structures at bud stage, and **E** and **F** show the enlargement of dorsal structures at 10-somite stage. Double-headed red arrows indicate the widening of somite structures in *swap70b* morphants. Blue arrows indicate the weakened expression of *myoD* in *swap70b* morphants.

### 3.2.3 *Swap70b* knockdown does not affect cell fate specification

Defects in cell specification may be mistaken for CE defects. In particular, alterations in cell fate determination may hamper interpretation of the results obtained from *hgg1* & *dlx3* staining (van Eekelen et al., 2010) described earlier. To examine whether cell specification was impacted by *swap70b* knockdown, *in situ* hybridisation was carried out with *swap70b* morphants using a panel of markers, which are all identified to be involved in cell specification.

Dorsal cell fate specification was analysed with *chd* (*chordin*) and *gsc* (*goosecoid*), both of which encoding dorsalizing factors in the zebrafish organiser. At shield stage (6 hpf), they are supposed to be expressed in the dorsal region of embryos (Miller-Bertoglio et al., 1997; Schulte-Merker et al., 1994). Chordin inhibits ventral signals by directly binding to BMP (Piccolo et al., 1996), and therefore plays an important role in forming D-V axis. Gsc is the first discovered organiser gene (Blumberg et al., 1991), expressed in cells anterior to the presumptive notochord at early embryogenesis stage (Schulte-Merker et al., 1994), and its encoding protein was proposed to execute Chd-independent functions in D-V patterning (Dixon et al., 2009). As shown in **Figure 3.5A-D**, expression of *chd* (**Figure 3.5A, B**) and *gsc* (**Figure 3.5C, D**) both remained unchanged in *swap70b* morphants compared to wild type controls.

*Bmp2b* (*bone morphogenetic protein 2b*), which specifies cells with ventral fates, was also tested at shield stage. Similar to *chd* and *gsc*, *bmp2b* displayed no major difference when *swap70* knockdown embryos were compared to wild type embryos (**Figure 3.5E, F**). This was also the case for *cdx4* (*caudal homeo box transcription factor 4*), which is a non-axial mesodermal marker at shield stage embryos (Davidson et al., 2003). In zebrafish, Cdx4 governs caudal tissue specification through mediating Wnt signalling (Shimizu et al., 2005). It can be clearly seen that the expression of *cdx4* was similar in *swap70b* morphant embryos and un-injected controls (**Figure 3.5G, H**).



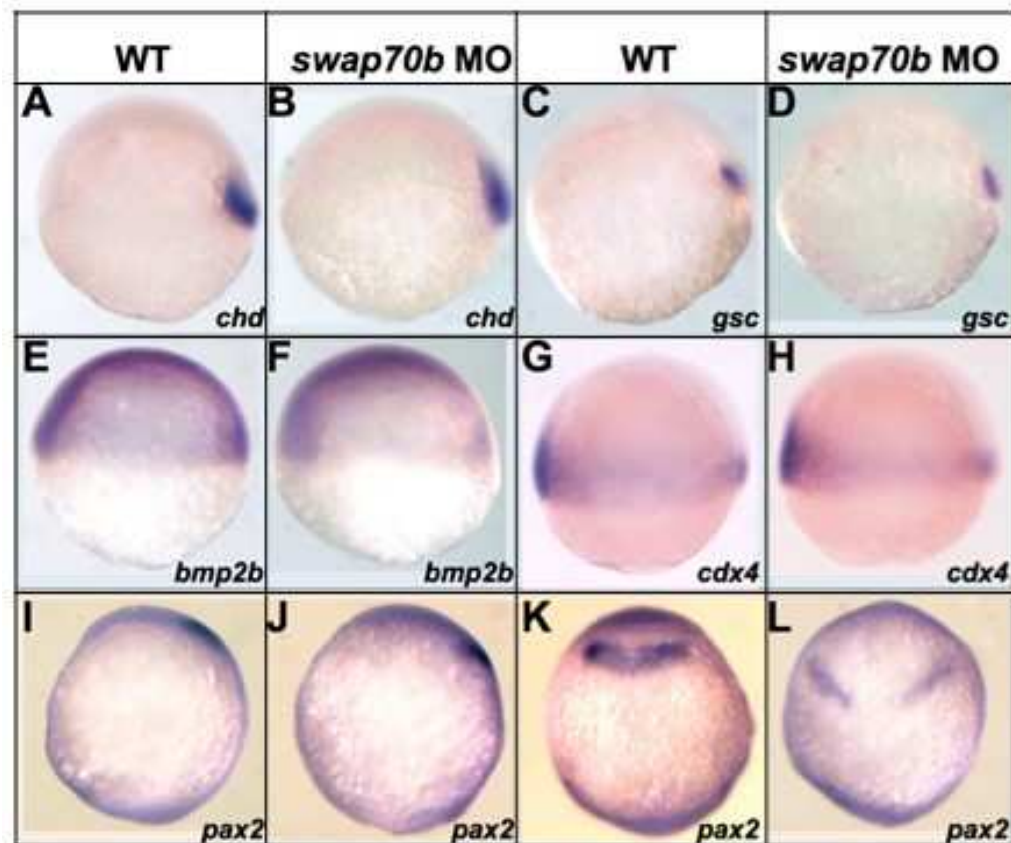


**Figure 3.5 Cell fate specification appears normal in *swap70b* morphants.**

Un-injected and 5 ng *swap70b* MO-injected embryos at 6 hpf were hybridised with various probes: *Chordin*, *chd* (**A, B**); *goosecoid*, *gsc* (**C, D**); *bone morphogenetic protein 2b*, *bmp2b* (**E, F**); *caudal homeobox transcription factor 4*, *cdx4* (**G, H**). At tail-bud stage, the expression pattern of an anterior specific gene *pax2* shifted posteriorly and became broader in *swap70b* morphants, but was still in the midbrain-hindbrain boundary (**I–L**). Lateral views (**A–J**) and dorsal views (**K, L**) with anterior to the top are shown.

Finally, the lack of certain brain structures, due to improper specification of the brain, can also lead to embryos with shortened body length (Jopling et al., 2007). Therefore, expression of a midbrain marker *pax2* (*paired box gene 2a*) was also tested at bud stage (10 hpf) embryos. As shown in **Figure 3.5I-L**, *pax2* was expressed in both wild type controls and Swap70b depleted embryos, indicating the brain structures were present. However, the expression domains were laterally expanded and posteriorly shifted, reflecting decreased convergence of the neural plate (**Figure 3.5K, L**).

Taken together, these results demonstrate that D-V specification and anterior structures were not affected in Swap70b-deficient embryos, and the observed defects in *swap70b* morphants were due to perturbed CE cell movements.

### 3.3 Discussion

Based on the results obtained from the injection with different types and amounts of *swap70b* MOs, early zebrafish embryogenesis was perturbed by the abrogation of Swap70b. In particular, *swap70b* morphants exhibited a variety of phenotypes indicative of aberrant gastrulation, including the reduction of body length and distortion in trunk at 24 hpf (**Figure 3.1**), as well as the failure of embryos to extend properly around the yolk at bud stage (**Figure 3.2**). Since these phenotypes could have resulted from defective CE cell movements, a series of molecular probes were utilised to assess CE cell movements in *swap70b* morphants. *Hgg1/dlx3/ntl* staining revealed that *swap70b* morphants exhibited abnormal convergence movement in the neural plate region, and the extension movement of the prospective hatching gland was also inhibited (**Figure 3.3A-D, G**). Subsequently, the dorsal posterior region was tested by *hgg1/ntl* staining, indicating that the CE cell movements of the notochord, which became both shorter and wider as assessed by *hgg1* staining (**Figure 3.3E, F, and H**), were impaired in *swap70b* morphants. Finally, a paraxial marker *myoD* was employed to reveal that somite structures became wider, thinner and disordered in *swap70b* morphants (**Figure 3.4**).

Since altered cell specification and loss of certain brain structures can also lead to the above phenotypes mediated by *swap70b* MO, a panel of well-characterised markers were used to address whether their expression patterns were affected by *swap70b* knockdown. None of these markers displayed any dramatic differences when *swap70b* knockdown embryos were compared to wild type embryos and the brain structures still existed after the knockdown of *swap70b* (**Figure 3.5**). The only change was noted in the expression of *pax2*, a mid-hindbrain boundary marker which was widened and posteriorly localised. The mislocalised *pax2* staining may indicate possible Swap70b dependent defects in brain development in addition to the defects in CE cell movements (**Figure 3.5I-L**).

Taken together, these data strongly suggest that Swap70b is required for proper CE cell movements during zebrafish gastrulation.

## **Chapter 4**

# **Swap70b regulates CE cell movements through the non-canonical Wnt/PCP pathway downstream of Wnt11**

### **4.1 Introduction**

As described in section 1.2, the non-canonical Wnt/PCP pathway is pivotal in vertebrate CE cell movements during gastrulation (Rohde et al., 2007). Results described in the previous chapter established an essential role for Swap70b in the modulation of CE cell movements. In particular, Swap70b abrogation disrupts CE without altering cell fate specification, strikingly resembling classical components in the non-canonical Wnt/PCP pathway (Roszko et al., 2009). Indeed, Def6a, which is the only GEF sharing a high degree of similarity with Swap70b, has been demonstrated to convey Wnt5b signals and synergise with Wnt11 in the non-canonical Wnt/PCP pathway to regulate CE (Goudevenou et al., 2011). Therefore, the possible link between Swap70b and the two non-canonical Wnt ligands, Wnt11 and Wnt5b, was explored in this chapter to determine whether Swap70b controls CE cell movements through the non-canonical Wnt/PCP pathway.

Because mutations in Wnt genes were found to exhibit remarkable phenotypes in a variety of model organisms, Wnt proteins have been recognized as one of the major families of developmentally important signalling molecules (Cadigan et al., 1997). Among them, the non-canonical Wnts, especially Wnt11 and Wnt5, are largely believed to act as permissive cues for cell movements during vertebrate development (Lin et al., 2010).

In 1996, a number of mutants that displayed defective gastrulation movements as well as tail formation were identified in zebrafish (Hammerschmidt et al., 1996; Heisenberg et al., 1996; Solnica-Krezel et al., 1996), providing valuable tools for the investigation of the various morphogenetic processes that occur during zebrafish embryogenesis.

In *silberblick* (*slb*) mutants, the extension of the axial mesendoderm is initially delayed, leading to an incomplete separation of the eyes later in development (Heisenberg et al., 1996). It was confirmed that the *slb*<sup>-/-</sup> phenotype is due to mutations in the *wnt11* gene (Heisenberg et al., 2000). Further analysis also provided both experimental and genetic evidence that Wnt11 regulates convergent extension movements in the nascent non-axial mesoderm during gastrulation (Heisenberg et al., 2000). Moreover, Dishevelled was found to act downstream of *slb/wnt11* and signal through a non-canonical Wnt pathway in zebrafish, revealing similarities between the intracellular pathways regulating planar polarity in *Drosophila* and CE cell movements in vertebrates. This led to the realisation that Wnt-mediated assignment of cell polarity might contribute to the morphogenetic movements of vertebrate gastrulation (Boutros et al., 1999; Heisenberg et al., 2000).

The *pipetail* (*ppt*) gene was originally found to be necessary for the development of the posterior end of the body axis in zebrafish (Hammerschmidt et al., 1996). In particular, *ppt* was considered to be uniquely required for tail development (Hammerschmidt et al., 1996). According to studies in *Xenopus*, tail formation shares elements of the same control system used in the trunk to be a continuation of gastrulation (Gont et

al., 1993; Tucker et al., 1995). In zebrafish, *ppt* mutants fail in the ventral cell movement of the tail bud on the yolk sac after germ ring closure, and the detachment of the tail tip from the yolk tube (Hammerschmidt et al., 1996). Subsequently, the zebrafish *ppt* gene was confirmed to be identical to *wnt5b* (Rauch et al., 1997). Wnt5b was then demonstrated to be essential for the regulation of CE cell movements in posterior mesendodermal and ectodermal regions, while its function in the anterior mesendoderm appears largely redundant to that of Wnt11 (Kilian et al., 2003).

In this chapter, in order to elucidate the intracellular pathway by which Swap70b modulates CE cell movements, rescue experiments were performed to characterise the interplay between Swap70b and the two Wnt ligands.

## 4.2 Results

### 4.2.1 *Swap70b* MO induced-defects resemble those of *wnt5b* and *wnt11* morphants at late developmental stage

Before exploring the possible relationship between Swap70b and Wnt ligands, it is pertinent to compare their loss-of-function phenotypes. As shown in **Figure 4.1**, *swap70b* morphants (**Figure 4.1B**) phenocopied *wnt5b* (**Figure 4.1C**) and *wnt11* morphants (**Figure 4.1D-F**) at 24hpf, especially in the posterior part.

Consistent with a previous study on Wnt5b, embryos injected with *wnt5b* MO exhibited a malformed head, reduced posterior extension and curved tail (**Figure 4.1C**) compared with control (**Figure 4.1A**) (Lin et al., 2010), and *swap70b* morphants displayed highly similar defects (**Figure 4.1B**). In terms of *wnt11* morphants, the situation seemed more complex. Mutant embryos showed three kinds of phenotypes: partly or completely fused eyes with normal tail, normal eyes with shortened and curved tail, or both (**Figure 4.1D-**

**F**, indicated by red arrows). In the following morphological analysis that was based on phenotypic classifications of 24 hpf embryos, the previous two, i.e. embryos with defects in only eye or tail phenotype were grouped as *wnt11* morphants with mild CE phenotypes. All others exhibiting defects in both eyes and tail were grouped according to their overall CE phenotypes.

Although no fused eyes or cyclopia were observed in *swap70b* morphants, the shortened and bent body axis in *swap70b* morphants highly phenocopies that of *wnt11* morphants. Therefore, it can be hypothesised that Swap70b executes its function in CE regulation through the non-canonical Wnt/PCP pathway.

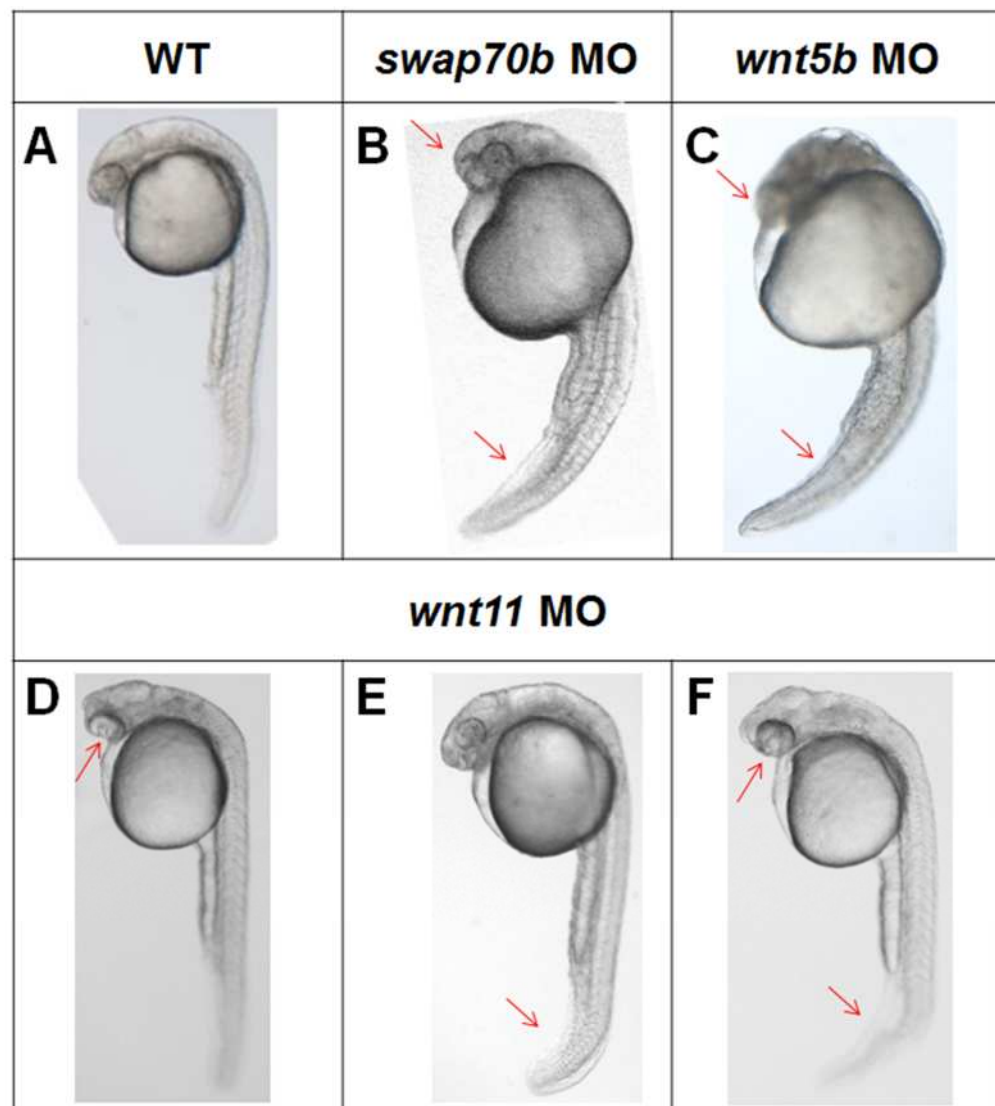


**Figure 4.1** *Swap70b* morphants phenocopy *wnt11* morphants and *wnt5b* morphants at 24hpf.

5 ng *swap70b* (B), *wnt5b* (C) or *wnt11* MO (D-F) was injected into 2-4 cell stage embryos that were allowed to grow until 24 hpf. Un-injected wild type embryos were used as control (A). *Swap70b* morphants (B) and *wnt5b* morphants (C) showed misshapen head and curved tail (red arrows), whereas *wnt11* morphants (D-F) displayed either fused eyes (D), or curved tail (E), or both (F) (red arrows).



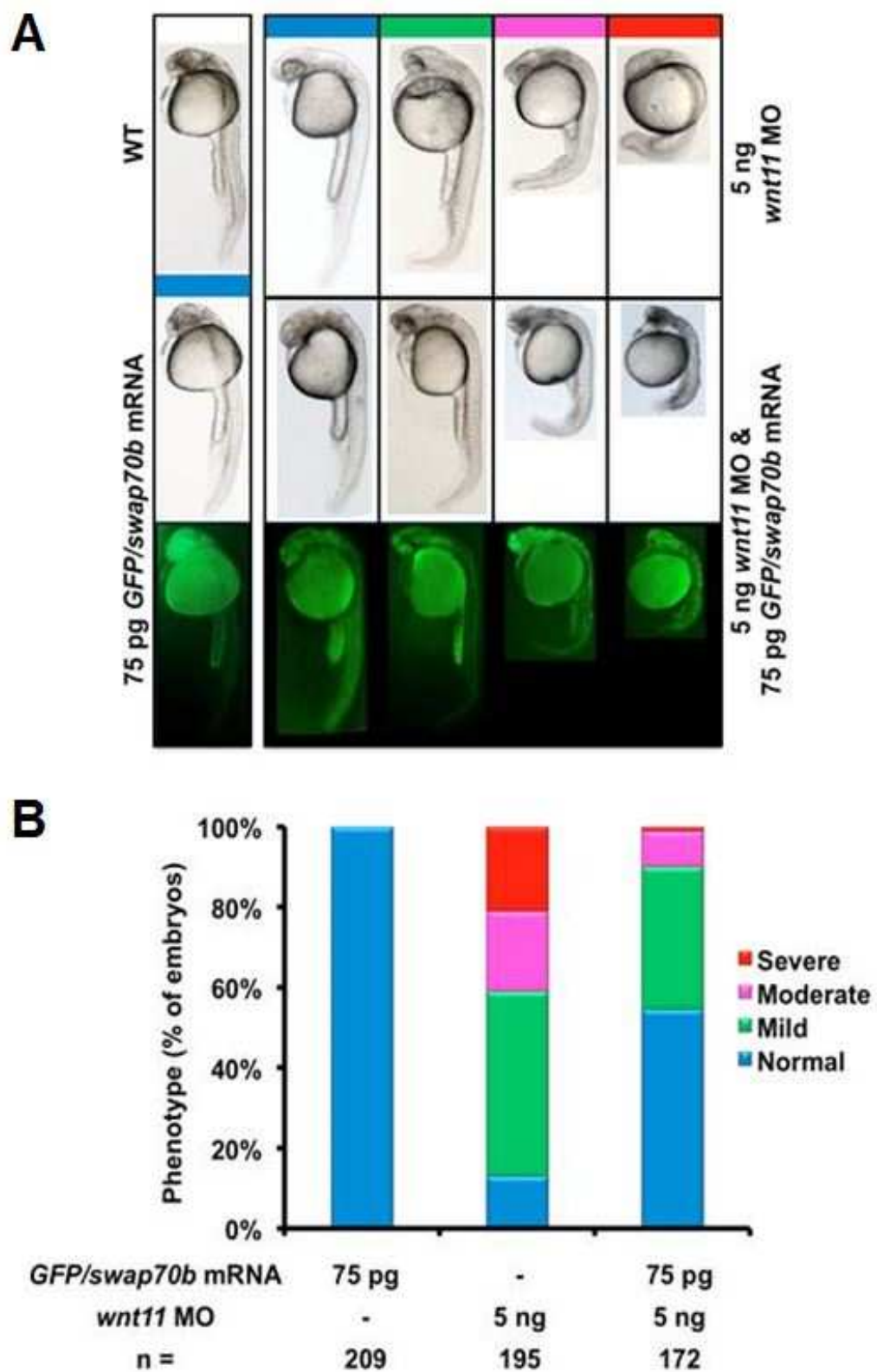
## 4.2.2 Swap70b modulates CE cell movements downstream of Wnt11

The Swap70b related protein Def6a has been demonstrated to regulate CE cell movements through Wnt5b signalling, whereas its over-expression failed to rescue *wnt11* morphants (Goudevenou et al., 2011). Therefore co-injection of 5 ng *wnt11* MO with various amounts of *GFP/swap70b* mRNA was carried out to test whether Swap70b function was sufficient to compensate for Wnt11-deficiency.

In agreement with previous experimental results, 150 pg of *GFP/swap70b* mRNA does not cause any abnormal phenotype on its own. However, compared with embryos injected with 5 ng of *wnt11* MO alone, preliminary results suggest that defective CE cell movements appeared more severe in embryos co-injected with 150 pg of *GFP/swap70b* mRNA and 5 ng of *wnt11* MO at 24 hpf (data not shown). When the amount of *GFP/swap70b* mRNA was reduced to 75 pg, which gave rise to no CE defects on its own, *GFP/swap70b* mRNA was sufficient to rescue *wnt11* morphants. This amount was also used for further investigation in early stage embryos (**Figure 4.2**).

**Figure 4.2 Wnt11-deficiency leads to aberrant CE cell movements that can be partially rescued by *GFP/swap70b* mRNA.**

(A) Zebrafish embryos were either un-injected (WT), injected with *GFP/swap70b* (75 pg), *wnt11* MO (5 ng) or co-injected with *GFP/swap70b* mRNA (75 pg) and *wnt11* MO (5 ng). All embryos at 24 hpf were grouped according to the severity of their morphological phenotypes into normal (blue), mild (green), moderate (pink) and severe (red). Images of representative embryos are shown. Each panel of the bottom two rows depict identical embryos. Green fluorescence in yolk and yolk extension is due to auto-fluorescence (data not shown). (B) Quantification of the phenotypic analysis. Bar graphs show the percentage of embryos with normal, mild, moderate and severe phenotypes. Wild type control embryos did not show any phenotypic alterations (data not shown). n: total number of embryos derived from at least three independent experiments.



As shown in **Figure 4.2**, compared with embryos injected with 5 ng *wnt11* MO alone, the percentage of normal embryos in the co-injection group dramatically rose from 10.8% (n=21) to 55.2% (n=95). Although the population with mild phenotype decreased from 47.7% (n=93) to 33.7% (n=58), the one with moderate and severe phenotypes significantly decreased from 20.0% (n=39) and 21.5% (n=42) to 9.9% (n=17) and 1.2% (n=2), respectively (**Figure 4.2B**), indicating a partial but successful rescue.

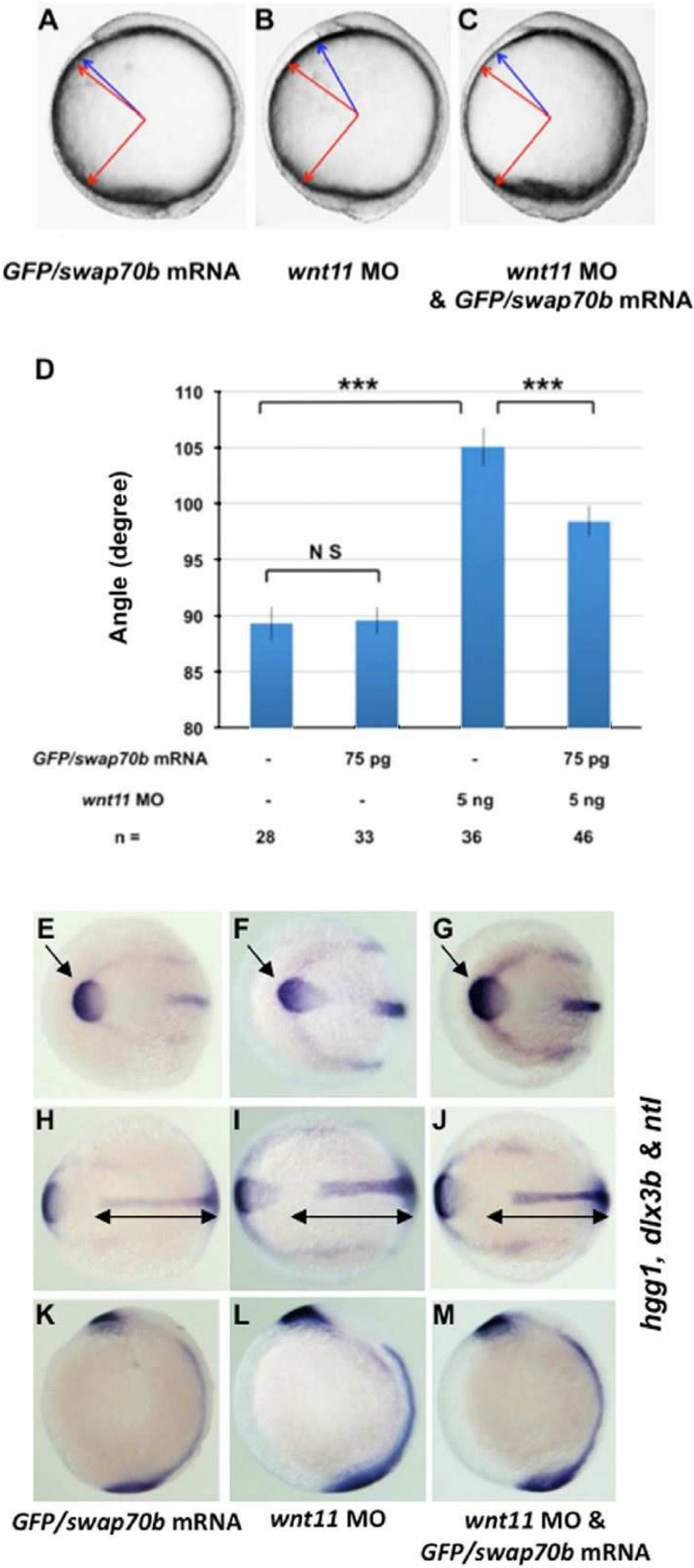
After this preliminary investigation, early stage embryos were tested. As described in section **3.2.1**, the extension of the embryonic axis at the one somite stage after co-injection of *wnt11* MO and *GFP/swap70b* mRNA was assessed, represented by the angle between the anterior and posterior ends in one somite stage embryos. Consistent with the morphology at 24 hpf, embryos injected with 75 pg of *GFP/swap70b* mRNA retained a wild type phenotype that was confirmed by two-tailed Student's *t*-tests (**Figure 4.3A, D**). The injection of *wnt11* MO resulted in a significant ( $p < 0.001$ ) increase in the angle (**Figure 4.3B, D**), which was then reversed dramatically ( $p < 0.001$ ) by the co-injection of 75 pg *GFP/swap70b* mRNA (**Figure 4.3C, D**), suggesting that Swap70b functions downstream of Wnt11 signalling during CE cell movements.

To further confirm these observations, *in situ* hybridisation with probes *hgg1*, *dlx3b* and *ntl* was also carried out in bud stage embryos (**Figure 4.3E–M**). It can be clearly seen that the ectopic Swap70b expression essentially reversed the characteristic phenotype (altered position and shape) of the polster/prechordal plate in *wnt11* morphants (**Figure 4.3E–G**, single head black arrows). In addition, the shortened and broadened notochord in *wnt11* morphants was also rescued by *GFP/swap70b* mRNA (**Figure 4.3H–J**, double head black arrows).

Taken together, these data suggest that Swap70b acts as a downstream effector of Wnt11 in the non-canonical Wnt/PCP pathway, which is different from Def6a (Goudevenou et al., 2011).

**Figure 4.3 *GFP/swap70b* mRNA successfully rescued *wnt11* morphants at early developmental stage.**

Zebrafish embryos at 2-cell stage were injected with *GFP/swap70b* mRNA (75 pg) (**A**), *wnt11* MO (5 ng) alone (**B**), or co-injected with *GFP/swap70b* mRNA (75 pg) and *wnt11* MO (5 ng) (**C**). (**D**) Quantification of A-P axis extension at 10  $\frac{1}{3}$  hpf. The angle between the most anterior and posterior embryonic structure was measured and quantified as described in **Figure 3.2**. Two-tailed Student's *t*-tests were used to determine statistical significance. \*\*\*:  $P < 0.001$ . N.S.: not significantly different. (**E–M**) Comparison of the shape of axial tissues between embryos injected with *GFP/swap70b* mRNA (75 pg) and stained with *hgg1*, *ntl* and *dlx3b* (**E**, **H**, **K**), *wnt11* MO (5 ng) alone (**F**, **I**, **L**), or co-injected with *GFP/swap70b* mRNA (75 pg) and *wnt11* MO (5 ng) (**G**, **J**, **M**) at bud stage. (**E–G**) Position and shape of the prechordal plate, marked by the expression of *hgg1* relative to the anterior edge of the neural plate, outlined by the expression of *dlx3*; animal views; anterior to the left. (**H–J**) Length of the notochord, marked by the expression of *ntl*; dorsal views; anterior to the left. (**K–M**) Lateral views; anterior to the left. Single head black arrows indicate the prechordal plate, and the double head ones indicate the notochord. Because embryos injected with 75 pg *GFP/swap70b* mRNA alone looked indistinguishable from wild type embryos (**Figure 3.3A, C**), the wild type control group is not presented in this figure.



### 4.2.3 Swap70b enhances the *ppt/wnt5b* phenotype in *wnt5b* morphants

Given the similarities observed in terms of phenotype in the *wnt5b* and *swap70b* morphants (**Figure 4.1**), rescue experiments were performed to characterise the interplay between Swap70b and Wnt5b, which has been illustrated to function upstream of Def6a in CE cell movements regulation (Goudevenou et al., 2011).

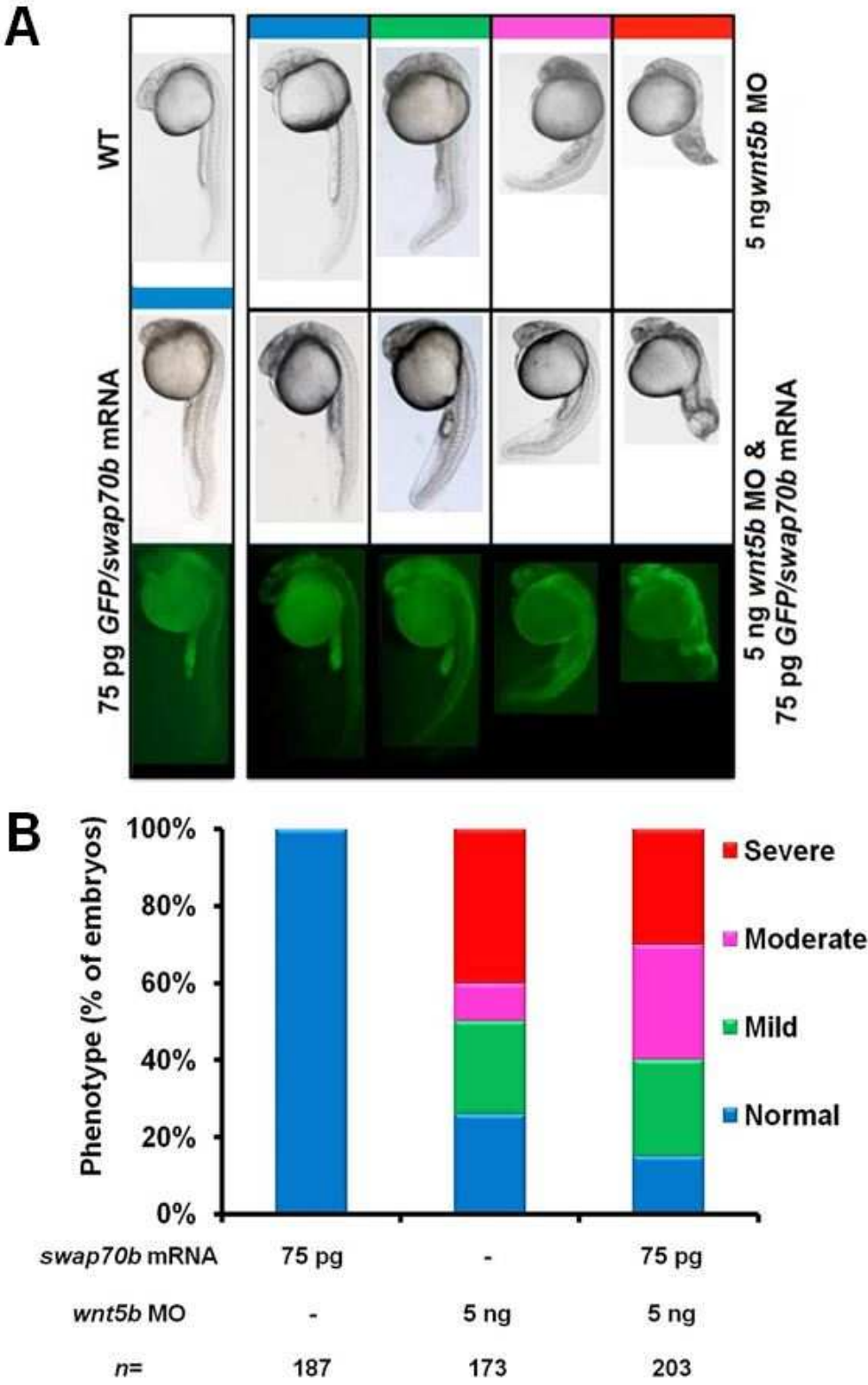
Firstly, 150 pg *swap70b* mRNA was used in the attempt to rescue the *ppt/wnt5b* phenotype mediated by Wnt5b knockdown. However, on the contrary, preliminary results suggest that it enhances the CE movement defects as in the case of Wnt11 (data not shown). Therefore, the amount was then reduced to 75 pg, which was still unable to rescue *wnt5b* morphants (**Figure 4.4**).

As shown in **Figure 4.4**, the percentage of embryos with severe phenotype decreased from 39.9% (n=69) to 31.0% (n=63) in the co-injection group, and the population with moderate phenotype rose from 9.8% (n=17) to 29.1% (n=59). In addition, the percentage of normal embryos decreased from 26.0% (n=45) to 13.8% (n=28), suggesting that there are no rescue effects, but instead the *ppt/wnt5b* phenotype was enhanced by the co-injection of 75 pg *swap70b* mRNA, which is different from the case of Def6a (Goudevenou et al., 2011).

**Figure 4.4** *Swap70b* mRNA failed to restore the *wnt5b* MO-induced CE movement defects.

(A) Zebrafish embryos were either un-injected (WT) or injected with *GFP/swap70b* (75 pg), *wnt5b* MO (5 ng) or co-injected with *GFP/swap70b* mRNA (75 pg) and *wnt5b* MO (5 ng). *Swap70b* morphants at 24 hpf were grouped according to the severity of their morphological phenotypes into normal (blue), mild (green), moderate (pink) and severe (red). Images of representative embryos are shown. Each panel of the bottom two rows depicts identical embryos. Green fluorescence in yolk and yolk extension is due to auto-fluorescence (data not shown). (B) Quantification of the phenotypic analysis. Bar graphs show the percentage of embryos with normal, mild, moderate and severe phenotypes. Wild type control embryos did not show any phenotypic alterations (data not shown). n: total number of embryos derived from at least three independent experiments.





According to the above experiments, it can be speculated that Swap70b does not function downstream of Wnt5b in the non-canonical Wnt/PCP pathway. Thus subsequently *swap70b* and *wnt5b* MOs were injected separately or together to determine if Swap70b and Wnt5b act in synergy in this pathway (**Figure 4.5**).

As shown in **Figure 4.5**, *in situ* hybridisation with combined *hgg1*, *dlx3b* and *ntl* was carried out in wild type embryos, *wnt5b* or *swap70b* single morphants, and Wnt5b/Swap70b double mutants. In the co-injected embryos, it can be clearly seen that the neural plate became largely widened and the notochord was obviously shortened. However, these two effects both seem to be a simple addition of the Wnt5b and Swap70b single knockdown phenotypes, further supporting that Swap70b functions in a parallel pathway rather downstream of Wnt5b. Nevertheless, due to technical difficulties, samples collected during the course of this project were not enough for quantification analysis. Therefore, the results are suggestive rather than conclusive and this experiment needs to be repeated.

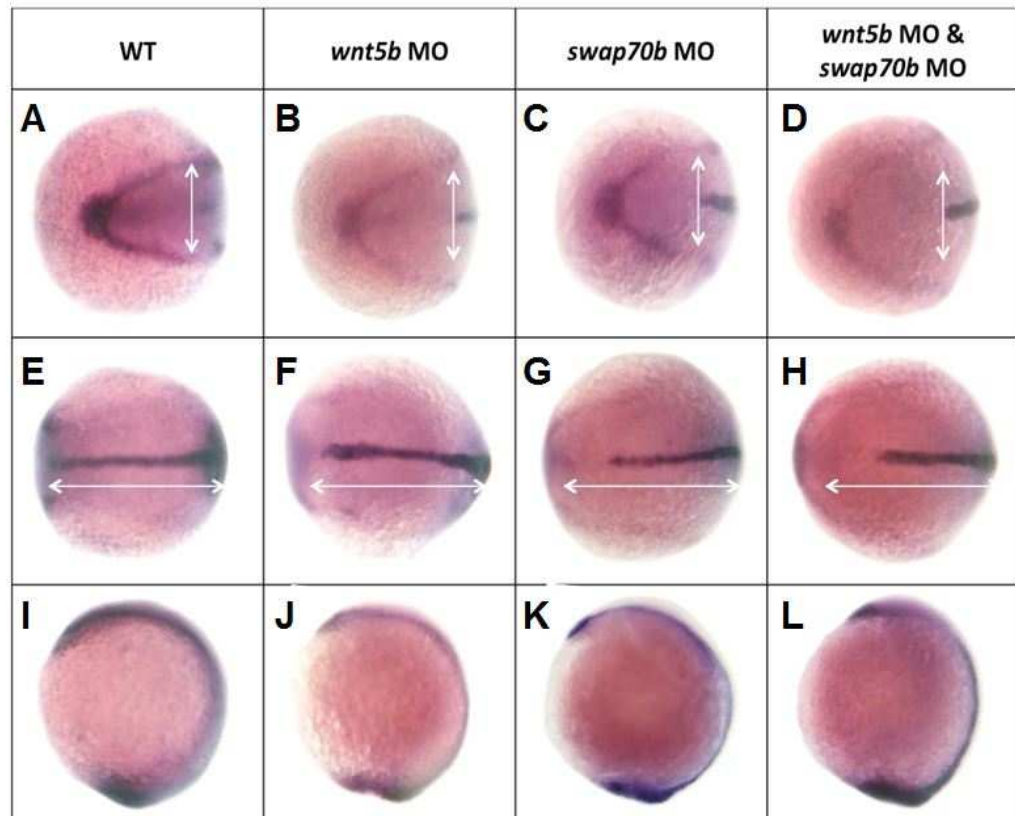


**Figure 4.5 Preliminary results suggest that Wnt5b/Swap70b double mutant embryos exhibit enhanced CE cell movement phenotype.**

Comparison of the shape of axial tissues between wild type embryos (**A, E, I**), embryos injected with *wnt5b* MO (2.5 ng) (**B, F, J**), or *swap70b* MO (2.5 ng) (**C, G, K**) alone, or co-injected with *wnt5b* MO (2.5 ng) and *swap70b* MO (2.5 ng) (**D, H, L**) at bud stage. (**A–D**) Position and shape of the prechordal plate, marked by the expression of *hgg1* relative to the anterior edge of the neural plate, outlined by the expression of *dlx3*; animal views; anterior to the left. (**E–H**) Length of the notochord, marked by the expression of *ntl*; dorsal views; anterior to the left. (**I–L**) Lateral views; anterior to the left. White double-headed arrows are given as a reference to the wild type.

## 4.3 Discussion

### 4.3.1 *Swap70b* morphants share similar CE cell movements defects with both *wnt11* and *wnt5b* morphants

The previous chapter showed that *Swap70b* loss-of-function results in perturbed CE cell movements without altering cell fate specification, reminiscent of the non-canonical Wnt/PCP pathway mutants (Roszko et al., 2009). Therefore, it was intriguing to explore whether *Swap70b* modulates CE cell movements through the non-canonical Wnt/PCP pathway like its closely related protein *Def6a*.

As detailed in section 1.2.1.2, *Wnt11* is considered to be predominantly required anteriorly, whereas *Wnt5b* is crucial in more posterior regions of the embryo (Tada et al., 2009). In addition, *Wnt11* and *Wnt5b* were found to perform partially redundant function in the anterior regions (Kilian et al., 2003).

Embryos injected with *swap70b*, or *wnt5b*, or *wnt11* MO were compared at 24 hpf to preliminarily investigate the possible relationship between *Swap70b* and the two Wnt proteins. As shown in **Figure 4.1**, *swap70b* morphants phenocopied both *wnt5b* and *wnt11* morphants to some extent, exhibiting reduced body length as well as curly and shortened tail, suggesting that *Swap70b* might be involved in the non-canonical Wnt/PCP pathway. In addition, because compared with *wnt11* morphants, the most common *slb/wnt11* phenotype characterised by partially or completely fused eyes was not observed in *swap70b* morphants, *Swap70b* might have little influence on the development of the anterior part in zebrafish, and *Swap70b* mediates part of but not all *Wnt11* signalling.

### 4.3.2 Swap70b functions downstream of Wnt11 in the non-canonical Wnt/PCP pathway

Studies in *Xenopus* showed that Wnt11 induces the accumulation of Fz7 receptor and Dsh at distinct sites of cell contacts (Witzel et al., 2006), leading to complex formation of Dsh, Daam1, RhoA, and WGEF that functions as a GEF protein to activate RhoA (Habas et al., 2001; Tanegashima et al., 2008). In zebrafish, Wnt11 signalling also results in RhoA activation with its downstream effector Rok2, which is necessary for modulating actin cytoskeleton reorganisation and CE cell movements (Marlow et al., 2002). However, it remains unknown which GEF protein is responsible for linking upstream Wnt11 signalling and RhoA activation during this process.

Given the similarity shared by *swap70b* and *wnt11* morphants, it was presumed that Swap70b conveys upstream Wnt11 signalling to regulate CE cell movements. Therefore, rescue experiments were carried out to examine whether *swap70b* mRNA can rescue CE defects induced by *wnt11* MO. Interestingly, at 24 hpf stage, the Wnt11 loss-of-function phenotype was worsened by 150pg *swap70b* mRNA, but suppressed significantly when the amount was halved (**Figure 4.2**), indicating that Wnt11 signalling is modulated through Swap70b and that a balanced Swap70b expression level is essential for appropriate downstream effects. When this rescue experiment was performed at an early developmental stage, 75pg *swap70b* mRNA was able to rescue the compromised CE defects induced by *wnt11* MO, further establishing Swap70b as an essential component of the non-canonical Wnt/PCP pathway as a downstream target of Wnt11 (**Figure 4.3**). In contrast, overexpression of Def6a failed to rescue Wnt11 morphants (Goudevenou et al., 2011), hence it can be speculated that Def6a and Swap70b are regulated by signals from different upstream Wnt ligands.

### 4.3.3 Swap70b and Wnt5b likely act in parallel pathways to regulate CE cell movements

As detailed in section 1.2.1.2, Wnt5b signals through Fz2 to regulate gastrulation movements especially in the posterior parts of the embryo (Tada et al., 2009). Unlike Wnt11, which was speculated to act as a permissive cue to components of the Wnt signalling pathway only, Wnt5b was proposed to also act as an instructive cue through Ryk in directional cell migration during gastrulation (Lin et al., 2010; Rohde et al., 2007; Simons et al., 2008). Furthermore, according to previous research on Def6a, the CE defects observed in *wnt5b* mutants, as well as impaired maturation of the cells that contribute to cartilaginous elements of the head skeleton, were phenocopied by *def6a* morphants, and ectopic overexpression of Def6a essentially rescues *wnt5b* morphants, which established Def6a as a novel member of the Wnt signalling pathway downstream of Wnt5b signalling (Goudevenou et al., 2011).

In order to analyse the possible relationship between Swap70b and Wnt5b, a comparison was first made between Swap70b and Wnt5b individual knockdowns. As shown in **Figure 4.1**, *swap70b* morphants resembled *wnt5b* morphants, as expected. However, attempts to rescue *wnt5b* morphants with overexpression of Swap70b failed, and instead the CE phenotype characteristic for Wnt5b knockdown was enhanced (**Figure 4.4**). This is reminiscent of the scenario that exogenous *wnt5b* mRNA was unable to rescue the *ppt/wnt5b* mutant phenotype, but instead caused variable malformations such as a shortened notochord and a misshaped prechordal plate (Kilian et al., 2003). It was thereby presumed that the posterior mesendoderm is generally more sensitive to *ppt/wnt5b* after Wnt5b loss-of-function (Kilian et al., 2003). Thus, 75pg *swap70b* mRNA, which causes no CE defects on its own, can interfere with normal CE cell movements in the posterior region.

Subsequently, the *swap70b* and *wnt5b* MOs were injected individually or together to further explore whether they function in parallel or overlapping pathways. As shown in **Figure 4.4**, co-injection of *swap70b* and *wnt5b* MOs resulted in a seemingly additive effect enhancing the CE phenotype. It seems therefore that Swap70b and Wnt5b act in parallel pathways without executing any redundant functions.

## Chapter 5

# Swap70b showed no apparent effects on F-actin assembly

### 5.1 Introduction

As mentioned in section **1.3.3.2**, in *Xenopus*, WGEF was demonstrated to be an immediate upstream activator of RhoA during CE, downstream of Wnt11 signalling. In zebrafish, RhoA was shown to regulate CE cell movements through Rho kinase 2 (Rok2), also downstream of Wnt11 (Marlow et al., 2002). However, it remains unknown which GEF is responsible for RhoA activation. According to a recent study in dendritic cells, Swap70 preferentially interacts with active GTP-RhoA and is required for RhoA-dependent cell motility (Ocana-Morgner et al., 2011). Considering the established role of Swap70b in zebrafish CE cell movements, it can be hypothesised that Swap70b acts upstream of RhoA in the non-canonical Wnt/PCP pathway to modulate CE cell movements. As detailed in section **1.3.1.1**, RhoA is involved in the reorganisation of the actin cytoskeleton through interactions with multiple downstream effectors. Therefore, it is worth investigating if the F-actin structure in gastrulating zebrafish is altered after Swap70b knockdown.

As shown in **Figure 5.1**, the cytoskeleton plays many important roles during zebrafish gastrulation. At early gastrulation, the blastoderm moves halfway towards the vegetal pole along with the yolk syncytial layer (YSL). In this



process, actin microfilaments form a dense structure that covers the vegetal cortical region of the yolk cell, which is still present at late gastrulation (**Figure 5.1A, B**; Solnica-Krezel, 2006). In addition, there are two actin rings at the vegetal margins of the deep cells and the enveloping layer (EVL) respectively (**Figure 5.1B**; Solnica-Krezel, 2006). Furthermore, a punctate actin ring forms in the external YSL vegetal to the blastoderm, where endocytosis takes place (**Figure 5.1B**; Solnica-Krezel, 2006).

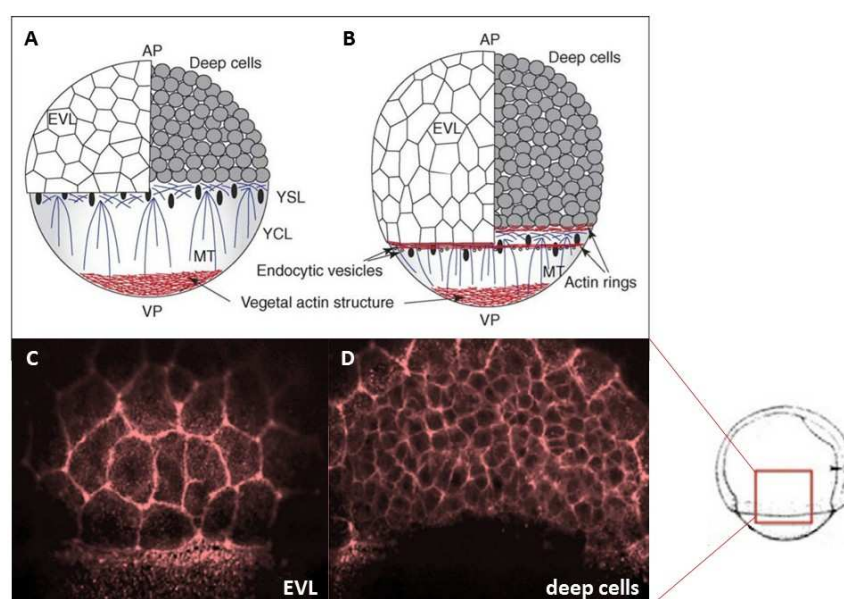


**Figure 5.1 Organisation of the cytoskeleton in the zebrafish yolk cell during gastrulation**

(A) Cytoskeletal structures at early gastrulation. AP, animal pole; EVL: enveloping layer; YSL, yolk syncytial layer; YCL: yolk cytoplasmic layer; MT: microtubules; VP, vegetal pole. (B) Cytoskeletal structures at late gastrulation. (C) F-actin of surface EVL cells stained with phalloidin at the 75% epiboly. (D) F-actin of deep cells stained with phalloidin at the 75% epiboly. Images A, B are adapted from (Solnica-Krezel, 2006), and C, D are adapted from (Yu et al., 2011).

## 5.2 Results

RhoA is known to modulate the formation of contractile actin–myosin filaments (stress fibers) and focal adhesions during cell migration (Ridley et al., 1992). In order to determine whether actin reorganisation during gastrulation was affected by Swap70b knockdown, *swap70b* morphants were fixed at 70% epiboly stage and rhodamine phalloidin staining was used to visualize F-actin under confocal microscopy.

As shown in **Figure 5.2**, F-actin was mainly located at cell boundaries corresponding to the cortical actin structure underneath the cell membrane in wild type embryos (**Figure 5.2A, C**). Both EVL and deep cells in embryos injected with 5 ng *swap70b* MO exhibited no obvious differences in terms of actin organisation (**Figure 5.2B, D**).

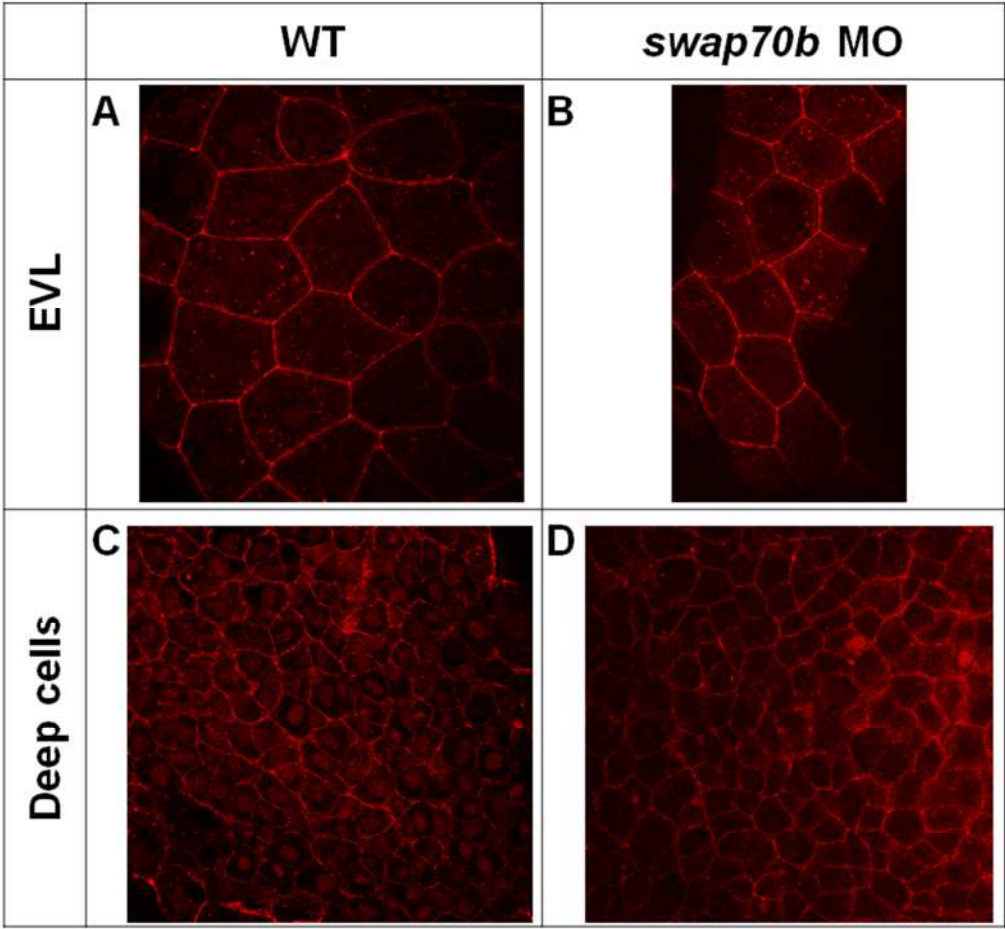


**Figure 5.2 Preliminary results suggest that knockdown of Swap70b has no significant effects on actin rearrangements.**

The wild type (**A, C**) and 5 ng *swap70b* MO (**B, D**) injected embryos were fixed at 70% epiboly, and photographed with lateral view under confocal microscopy after rhodamine phalloidin staining. Images **A, B** are EVL cells, and images **C, D** are deep cells.

## 5.3 Discussion

As detailed in section 1.3.1.1, Rac and RhoA both play prominent roles in the architecture of actin cytoskeleton. Mammalian Swap70 was shown to function as a guanine nucleotide exchange factor for Rac regulating F-actin cytoskeletal reorganisation, and it directly binds activated Rac and RhoA in dendritic cells (Ocana-Morgner et al., 2011; Shinohara et al., 2002). It was also found that coactivation of Rac and RhoA by Wnt/Frizzled signaling is required for vertebrate gastrulation (Habas et al., 2003). Therefore, actin staining using phalloidin was carried out to examine if the actin network structure changed after the depletion of Swap70b in gastrulating zebrafish embryos.

As shown in **Figure 5.2**, there seems no distinguishable difference between *swap70b* morphants and their wild type siblings. Therefore, it could be speculated that Swap70b is not indispensable in the control of F-actin assembly. However, this experiment design itself has some disadvantages and limitations. On one hand, there are some technical difficulties to position all embryos properly as shown in **Figure 5.1**. On the other hand, it is much more reasonable to disperse a single layer of tissue, place it on a glass, and look at the protrusions of cells. Thus, this experiment needs to be repeated to make firm conclusions.

## Chapter 6

# Swap70b and Def6a perform overlapping and distinct function in the non-canonical Wnt/PCP pathway

### 6.1 Introduction

Given the strong similarity in amino acid sequence and domain structure, it is highly likely that Def6a overexpression could compensate for Swap70b loss-of-function and vice versa. Therefore, rescue experiments using phenotypic analysis combined with *in situ* hybridisation were carried out to test this hypothesis.

As detailed in section **1.3.3.1**, Def6 and Swap70 characterise a novel type of GEF protein due to their unique domain organisation, i.e. an unusual N-terminal PH and C-terminal DH-like domain configuration (Gupta et al., 2003; Hotfilder et al., 1999; Mavrakis et al., 2004; **Figure 1.8**). Def6 has been demonstrated to be an upstream activator of Rho GTPases, including Rac1, Cdc42 (Goudevenou et al., 2011; Gupta et al., 2003). In particular, Def6 was shown to regulate cell shape, polarity, and movement through interacting with the actin cytoskeleton in several publications (Mavrakis et al., 2004; Oka et al., 2007; Samson et al., 2007).

Utilising zebrafish as a model system, Katerina Goudevenou and colleagues in the lab established the essential role of Def6a, the zebrafish homolog of mammalian Def6, in the control of CE cell movements during zebrafish embryogenesis (Goudevenou et al., 2011). Data from this thesis suggested that Swap70b is also necessary for CE cell movements during zebrafish gastrulation. In addition, comparing the phenotypes of Def6a and Swap70b individual knockdowns (Goudevenou, PhD thesis, 2010; Shuen, MRes thesis, 2010), it seemed obvious that *def6a* and *swap70b* morphants resemble each other to a great extent from the very beginning of gastrulation until late developmental stages (Goudevenou, PhD thesis, 2010; Shuen, MRes thesis, 2010), which is as expected considering their high similarity.

Nevertheless, according to the results obtained by Katerina Goudevenou and colleagues (Goudevenou et al., 2011), as well as conclusions from Chapter 4 and 5, Def6a and Swap70b not only transduce signals from different upstream Wnt ligands, but also regulate distinct downstream Rho GTPases, as RhoA could not rescue *def6a* morphants (Goudevenou et al., 2011), indicating that Swap70b and Def6a perform distinct functions in the non-canonical Wnt/PCP pathway, differentiating Wnt11 from Wnt5b signalling. Thus, *def6a* and *swap70b* MOs were injected separately or together to further dissect the interplay between these two closely related GEFs.

## 6.2 Results

### 6.2.1 Swap70b and Def6a partially rescued each other when expressed ectopically

Rescue experiments were firstly employed to determine whether Swap70b and Def6a can compensate for each other in the modulation of CE cell movements. Since 150 pg *GFP/swap70b* mRNA did not cause any abnormal

phenotype on its own, it was used in the attempt to restore CE defects induced by *def6a* MO.

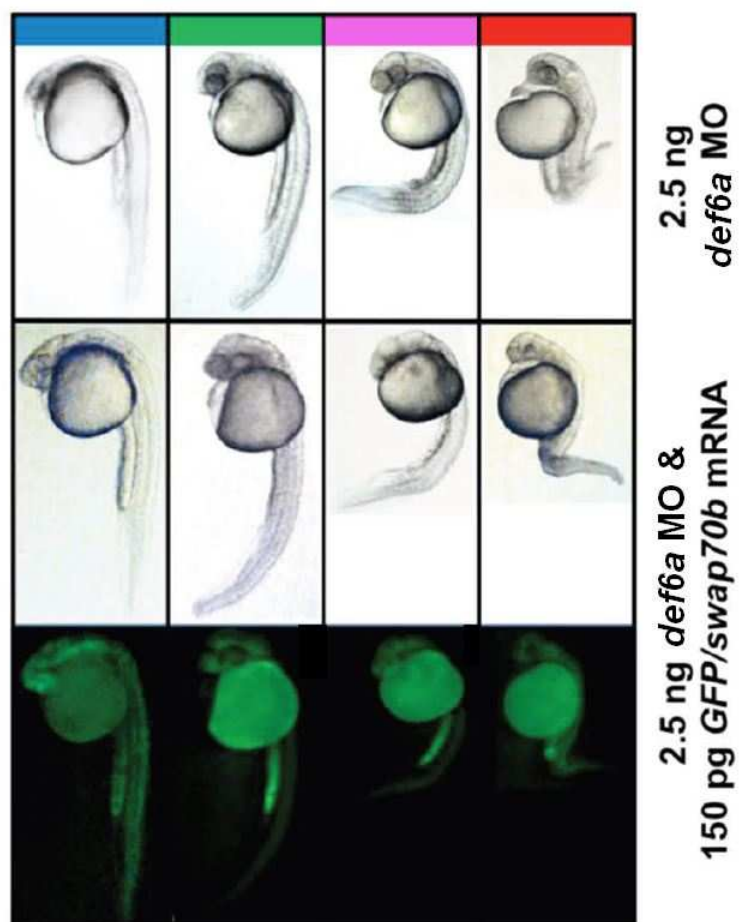
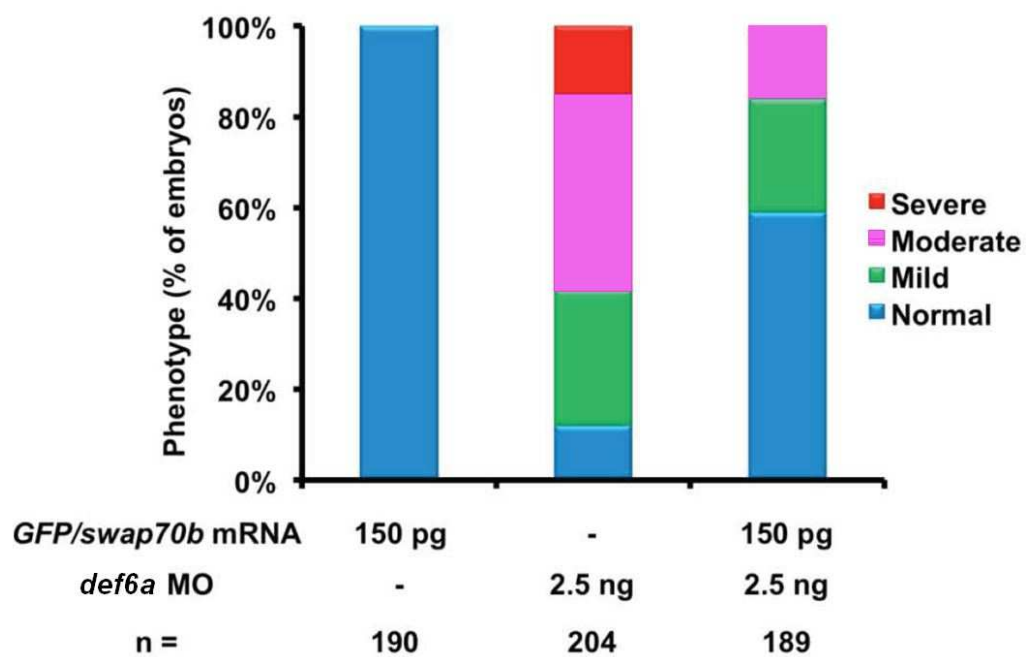
Def6a loss-of-function induced by 2.5 ng *def6a* MO led to the same phenotypes described in Katerina Goudevenou's thesis (Goudevenou, PhD thesis, 2010), such as malformed head, shortened body axis and curved tail at 24hpf, which is highly similar to *swap70b* morphants. According to the severity degree of these CE phenotypes, embryos injected with 2.5 ng *def6a* MO, 150 pg *GFP/swap70b* mRNA individually or together were separated into four groups at 24hpf (**Figure 6.1A**). Quantification made it apparent that Swap70b overexpression resulted in a robust rescue of *def6a* morphants (**Figure 6.1B**).

In comparison to embryos injected with 2.5 ng *def6a* MO alone, the percentage of embryos with severe or moderate defects declined from 15.2% (n=31) and 43.1% (n=88) to 0.5% (n=1) and 15.9% (n=30) in the group co-injected with *def6a* MO and *swap70b* mRNA. Although the percentage of embryos with mild defects decreased slightly from 29.9% (n=61) to 24.3% (n=46) in the co-injection group, the percentage of normal-looking embryos increased significantly from 11.8% (n=24) to 59.3% (n=112), indicating a partial but successful rescue (**Figure 6.1B**).

**Figure 6.1 Ectopic expression of GFP/Swap70b fusion protein rescued *def6a* morphants.**

(A) Embryos at 2-cell stage were injected with *GFP/swap70b* mRNA (150 pg), *def6a* MO (2.5 ng) alone, or *GFP/swap70b* mRNA (150 pg) and *def6a* MO (2.5 ng). All embryos at 24 hpf were grouped into normal (blue), mild (green), moderate (pink) and severe (red) according to their morphological phenotype. Representative images of embryos are shown. Each pair of panels in the bottom depicts identical embryos. Green fluorescence in yolk and yolk extension is due to auto-fluorescence (data not shown). (B) Quantification of the phenotypic analysis. Bar graphs show the percentage of embryos with normal, mild, moderate and severe phenotypes. Wild type embryos did not show any phenotypic alterations (data not shown). n: total number of embryos derived from at least three independent experiments.



**A****B**

Subsequently, the bud-stage embryos were also tested, using the same quantification method with combined probes *dlx3b* and *hgg1* that was described in section 3.2.2 (**Figure 3.3A, B, and G**). Embryos injected with 150 pg *GFP/swap70b* mRNA, or 2.5 ng *def6a* MO, or both, were stained with *dlx3b* and *hgg1*, in which CE phenotypes were assessed by measuring the widening of the *dlx3b* staining (**Figure 6.2**).

As shown in **Figure 6.2A**, the injection of 150 pg *GFP/swap70b* mRNA did not give rise to any phenotype, which is consistent with previous results in section 3.2.1 (**Figure 3.1; Figure 3.2**). The injection of 2.5 ng *def6a* MO resulted in a significant increase in the width of the neural plate (**Figure 6.2B, D**), which was essentially reversed by 150 pg *GFP/swap70b* mRNA (**Figure 6.2C, D**). Therefore, it can be concluded that the ectopic expression of GFP/Swap70b successfully rescued the CE defects mediated by *def6a* MO.

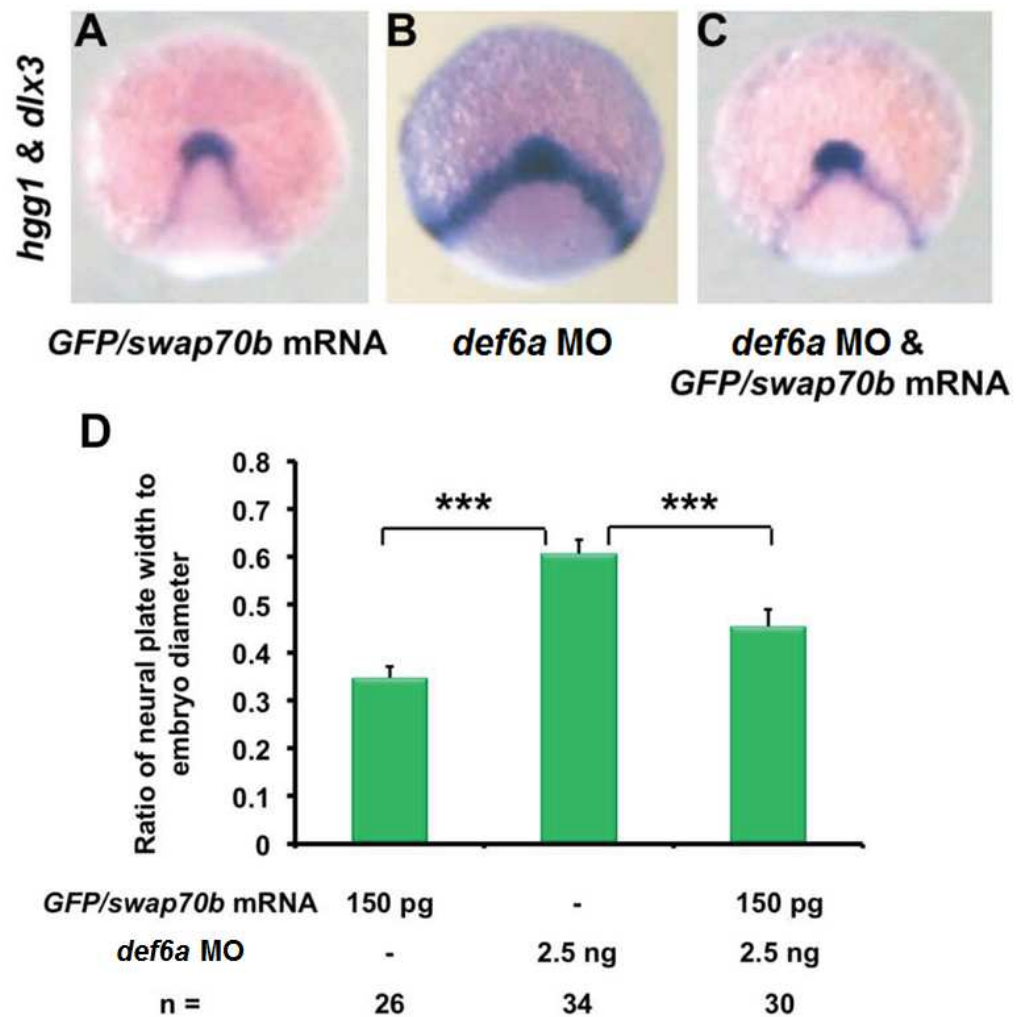


**Figure 6.2** *GFP/swap70b* mRNA successfully rescues *def6a* morphants at early developmental stage.

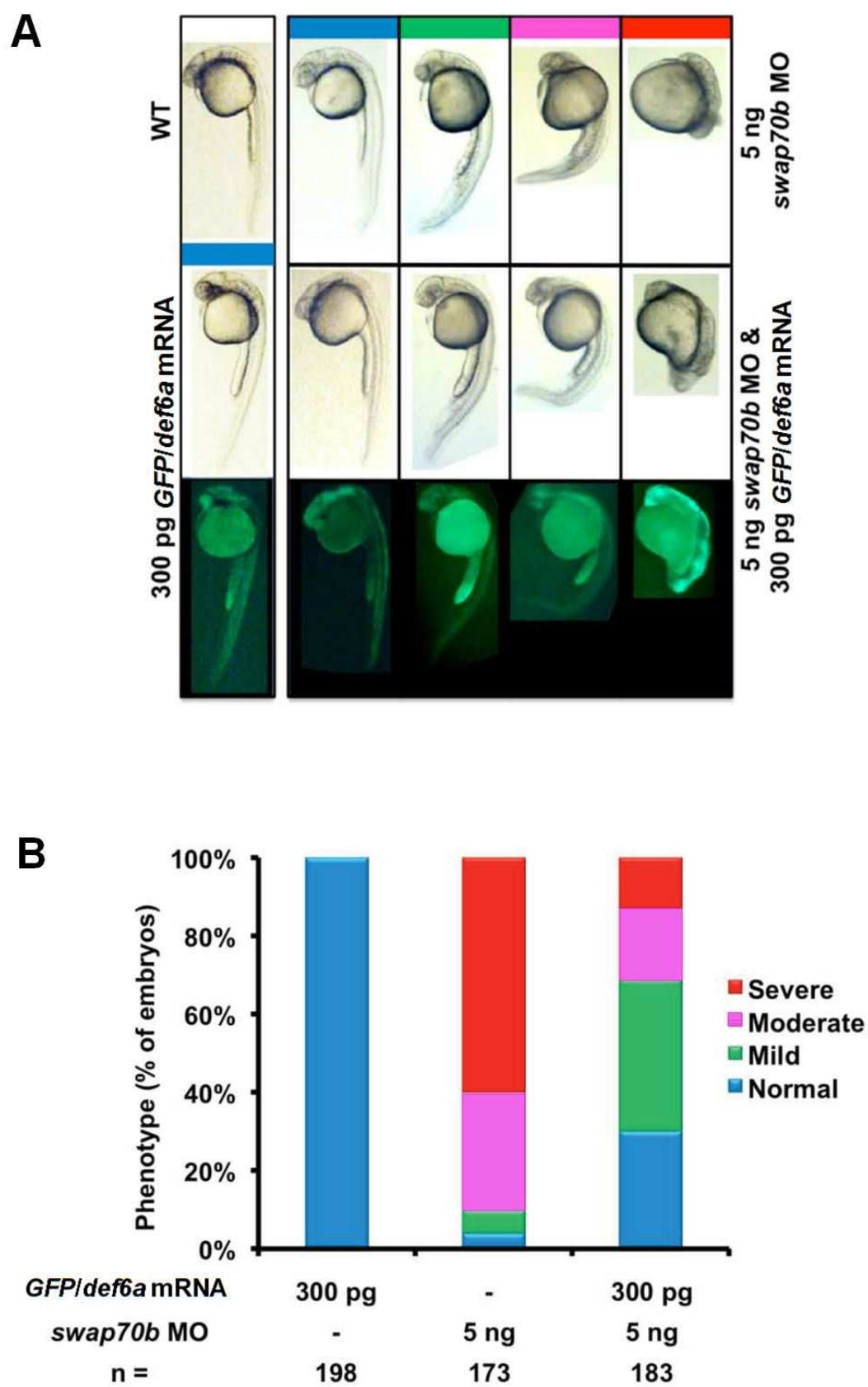
Embryos at 2-cell stage were injected with *GFP/swap70b* mRNA (150 pg) (A), *def6a* MO (2.5 ng) alone (B), or *GFP/swap70b* mRNA (150 pg) and *def6a* MO (2.5 ng) (C) and were stained at tail-bud stage with *hgg1* and *dlx3b* to evaluate CE using the same quantification method described in **Figure 3.3A, B, and G**. (D) Two-tailed Student's *t*-tests were used to determine statistical significance. \*\*\*:  $P < 0.001$ . Because embryos injected with 150 pg *GFP/swap70b* mRNA alone looked indistinguishable from wild type embryos (**Figure 3.3A, C**), the wild type control group is not presented in this figure.

Next the reciprocal experiment was also performed using the same approach, in which 300 pg *GFP/def6a* mRNA was employed in the attempt to restore the compromised CE cell movements induced by 5 ng *swap70b* MO.

Embryos were injected with 300 pg *GFP/def6a* mRNA, or 5 ng *swap70b* MO, or both, and grouped at 24 hpf using the same classification criteria for *swap70b* morphants specified in section 3.2.1 (**Figure 6.3A**). According to the quantification results in **Figure 6.3B**, embryos injected with 300 pg *GFP/def6a* mRNA alone did not exhibit any abnormal phenotype, which was consistent with previous data (Goudevenou, PhD thesis, 2010). In addition, it can be clearly seen that this amount was sufficient to rescue the impaired CE cell movements resulting from *Swap70b* loss-of-function. Compared to embryos injected with 5 ng *swap70b* MO only, the population with severe and moderate CE phenotypes decreased significantly from 60.1% (n=104) and 30.1% (n=52) to 13.1% (n=24) and 18.0% (n=33) separately. On the contrary, the population with normal phenotype and mild CE defects rose from 4.0% (n=7) and 5.8% (n=10) to 30.1% (n=55) and 38.8% (n=71), which implied a partial but robust rescue (**Figure 6.3B**).

**Figure 6.3 Ectopic expression of GFP/Def6a fusion protein rescues *swap70b* morphants.**

(A) Embryos at 2-cell stage were injected with *GFP/def6a* mRNA (300 pg), *swap70b* MO (5 ng) alone, or *GFP/def6a* mRNA (300 pg) and *swap70b* MO (5 ng). All embryos at 24 hpf were grouped into normal (blue), mild (green), moderate (pink) and severe (red) according to their morphological phenotype. Representative images of embryos are shown. Each panel of the bottom two rows depict identical embryos. Green fluorescence in yolk and yolk extension is due to auto-fluorescence (data not shown). (B) Quantification of the phenotypic analysis. Bar graphs show the percentage of embryos with normal, mild, moderate and severe phenotypes. Wild type embryos did not show any phenotypic alterations (data not shown). n: total number of embryos derived from at least three independent experiments.



*In situ* hybridisation carried out in bud-stage embryos further confirmed the rescue effects of Def6a on the loss of Swap70b function. As shown in **Figure 6.4A**, embryos injected with 300 pg *GFP/def6a* mRNA alone did not show any phenotype. While the injection of 5 ng *swap70b* MO alone led to a great increase in the neural plate width of *swap70b* morphants (as indicated by the expression domains of *hgg1* and *dlx3b*; **Figure 6.4B, D**), co-injection of 5 ng *swap70b* MO and 300 pg *GFP/def6a* mRNA resulted in a significant reduction (**Figure 6.4C, D**).

Taken together, Swap70b and Def6a can partially compensate for each other in the regulation of CE cell movements when expressed ectopically, which is not surprising given their high similarity in structure. Therefore, it can be presumed that they are functionally largely redundant in the non-canonical Wnt/PCP pathway.

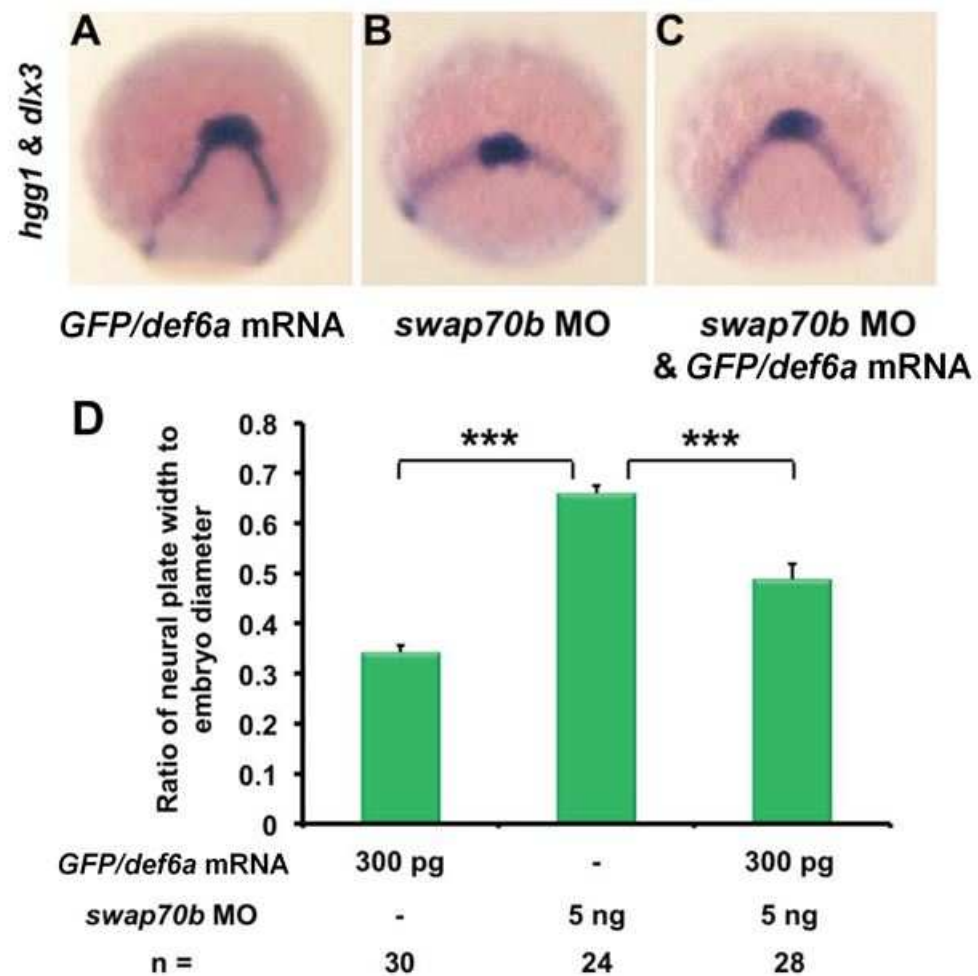


**Figure 6.4** *GFP/def6a* mRNA successfully rescues *swap70b* morphants at early developmental stage.

Embryos at 2-cell stage were injected with *GFP/def6a* mRNA (300 pg) (A), *swap70b* MO (5 ng) alone (B), or *GFP/def6a* mRNA (300 pg) and *swap70b* MO (5 ng) (C) and were stained at tail-bud stage with *hgg1* and *dlx3b* to evaluate CE using the same quantification method described in **Figure 3.3A, B, and G**. (D) Two-tailed Student's *t*-tests were used to determine statistical significance. \*\*\*:  $P < 0.001$ . Because embryos injected with 300 pg *GFP/def6a* mRNA alone looked indistinguishable from wild type embryos (**Figure 3.3A, C**), the wild type control group is not presented in this figure.



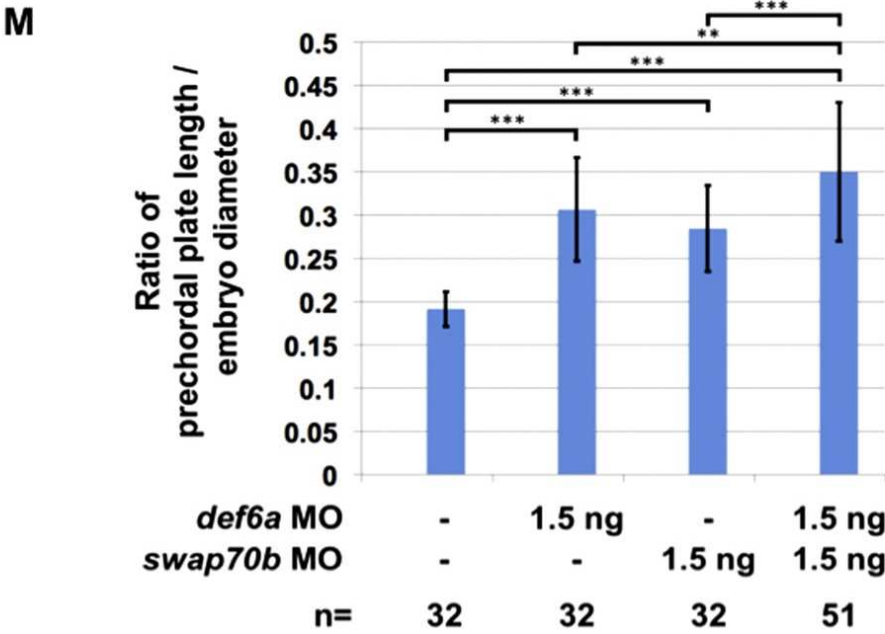
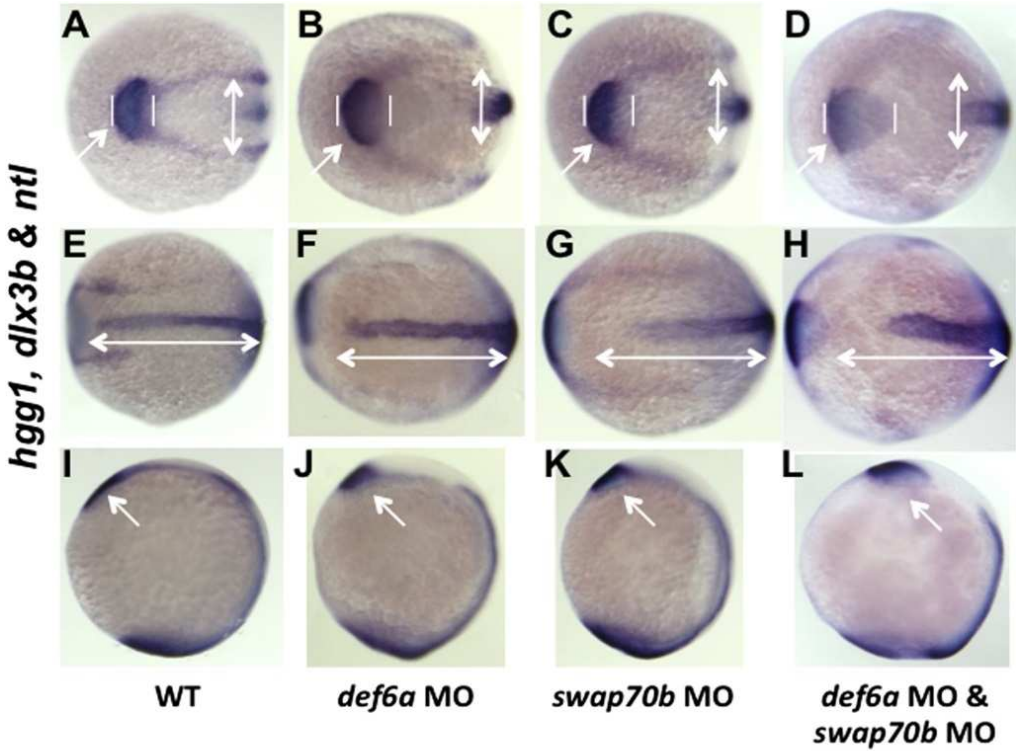
## 6.2.2 Swap70b and Def6a knockdown results in an additive effect on CE cell movements

While Swap70b and Def6a appear to perform largely redundant functions, they have been demonstrated to link to distinct upstream Wnt ligands and downstream Rho GTPases, thereby being supposed to play different roles in the non-canonical Wnt/PCP pathway (Goudevenou et al., 2011 and this thesis). Therefore, a comparison was made between the single and double knockdown of Swap70b and Def6a to further explore their relationship.

As shown in **Figure 6.5**, the position and shape of the polster/prechordal plate (labelled by *hgg1*) that was altered in *def6a* as well as *swap70b* morphants (**Figure 6.5B** and **C** compared to **A**) was more severely affected in *def6a/swap70b* double mutants (**Figure 6.5D** compared to **B** and **C**). The ratio of prechordal plate length to embryo diameter was established in order to reveal whether these differences were statistically significant, (**Figure 6.5M**). While wild type embryos (n=32) showed a ratio of  $0.19 \pm 0.02$ , *def6a* morphants (n=32) exhibited a ratio of  $0.31 \pm 0.06$  and *swap70b* morphants (n=32) a ratio of  $0.29 \pm 0.05$ , which are both statistically different from wild type ( $p < 0.001$ ). Similarly, double mutant morphants (n=51) showed a ratio of  $0.35 \pm 0.08$  that was significantly different from *def6a* ( $p < 0.01$ ) and *swap70b* ( $p < 0.001$ ) morphants (**Figure 6.5M**). In addition, the body axis indicated by the length of the notochord was further reduced in double mutant morphants (**Figure 6.5H** compared to **F** and **G**) than in *def6a* and *swap70b* morphants (**Figure 6.5F** and **G** compared to **E**). Together, co-injection of *swap70b* and *def6a* MOs resulted in an additive influence on CE cell movements, supporting the hypothesis that they have different functions in the non-canonical Wnt/PCP pathway. Alternatively, this might support the idea that one protein can compensate for the loss of the other.

**Figure 6.5 Def6a and Swap70b have partially redundant functions in CE cell movement.**

*In situ* hybridisation with *hgg1*, *dlx3b* and *ntl* as indicated comparing wild type embryos (**A**, **E**, **I**) with either *def6a* (**B**, **F**, **J**), *swap70b* (**C**, **G**, **K**) single morphants or *def6a/swap70b* double mutants (**D**, **H**, **L**). White double-headed arrows in **E–H** are given as reference to the wild type control. Arrows and vertical lines mark the *hgg1* expression domain indicating the altered position and shape of the polster/prechordal plate in *def6a* (**B**, **J**), *swap70b* (**C**, **K**) and *def6a/swap70b* (**D**, **L**) morphants compared to wild type (**A**, **I**). (**M**) Quantification of the altered shape of the polster/prechordal plate. The ratio of prechordal plate length to embryo diameter is shown for wild type embryos ( $0.19 \pm 0.02$ ), *def6a* morphants ( $0.31 \pm 0.06$ ), *swap70b* morphants ( $0.29 \pm 0.05$ ) and double mutant morphants ( $0.35 \pm 0.08$ ). Two-tailed Student's *t*-tests were used to determine statistical significance. \*\*\*:  $P < 0.001$ . \*\*:  $P < 0.01$ . Number of embryos (*n*) in each group analysed as indicated.



## 6.3 Discussion

### 6.3.1 Swap70b and Def6a play partially redundant roles in the regulation of CE cell movements

As shown in section 6.2.1, the ectopic expression of Swap70b can rescue the aberrant CE cell movements mediated by the abrogation of Def6a, and vice versa, providing clear evidence for a partial functional redundancy between these two GEF proteins. In terms of the underlying reason, the most possible one is that they share strong similarity in three dimensional structure (**Figure 6.6A, B**), which is dependent on amino acid sequence (**Figure 1.8**) and directly determines their functions.

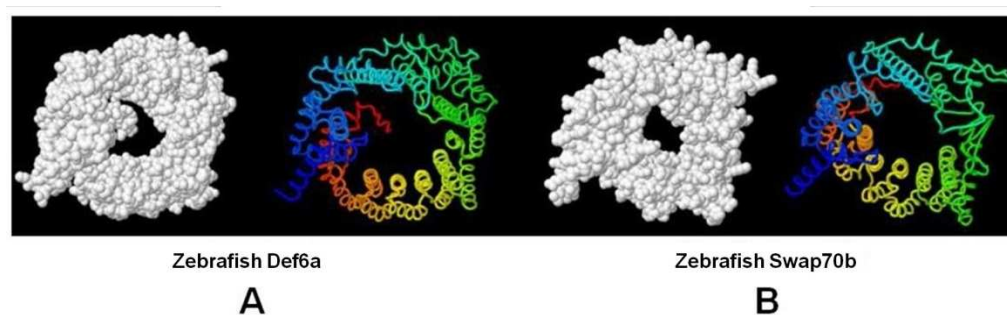


**Figure 6.6 Three dimensional structure predictions of Def6a and Swap70b**

Full length amino acid sequences of Def6a and Swap70b were submitted to I-TASSER to generate predicted 3D structure models. (A) Predicted 3D structure of Def6a. (B) Predicted 3D structure of Swap70b. N-terminus is in blue and C-terminus is in red. Adapted from (Shuen, MRes thesis, 2010)

### 6.3.2 Swap70b and Def6a execute distinct functions in the non-canonical Wnt/PCP pathway

Although Swap70b and Def6a display some functional redundancy in modulating CE cell movements, they appear to link different upstream Wnt ligands and downstream effectors (Goudevenou et al., 2011; Shuen, MRes thesis, 2010 and this thesis). To further investigate their relationship, *swap70b* and *def6a* MOs were injected separately or mixed, followed by the assessment of CE phenotype through the migration of polster/prechordal plate and the extension of notochord (**Figure 6.5**).

Interestingly, the co-injection of *swap70b* and *def6a* MOs showed a strongly enhanced CE phenotype, reminiscent of the *slb;ppt* double mutant phenotype which is much more severe than that of each single mutant (Kilian et al., 2003). Moreover, the double knockdown of *wnt5b* and *swap70b* also led to an additive effect of each single knockdown (**Figure 4.5**), further confirming that Swap70b and Def6a perform non-redundant functions in the non-canonical Wnt/PCP pathway, delineating Wnt11 from Wnt5b signalling.

Taken together, Swap70b and Def6a have both overlapping and non-overlapping roles in the modulation of CE cell movements. This may explain the previous finding that despite their functional diversification, Wnt11 and Wnt5b act redundantly to regulate gastrulation particularly in the anterior region (Kilian et al., 2003).

## **Chapter 7**

# **Essential role for SYK in zebrafish gastrulation via Swap70b**

### **7.1 Introduction**

As mentioned in section 1.6, SYK has been demonstrated to be an upstream regulator of Swap70, which phosphorylates Swap70 in B cells migration (Pearce et al., 2011). In addition, SYK was found to play an important role in the regulation of cytoskeleton through its association with Vav protein, which is a GEF for Rho GTPases (Bertagnolo et al., 2001; Deckert et al., 1996; Zou et al., 2010). Considering the close relationship between SYK and Swap70, coupled with the Wnt11/Swap70b signalling model proposed in this thesis, it was intriguing to investigate if SYK exerts its cytoskeleton-organising effect in zebrafish gastrulation through a similar mechanism. Therefore rescue experiments were carried out in this chapter to examine the possible relationship between SYK and Swap70b during zebrafish gastrulation.

It has been established that SYK plays necessary roles in cell adhesion through various integrins, which use similar mechanisms to classical immunoreceptors described in section 1.6 (Mocsai et al., 2010). In osteoclasts, for example, SYK is initially recruited by the complex formed by  $\alpha V\beta 3$  integrin and another tyrosine kinase c-Src. This event is mediated by the interaction between SYK and the c-Src-phosphorylated tyrosines of two ITAM proteins, Dap12 and FcR $\gamma$ . Meanwhile, SYK is also phosphorylated by c-Src and becomes activated.

SYK, in turn, activates Vav3 that serves as a GEF for Rho GTPases. Thus,  $\alpha\text{v}\beta 3$  activation recruits a signalling complex consisting of c-Src, SYK, ITAM proteins, Vav3, and Rho GTPases, organising the osteoclast cytoskeleton (Zou et al., 2010).

Utilising zebrafish as an *in vivo* system, a recent study demonstrated zebrafish SYK and Zap-70 to play unexpectedly redundant roles in promoting the migration of angioblasts to form both blood vascular and lymphatic vascular systems (Christie et al., 2010). This is the first time that the function of SYK has been studied in zebrafish, particularly the vascular development process. In this research, the gene sequence of SYK in zebrafish was identified from the genomic database. Similar to mammals, zebrafish SYK contains two N-terminal SH2 domains and a C-terminal tyrosine kinase domain (Christie et al., 2010). For functional analysis of SYK and Zap-70, MO mediated gene knockdown was used. Based on the efficiency and specificity of the MOs that had been evaluated in this research, one splice MO, *syk*<sup>e2i2</sup> (5'-AGTGAAGAAGACTTACAGAAATTTG-3') MO that targets exon 2-intron 2 (e2i2) of *syk* was employed in this thesis. This MO was abbreviated to *syk* MO in this thesis.

## 7.2 Results

### 7.2.1 *Syk* morphants display similar phenotypes to *swap70b* morphants

The amount of 5ng *syk* MO was chosen because it gave an obvious gastrulation phenotype at 24hpf, and a comparison was made between *syk* morphants and *swap70b* morphants at 24hpf. As shown in Figure 7.1, embryos injected with *syk* MO and *swap70b* MO exhibited strikingly similar phenotypes, both indicating disruptive gastrulation movements. Compared

with wild type controls (**Figure 7.1A**), *syk* morphants and *swap70b* morphants both showed obviously bent and shortened trunks (**Figure 7.1B, C**). The only difference seemed to exist in the somite structures (**Figure 7.1B, C**); the somites of *syk* morphants appeared more organised and more of a normal chevron shape than those of *swap70b* morphants (**Figure 7.1B, C** red arrows), suggesting that SYK loss-of-function has little influence on the development of somites.

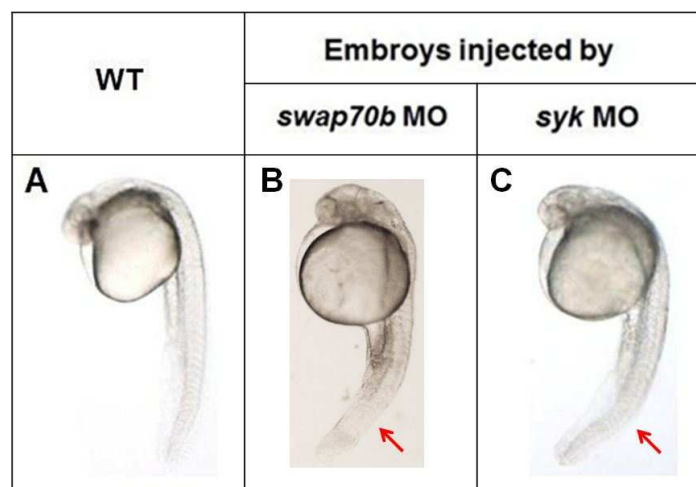


**Figure 7.1** *Syk* morphants resemble *swap70b* morphants at 24hpf.

Zebrafish embryos were un-injected (**A**), injected with 5ng *swap70b* MO (**B**) or 5ng *syk* MO (**C**), and allowed to grow until 24hpf. Red arrows indicate the somite structures of representative embryos in each group.



## 7.2.2 *Swap70b* enhances gastrulation defects in *syk* morphants

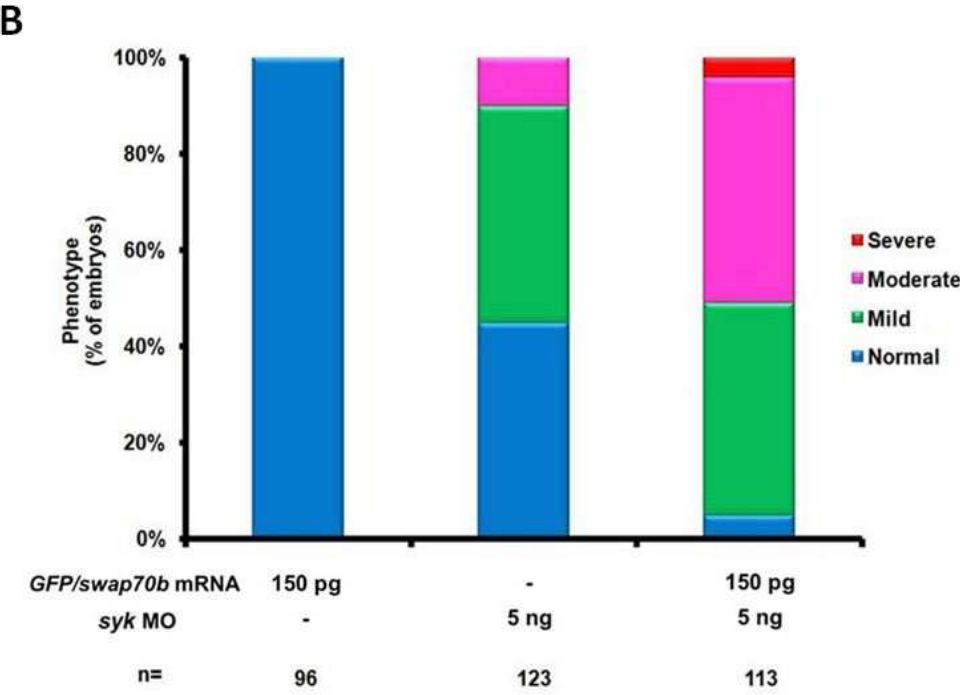
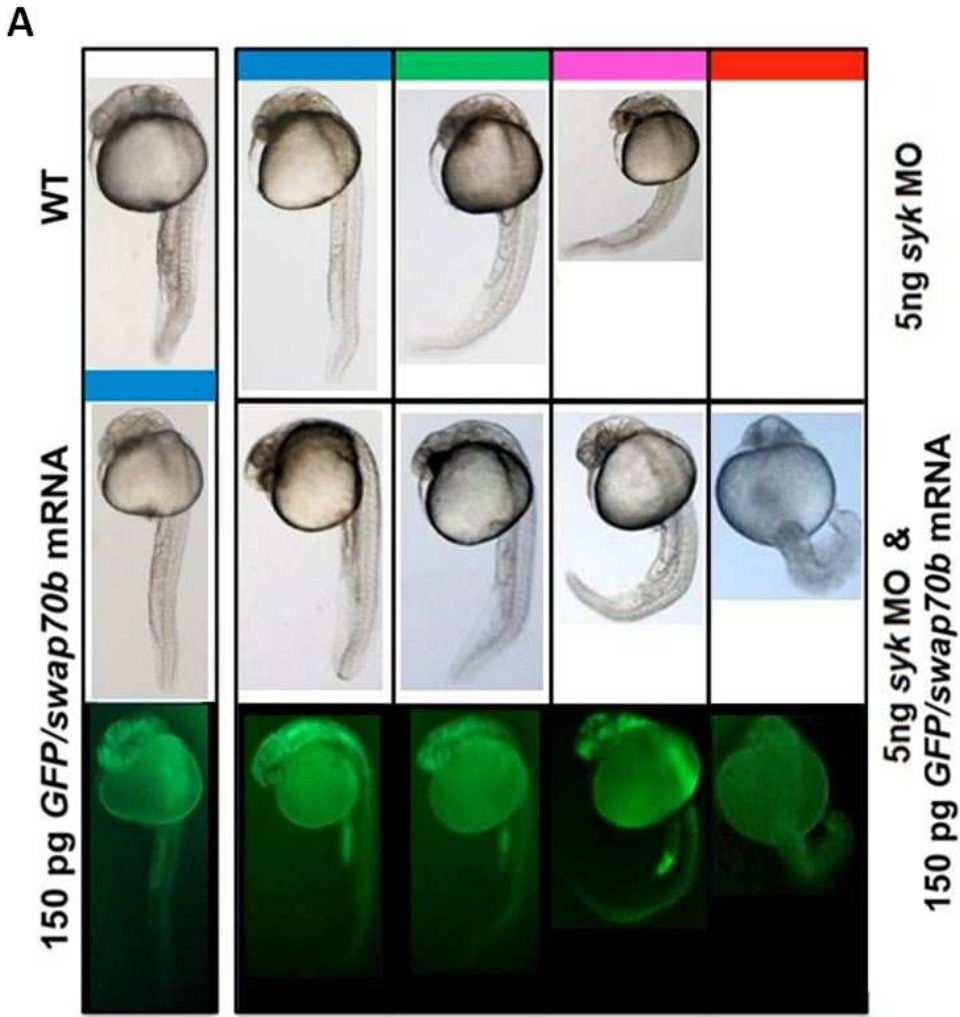
Given that *syk* and *swap70b* knockdowns produced similar phenotypes associated with gastrulation defectiveness, rescue experiments were then carried out attempting to rescue *syk* MO-mediated gastrulation defects with *swap70b* mRNA. Since the injection of 150pg GFP/*swap70* mRNA by itself was confirmed to not generate any obvious defects during zebrafish development, this amount was chosen for the rescue experiment.

As described above, *syk* morphants phenocopy *swap70b* morphants except that their somites appear more orderly. Therefore, the classification criteria used in *syk* morphants are similar to the one used in *swap70b* morphants, i.e. the bending degree and length of embryonic body, and the following quantification method was the same. All embryos injected with 150pg GFP/*swap70b* mRNA or 5ng *syk* MO alone, or both, were classified into four groups, with the un-injected embryos as the standard of the normal group (**Figure 7.2A**). Subsequently, the mild, moderate and severe groups were judged according to the severity extent of gastrulation defects, particularly the bending extent of trunk and length of body axis (**Figure 7.2A**).

Based on the quantification, it seems obvious that the addition of GFP/*swap70b* mRNA worsened gastrulation defects induced by *syk* MO. Consistent with previous experiments, none of embryos injected with 150pg GFP/*swap70b* mRNA displayed any obvious defects. In the group of embryos injected with 5ng *syk* MO, the percentage of embryos with normal phenotype was 44.7% (n=55), which decreased to only 4.4% (n=5) in the co-injection group. Embryos with mild phenotype remained almost unchanged, taking up 45.5% (n=56) and 45.1% (n=51) in the 5ng *swap70b* MO injected group and the co-injection group respectively, whereas the population with moderate phenotype increased dramatically from 9.8% (n=12) to 46.0% (n=52).

**Figure 7.2 Swap70b worsens gastrulation defects in *syk* morphants.**

(A) Zebrafish embryos were un-injected (WT), injected with 150pg GFP/*swap70b* mRNA, or 5ng *syk* MO, or co-injected with 5ng *syk* MO and 150pg GFP/*swap70b* mRNA, and then were grouped into normal (blue), mild (green), moderate (pink) and severe (red) according to their phenotype at 24hpf. Representative images of embryos in each group are shown. (B) Bar graph shows the percentage of embryos with normal, mild, moderate and severe phenotypes. Wild type embryos did not show any phenotypic alterations (data not shown). n, total number of embryos in at least three independent experiments.



Moreover, in embryos injected with 5ng *syk* MO, none with severe phenotype were observed, whereas after the co-injection of GFP/*swap70b* mRNA, there were 4.4% (n=5) embryos showing severe gastrulation defects, especially, with significantly shorter and distorted trunk and misshaped head (**Figure 7.2A, B**).

## 7.3 Discussion

As described in section 1.6, SYK has been shown to directly phosphorylate Swap70b, which is a key event during B cell polarisation and regulation of B cell migration *in vivo* (Pearce et al., 2011). Given such a close relationship between SYK and Swap70b, coupled with the large-scale cell migration occurring in CE cell movements, in this chapter, SYK was depleted in zebrafish to determine whether it plays a role in gastrulating zebrafish.

Excitingly, SYK-deficient zebrafish displayed obvious gastrulation impairment, such as decreased body length and curved trunk, which resembled *swap70b* morphants at 24hpf. This spectrum of defects was not reversed but significantly exaggerated by co-expression of *swap70b* mRNA. This phenotype is reminiscent of RacV12, a constitutively active Rac, which worsened the gastrulation defects caused by Fyn/Yes knockdown in zebrafish (Jopling et al., 2005). In addition, it was demonstrated that Fyn/Yes and non-canonical Wnt signalling converge on RhoA in gastrulation cell movements (Jopling et al., 2005). Coupled with the conclusion obtained from research on SYK and Swap70 in other organic systems, it can be speculated that through a mechanism likely to be direct phosphorylation, SYK negatively regulates Swap70b during zebrafish gastrulation. If this is the case, the knockdown of *syk* would result in more active Swap70b, which would be expected to generate phenotypes equivalent to that of *swap70b* overexpression, and finally the addition of *swap70b* mRNA would just worsen these defects.

## **Chapter 8    Conclusions & Prospects**

This thesis establishes the crucial role of Swap70b in modulating convergence and extension (CE) cell movements during zebrafish gastrulation, and elucidates the underlying mechanism. In particular, Swap70b is demonstrated to regulate CE cell movements through acting downstream of Wnt11 in the non-canonical Wnt/PCP pathway. In addition, Swap70b is also shown to perform both overlapping and distinct functions with Def6a.

### **8.1 Conclusions**

#### **8.1.1 Swap70b is essential for normal CE cell movements during zebrafish gastrulation**

During vertebrate gastrulation, a series of morphogenetic cell movements give rise to the three germ layers and create the basic body plan of the embryo (Warga et al., 1990). One such movements is convergence and extension (CE) cell movements, in which mesoderm and ectoderm undergo cell intercalations along the medial-lateral axis, narrowing the tissues dorsalwards (convergence) and extending them along the anterior-posterior axis (extension) (Concha et al., 1998). While rapid progress has been made in the understanding of the cellular behaviour underlying this process, relatively less is known about the corresponding molecular mechanisms.

Recently, our lab has reported that Def6a is required for CE cell movements during zebrafish gastrulation (Goudevenou et al., 2011). Preliminary research performed by Wai Ho Shuen suggested an important role of Swap70b, the

closely-related GEF protein of Def6a, in CE regulation (Shuen, MRes thesis, 2010). This thesis continued this investigation by carrying out experiments in both late and early stage zebrafish embryos to provide more robust evidence.

Phenotypic analysis of 24 hpf embryos showed that Swap70b loss-of-function led to gastrulation defects reflected by reduced body length and curly tail. Subsequently, the early stage of gastrulation, i.e. the bud stage and one somite stage embryos were tested, firmly supporting that Swap70b plays a critical role during CE cell movements. In particular, the abrogation of Swap70b resulted in the failure of embryos to extend properly around the yolk, the inhibition of axial mesendodermal cells migration indicated by the convergence of neural plate cells, and the extension of notochord. Next, the paraxial mesoderm at early and late stages of gastrulation were assessed, using the probe *myoD*. In both cases the two stripes of adaxial cells were medio-laterally expanded and anterior-posteriorly shortened in *swap70b* morphants. Collectively, it has been established that Swap70b is required for normal CE cell movements during the course of zebrafish gastrulation. Importantly, the following examination of cell fate specification in *swap70b* morphants revealed that Swap70b has no substantial influence on the determination of cell fate. This phenotype is reminiscent of members of the non-canonical Wnt/PCP pathway, and therefore raised the possibility that Swap70b is also involved in this pathway, like its close-relative Def6a.

### **8.1.2 Proposed model of Swap70b signalling in regulating CE cell movements**

The non-canonical Wnt/PCP pathway was originally discovered to mediate the establishment of cell polarity in the plane of epithelia in *Drosophila*. Large-scale mutagenesis screens in zebrafish revealed its essential function in regulating CE and other cell migration during gastrulation (Roszko et al., 2009; Wang et al., 2006; Ybot-Gonzalez, et al., 2007; Yen et al., 2009).

Zebrafish embryos carrying mutations in the non-canonical Wnt pathway components displayed a shorter and broader body axis at the end of gastrulation indicative of CE movement defects yet with normal cell fate specification (Adler, 2002; Driever et al., 1996; Haffter et al., 1996; Hammerschmidt et al., 1996; Heisenberg et al., 1997; Solnica-Krezel et al., 1996). Two of these mutants named *silberblick* (*slb*) and *pipetail* (*ppt*) were identified as alleles of *wnt11* and *wnt5b* (previous name *wnt5a*, renamed after Stoick-Cooper et al. (2007)), respectively (Heisenberg et al., 2000; Rauch et al., 1997).

In *Xenopus*, Wnt11-Fz7 signalling leads to the formation of a complex consisting of Dsh, the adaptor protein Daam1, RhoA and WGEF (Habas et al., 2001; Tanegashima et al., 2008). Daam1 lacks GEF activity (Habas et al., 2001), but WGEF was identified as a Rho-GEF responsible to activate RhoA during this process (Tanegashima et al., 2008). In zebrafish, overexpression of either RhoA or its downstream effector Rok2 that modulates actin cytoskeleton rearrangements and CE cell movements (Gray et al., 2011; Roszko et al., 2009; Tada et al., 2009), partially restores the *wnt11/sl*b mutant phenotype (Jopling et al., 2005; Marlow et al., 2002; Zhu et al., 2006). However, it is yet unknown which GEF is required for RhoA activation. In this thesis, rescue experiments were carried out in both early and late stage embryos, showing that Swap70b acts downstream of Wnt11 in the control of CE cell movements. It remains to be seen whether Swap70b acts upstream of RhoA.

The relationship between Swap70b and Def6a was also explored. Firstly rescue experiments were carried out, which showed that Swap70b overexpression substantially rescued *def6a* morphants, and vice versa. Therefore it can be speculated that these two GEF proteins execute overlapping functions in the non-canonical Wnt/PCP pathway. This possibly explains the synergistic effect between Wnt11 and Def6a observed previously (Goudevenou et al., 2011). In particular, Def6a might be able to perform part of the functions of Swap70b. Furthermore, in the following experiments

where *swap70b* and *def6a* MOs were injected individually or in combination, the double mutant morphants exhibited a far more severe CE phenotype than each single mutant morphant. This is reminiscent of the data by Kilian et al. (2003) showing that Ppt-Wnt5b/Slb-Wnt11 double mutants exhibited an additive CE effect of each single mutant, which suggest that Slb/Wnt11 and Ppt/Wnt5b act redundantly in the non-canonical Wnt/PCP pathway to modulate morphogenetic movements during the course of gastrulation (Kilian et al., 2003). This is reasonable given the previous findings that Swap70b and Def6a mediate different upstream signalling pathways from these two Wnt ligands, and further support that they execute partially overlapping functions in CE cell movements.

Taken together, a model of Swap70b signalling in the regulation of CE cell movements can be established as shown in **Figure 8.1**, which makes the picture of the Wnt signalling network more complete.



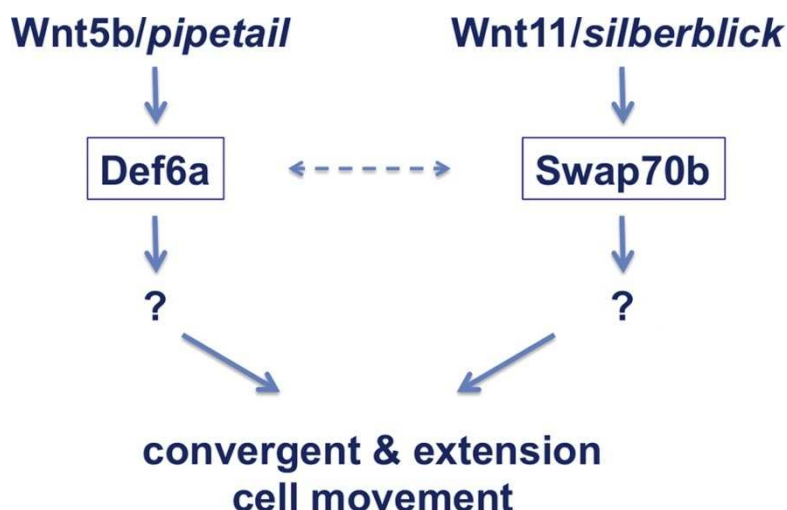


**Figure 8.1 A proposed model of Swap70b signalling**

Based on all the data that have been obtained, a model of Swap70b signalling was proposed. During the process of CE cell movements, Def6a and Swap70b act downstream of Wnt5b and Wnt11 respectively, which can compensate for each other. In addition, the downstream effectors of Swap70b and Def6a remain to be uncovered.

## 8.2 Prospects

While this thesis has shed some light on the role of Swap70b in zebrafish embryogenesis as well as the underlying molecular mechanisms, there are still some fascinating topics to be explored.

### 8.2.1 Additional potential functions of Swap70b in zebrafish development

During the functional investigation of Swap70b, other phenotypes also came to notice besides CE, implying the involvement of Swap70b in various developmental processes.

As shown in **Figure 1.14** and **Figure 1.15**, Swap70b is maternally expressed during zebrafish embryogenesis, and AUG MO that can interfere with maternal Swap70b indeed caused obvious gastrulation defects (**Figure 1.18**). Therefore, Swap70b may play unknown roles in earlier developmental processes. Because maternal factors inducing mesoderm were found to simultaneously initiate CE cell movements in *Xenopus*, it has been proposed that the early steps of pattern formation and gastrulation may be coupled and share elements of the same genetic control system (Smith et al., 1992). Although *swap70b* knockdown does not affect cell fate specification in gastrulating zebrafish embryos (**Figure 3.5**), it cannot be excluded that it may contribute to the early procedures of pattern formation.

Wai Ho Shuen noticed in his research that Swap70b gain and loss-of-function both led to abnormal numbers of ear otoliths in the otic vesicles, suggesting a possible implication of Swap70b in otolith development (Shuen, MRes thesis, 2010). This unanticipated phenotype was reminiscent of another zebrafish Rho GEF, *Arhgef11*, which was demonstrated to be essential for proper development of otoliths. Interestingly, overexpression of either *Arhgef11* or its human homolog in zebrafish led to disturbed gastrulation movements. Similarly, its fruit fly homolog, *RhoGEF2* was proved to be required during gastrulation for cell shape changes (Panizzi et al., 2007). Considering that GEF proteins can modulate cell polarisation via downstream Rho GTPases (Garcia et al., 2006), it can be hypothesised that Swap70b may be involved in the formation of cilia, and thus play an important role in the development of cells within this structure.

## **8.2.2 In-depth analysis of mechanisms underlying Swap70b function**

The results presented in this thesis suggest that Swap70b is a component of the non-canonical Wnt/PCP pathway downstream of Wnt11 signalling. The

downstream effectors of Swap70b in this pathway need to be explored through rescue experiments, particularly Rho GTPases. Moreover, the role of Swap70b in CE cell movements, as well as the underlying mechanism, can also be explored by cell tracing experiments in the future when proper materials are available (Pan et al., 2013).

In addition, biochemical assays must be carried out to further explore the mechanism of Swap70b's function. In particular, the probable interactions between Swap70b and the members of the non-canonical Wnt/PCP pathway, such as Dsh and Daam1, need be examined through co-IP or GST-pulldown experiments (Tanegashima et al., 2008). Cell biology experiments should also be carried out to examine the localisation of Swap70b during CE cell movements. As detailed in section **1.4.1**, Swap70 has a nuclear exit signal (NES) and three nuclear localisation signals (NLSs), which enable it to shuttle between the nucleus and the cytosol to execute multiple functions. In particular, Swap70 accumulates at the cell membrane to promote membrane ruffling (Shinohara et al., 2002), moves to the nucleus to influence B cell switching (Borggreffe et al., 1998), and localises to the cytoplasm in most cells during migration of neural precursors (Takada et al., 2011). Therefore, the subcellular positioning of Swap70 in gastrulating embryos can be investigated in order to better understand the mechanisms of its action.

As shown in **Figure 1.10**, Swap70 consists of a unique combination of amino acid motifs and domains. Thus, the structural basis of Swap70b's functional effects and subcellular localisation in CE cell movements can be investigated through the constructs containing different functional regions of Swap70b, using biochemical and cell biology techniques, respectively.

### 8.2.3 The potential role of SYK in the regulation of CE cell movements

As introduced in section 1.6, mammalian SYK has been reported to phosphorylate Swap70 at tyrosine 517, resulting in the inhibition of its binding to F-actin, which is required for regulating B cell migration (Pearce et al., 2011). Subsequent research in zebrafish revealed its ubiquitous expression throughout zebrafish embryogenesis, as well as its unexpected essential role in promoting the migration of angioblasts during vascular growth (Christie et al., 2010). It seems thereby SYK is involved in the movements of various types of cells, and of its downstream effectors is Swap70b that directly controls cytoskeletal rearrangements through activating Rho GTPases (Pearce et al., 2011). Hence, as presented in Chapter 7 in this thesis, some preliminary analysis was performed to investigate SYK's possible function, perhaps related to Swap70b, in zebrafish gastrulation.

Interestingly, the knockdown of SYK led to phenotypes associated with impaired gastrulation movements that resembled Swap70b loss-of-function. It was therefore assumed that SYK might act upstream of Swap70b to modulate zebrafish gastrulation. However, in the following rescue experiment, the injection of 150pg *swap70b* mRNA worsened the gastrulation defects in *syk* morphants (**Figure 7.2**). There might be two possibilities to interpret this result: 1) SYK negatively regulates Swap70b in this process, for which the deletion of *syk* is equivalent to the overexpression of Swap70b. 2) The amount of 150pg *swap70b* mRNA is relatively too high to get a rescue effect, and therefore it is worth trying a decreasing amount of *swap70b* mRNA to repeat this experiment.

In addition, as described in section 3.2.2 and 3.2.3, *in situ* hybridisation with probes used to assess CE cell movements and cell fate specification can be carried out to determine if SYK is required for CE cell movements. Next whether SYK functions directly in the non-canonical Wnt/PCP pathway, or

indirectly by influencing *Swap70b*, will also be interesting to investigate through rescue experiment, i.e. the separate and co-injection of *syk* mRNA and the MOs of Wnt ligands, as well as synergy experiment, i.e. the separate and co-injection of *syk* MO and *wnt11* or *wnt5b* MO.

Similarly, the inducible T-cell kinase (*Itk*), a tyrosine kinase that has been demonstrated to phosphorylate mammalian Def6 (Hey et al., 2012), can also be tested to determine whether it is implicated in the regulation of zebrafish gastrulation, particularly CE cell movements.

## References

- Adler, P. N. "Planar Signaling and Morphogenesis in *Drosophila*." *Dev Cell* 2, no. 5 (2002): 525-35.
- Babb, S. G. and J. A. Marrs. "E-Cadherin Regulates Cell Movements and Tissue Formation in Early Zebrafish Embryos." *Dev Dyn* 230, no. 2 (2004): 263-77.
- BALLARD, WILLIAM W. "Morphogenetic Movements and Fate Maps of Vertebrates." *American Zoologist* 21, no. 2 (1981): 391-399.
- Baron, R. and M. Kneissel. "Wnt Signaling in Bone Homeostasis and Disease: From Human Mutations to Treatments." *Nat Med* 19, no. 2 (2013): 179-92.
- Bastock, R., H. Strutt and D. Strutt. "Strabismus Is Asymmetrically Localised and Binds to Prickle and Dishevelled During *Drosophila* Planar Polarity Patterning." *Development* 130, no. 13 (2003): 3007-14.
- Bedell, V. M., S. E. Westcot and S. C. Ekker. "Lessons from Morpholino-Based Screening in Zebrafish." *Brief Funct Genomics* 10, no. 4 (2011): 181-8.
- Behrndt, M., G. Salbreux, P. Campinho, R. Hauschild, F. Oswald, J. Roensch, S. W. Grill and C. P. Heisenberg. "Forces Driving Epithelial Spreading in Zebrafish Gastrulation." *Science* 338, no. 6104 (2012): 257-60.
- Bennett, J. T., H. L. Stickney, W. Y. Choi, B. Ciruna, W. S. Talbot and A. F. Schier. "Maternal Nodal and Zebrafish Embryogenesis." *Nature* 450, no. 7167 (2007): E1-2; discussion E2-4.
- Bertagnolo, V., M. Marchisio, F. Brugnoli, A. Bavelloni, L. Boccafogli, M. L. Colamussi and S. Capitani. "Requirement of Tyrosine-Phosphorylated Vav for Morphological Differentiation of All-Trans-Retinoic Acid-Treated HI-60 Cells." *Cell Growth Differ* 12, no. 4 (2001): 193-200.
- Birkenfeld, J., P. Nalbant, B. P. Bohl, O. Pertz, K. M. Hahn and G. M. Bokoch. "Gef-H1 Modulates Localized RhoA Activation During Cytokinesis under the Control of Mitotic Kinases." *Dev Cell* 12, no. 5 (2007): 699-712.
- Birkenfeld, J., P. Nalbant, S. H. Yoon and G. M. Bokoch. "Cellular Functions of Gef-H1, a Microtubule-Regulated Rho-Gef: Is Altered Gef-H1 Activity a Crucial Determinant of Disease Pathogenesis?" *Trends Cell Biol* 18, no. 5 (2008): 210-9.

- Birsoy, B., M. Kofron, K. Schaible, C. Wylie and J. Heasman. "Vg 1 Is an Essential Signaling Molecule in Xenopus Development." *Development* 133, no. 1 (2006): 15-20.
- Biswas, P. S., G. Bhagat and A. B. Pernis. "Irf4 and Its Regulators: Evolving Insights into the Pathogenesis of Inflammatory Arthritis?" *Immunol Rev* 233, no. 1 (2010): 79-96.
- Biswas, P. S., S. Gupta, R. A. Stirzaker, V. Kumar, R. Jessberger, T. T. Lu, G. Bhagat and A. B. Pernis. "Dual Regulation of Irf4 Function in T and B Cells Is Required for the Coordination of T-B Cell Interactions and the Prevention of Autoimmunity." *J Exp Med* 209, no. 3 (2012): 581-96.
- Borggreffe, T., S. Keshavarzi, B. Gross, M. Wabl and R. Jessberger. "Impaired Ige Response in Swap-70-Deficient Mice." *Eur J Immunol* 31, no. 8 (2001): 2467-75.
- Borggreffe, T., M. Wabl, A. T. Akhmedov and R. Jessberger. "A B-Cell-Specific DNA Recombination Complex." *J Biol Chem* 273, no. 27 (1998): 17025-35.
- Boutros, M. and M. Mlodzik. "Dishevelled: At the Crossroads of Divergent Intracellular Signaling Pathways." *Mech Dev* 83, no. 1-2 (1999): 27-37.
- Bruce, A. E., C. Howley, M. Dixon Fox and R. K. Ho. "T-Box Gene Eomesodermin and the Homeobox-Containing Mix/Bix Gene Mtx2 Regulate Epiboly Movements in the Zebrafish." *Dev Dyn* 233, no. 1 (2005): 105-14.
- Bubeck Wardenburg, J., C. Fu, J. K. Jackman, H. Flotow, S. E. Wilkinson, D. H. Williams, R. Johnson, G. Kong, A. C. Chan and P. R. Findell. "Phosphorylation of Slp-76 by the Zap-70 Protein-Tyrosine Kinase Is Required for T-Cell Receptor Function." *J Biol Chem* 271, no. 33 (1996): 19641-4.
- Carmany-Rampey, A. and A. F. Schier. "Single-Cell Internalization During Zebrafish Gastrulation." *Curr Biol* 11, no. 16 (2001): 1261-5.
- Carreira-Barbosa, F., M. L. Concha, M. Takeuchi, N. Ueno, S. W. Wilson and M. Tada. "Prickle 1 Regulates Cell Movements During Gastrulation and Neuronal Migration in Zebrafish." *Development* 130, no. 17 (2003): 4037-46.

- Carreira-Barbosa, F., M. Kajita, V. Morel, H. Wada, H. Okamoto, A. Martinez Arias, Y. Fujita, S. W. Wilson and M. Tada. "Flamingo Regulates Epiboly and Convergence/Extension Movements through Cell Cohesive and Signalling Functions During Zebrafish Gastrulation." *Development* 136, no. 3 (2009): 383-92.
- Chan, A. C., N. S. van Oers, A. Tran, L. Turka, C. L. Law, J. C. Ryan, E. A. Clark and A. Weiss. "Differential Expression of Zap-70 and Syk Protein Tyrosine Kinases, and the Role of This Family of Protein Tyrosine Kinases in Tcr Signaling." *J Immunol* 152, no. 10 (1994): 4758-66.
- Charest, P. G. and R. A. Firtel. "Big Roles for Small Gtpases in the Control of Directed Cell Movement." *Biochem J* 401, no. 2 (2007): 377-90.
- Chen, K., W. Zhang, J. Chen, S. Li and G. Guo. "Rho-Associated Protein Kinase Modulates Neurite Extension by Regulating Microtubule Remodeling and Vinculin Distribution." *Neural Regen Res* 8, no. 32 (2013): 3027-35.
- Chen, W. S., D. Antic, M. Matis, C. Y. Logan, M. Povelones, G. A. Anderson, R. Nusse and J. D. Axelrod. "Asymmetric Homotypic Interactions of the Atypical Cadherin Flamingo Mediate Intercellular Polarity Signaling." *Cell* 133, no. 6 (2008): 1093-105.
- Chen, X., H. Xu, P. Yuan, F. Fang, M. Huss, V. B. Vega, E. Wong, Y. L. Orlov, W. Zhang, J. Jiang, Y. H. Loh, H. C. Yeo, Z. X. Yeo, V. Narang, K. R. Govindarajan, B. Leong, A. Shahab, Y. Ruan, G. Bourque, W. K. Sung, N. D. Clarke, C. L. Wei and H. H. Ng. "Integration of External Signaling Pathways with the Core Transcriptional Network in Embryonic Stem Cells." *Cell* 133, no. 6 (2008): 1106-17.
- Chen, Z., D. Borek, S. B. Padrick, T. S. Gomez, Z. Metlagel, A. M. Ismail, J. Umetani, D. D. Billadeau, Z. Otwinowski and M. K. Rosen. "Structure and Control of the Actin Regulatory Wave Complex." *Nature* 468, no. 7323 (2010): 533-8.
- Cheng, J. C., A. L. Miller and S. E. Webb. "Organization and Function of Microfilaments During Late Epiboly in Zebrafish Embryos." *Dev Dyn* 231, no. 2 (2004): 313-23.
- Choi, J., J. Ko, E. Park, J. R. Lee, J. Yoon, S. Lim and E. Kim. "Phosphorylation of Stargazin by Protein Kinase a Regulates Its Interaction with Psd-95." *J Biol Chem* 277, no. 14 (2002): 12359-63.
- Chopin, M., L. Quemeneur, T. Ripich and R. Jessberger. "Swap-70 Controls Formation of the Splenic Marginal Zone through Regulating T1b-Cell Differentiation." *Eur J Immunol* 40, no. 12 (2010): 3544-56.



- Ciruna, B., A. Jenny, D. Lee, M. Mlodzik and A. F. Schier. "Planar Cell Polarity Signalling Couples Cell Division and Morphogenesis During Neurulation." *Nature* 439, no. 7073 (2006): 220-4.
- Concha, M. L. and R. J. Adams. "Oriented Cell Divisions and Cellular Morphogenesis in the Zebrafish Gastrula and Neurula: A Time-Lapse Analysis." *Development* 125, no. 6 (1998): 983-94.
- Coonrod, S. A., L. C. Bolling, P. W. Wright, P. E. Visconti and J. C. Herr. "A Morpholino Phenocopy of the Mouse Mos Mutation." *Genesis* 30, no. 3 (2001): 198-200.
- Coque, E., C. Raoul and M. Bowerman. "Rock Inhibition as a Therapy for Spinal Muscular Atrophy: Understanding the Repercussions on Multiple Cellular Targets." *Front Neurosci* 8, (2014): 271.
- Couzin, Jennifer. "Method to Silence Genes Earns Loud Praise." *Science* 314, no. 5796 (2006): 34.
- Daggett, D. F., C. A. Boyd, P. Gautier, R. J. Bryson-Richardson, C. Thisse, B. Thisse, S. L. Amacher and P. D. Currie. "Developmentally Restricted Actin-Regulatory Molecules Control Morphogenetic Cell Movements in the Zebrafish Gastrula." *Curr Biol* 14, no. 18 (2004): 1632-8.
- Debant, A., C. Serra-Pages, K. Seipel, S. O'Brien, M. Tang, S. H. Park and M. Streuli. "The Multidomain Protein Trio Binds the Lar Transmembrane Tyrosine Phosphatase, Contains a Protein Kinase Domain, and Has Separate Rac-Specific and Rho-Specific Guanine Nucleotide Exchange Factor Domains." *Proc Natl Acad Sci U S A* 93, no. 11 (1996): 5466-71.
- Deckert, M., S. Tartare-Deckert, C. Couture, T. Mustelin and A. Altman. "Functional and Physical Interactions of Syk Family Kinases with the Vav Proto-Oncogene Product." *Immunity* 5, no. 6 (1996): 591-604.
- Djiane, A., J. Riou, M. Umbhauer, J. Boucaut and D. Shi. "Role of Frizzled 7 in the Regulation of Convergent Extension Movements During Gastrulation in *Xenopus Laevis*." *Development* 127, no. 14 (2000): 3091-100.
- Doye, Anne, Amel Mettouchi, Guillaume Bossis, René Clément, Caroline Buisson-Touati, Gilles Flatau, Laurent Gagnoux, Marc Piechaczyk, Patrice Boquet and Emmanuel Lemichez. "Cnf1 Exploits the Ubiquitin-Proteasome Machinery to Restrict Rho Gtpase Activation for Bacterial Host Cell Invasion." *Cell* 111, no. 4: 553-564.

- Draper, B. W., P. A. Morcos and C. B. Kimmel. "Inhibition of Zebrafish Fgf8 Pre-Mrna Splicing with Morpholino Oligos: A Quantifiable Method for Gene Knockdown." *Genesis* 30, no. 3 (2001): 154-6.
- Driever, W., L. Solnica-Krezel, A. F. Schier, S. C. Neuhauss, J. Malicki, D. L. Stemple, D. Y. Stainier, F. Zwartkruis, S. Abdelilah, Z. Rangini, J. Belak and C. Boggs. "A Genetic Screen for Mutations Affecting Embryogenesis in Zebrafish." *Development* 123, (1996): 37-46.
- Eckfeldt, C. E., E. M. Mendenhall, C. M. Flynn, T. F. Wang, M. A. Pickart, S. M. Grindle, S. C. Ekker and C. M. Verfaillie. "Functional Analysis of Human Hematopoietic Stem Cell Gene Expression Using Zebrafish." *PLoS Biol* 3, no. 8 (2005): e254.
- Eden, S., R. Rohatgi, A. V. Podtelejnikov, M. Mann and M. W. Kirschner. "Mechanism of Regulation of Wave1-Induced Actin Nucleation by Rac1 and Nck." *Nature* 418, no. 6899 (2002): 790-3.
- Eisen, J. S. and J. C. Smith. "Controlling Morpholino Experiments: Don't Stop Making Antisense." *Development* 135, no. 10 (2008): 1735-43.
- Ekker, M., M. A. Akimenko, R. Bremiller and M. Westerfield. "Regional Expression of Three Homeobox Transcripts in the Inner Ear of Zebrafish Embryos." *Neuron* 9, no. 1 (1992): 27-35.
- Ekker, S. C. "Morphants: A New Systematic Vertebrate Functional Genomics Approach." *Yeast* 17, no. 4 (2000): 302-306.
- Ellerbroek, S. M., K. Wennerberg and K. Burridge. "Serine Phosphorylation Negatively Regulates RhoA in Vivo." *J Biol Chem* 278, no. 21 (2003): 19023-31.
- Fedon, Yann, Anne Bonnieu, Barbara Vernus, Francis Bacou, Henri Bernardi and Stéphanie Gay. *Role and Function of Wnts in the Regulation of Myogenesis: When Wnt Meets Myostatin* Skeletal Muscle - from Myogenesis to Clinical Relations, 2012.
- Feiguin, F., M. Hannus, M. Mlodzik and S. Eaton. "The Ankyrin Repeat Protein Diego Mediates Frizzled-Dependent Planar Polarization." *Dev Cell* 1, no. 1 (2001): 93-101.
- Finney, B. A., E. Schweighoffer, L. Navarro-Nunez, C. Benezech, F. Barone, C. E. Hughes, S. A. Langan, K. L. Lowe, A. Y. Pollitt, D. Mourao-Sa, S. Sheardown, G. B. Nash, N. Smithers, C. Reis e Sousa, V. L. Tybulewicz and S. P. Watson. "Clec-2 and Syk in the Megakaryocytic/Platelet Lineage Are Essential for Development." *Blood* 119, no. 7 (2012): 1747-56.

- Fire, A., S. Xu, M. K. Montgomery, S. A. Kostas, S. E. Driver and C. C. Mello. "Potent and Specific Genetic Interference by Double-Stranded Rna in *Caenorhabditis Elegans*." *Nature* 391, no. 6669 (1998): 806-11.
- Flatau, G., E. Lemichez, M. Gauthier, P. Chardin, S. Paris, C. Fiorentini and P. Boquet. "Toxin-Induced Activation of the G Protein P21 Rho by Deamidation of Glutamine." *Nature* 387, no. 6634 (1997): 729-33.
- Formstone, C. J. and I. Mason. "Combinatorial Activity of Flamingo Proteins Directs Convergence and Extension within the Early Zebrafish Embryo Via the Planar Cell Polarity Pathway." *Dev Biol* 282, no. 2 (2005): 320-35.
- Galandrini, R., G. Palmieri, M. Piccoli, L. Frati and A. Santoni. "Role for the Rac1 Exchange Factor Vav in the Signaling Pathways Leading to Nk Cell Cytotoxicity." *J Immunol* 162, no. 6 (1999): 3148-52.
- Gao, C. and Y. G. Chen. "Dishevelled: The Hub of Wnt Signaling." *Cell Signal* 22, no. 5 (2010): 717-27.
- Gebiski, B. L., C. J. Mann, S. Fletcher and S. D. Wilton. "Morpholino Antisense Oligonucleotide Induced Dystrophin Exon 23 Skipping in Mdx Mouse Muscle." *Hum Mol Genet* 12, no. 15 (2003): 1801-11.
- Georgiou, Marios and Buzz Baum. "Polarity Proteins and Rho Gtpases Cooperate to Spatially Organise Epithelial Actin-Based Protrusions." *Journal of Cell Science* 123, no. 7 (2010): 1089-1098.
- Georgiou, Marios, Eliana Marinari, Jemima Burden and Buzz Baum. "Cdc42, Par6, and Apkc Regulate Arp2/3-Mediated Endocytosis to Control Local Adherens Junction Stability." *Current Biology* 18, no. 21 (2008): 1631-1638.
- Glickman, N. S., C. B. Kimmel, M. A. Jones and R. J. Adams. "Shaping the Zebrafish Notochord." *Development* 130, no. 5 (2003): 873-87.
- Goh, L. L. and E. Manser. "The Rhoa Gef Syx Is a Target of Rnd3 and Regulated Via a Raf1-Like Ubiquitin-Related Domain." *PLoS One* 5, no. 8 (2010): e12409.
- Gomez-Orte, E., B. Saenz-Narciso, S. Moreno and J. Cabello. "Multiple Functions of the Noncanonical Wnt Pathway." *Trends Genet* 29, no. 9 (2013): 545-53.

- Gong, Y., C. Mo and S. E. Fraser. "Planar Cell Polarity Signalling Controls Cell Division Orientation During Zebrafish Gastrulation." *Nature* 430, no. 7000 (2004): 689-93.
- Goodrich, Lisa V. and David Strutt. "Principles of Planar Polarity in Animal Development." *Development* 138, no. 10 (2011): 1877-1892.
- Gore, A. V., S. Maegawa, A. Cheong, P. C. Gilligan, E. S. Weinberg and K. Sampath. "The Zebrafish Dorsal Axis Is Apparent at the Four-Cell Stage." *Nature* 438, no. 7070 (2005): 1030-5.
- Goto, T. and R. Keller. "The Planar Cell Polarity Gene Strabismus Regulates Convergence and Extension and Neural Fold Closure in Xenopus." *Dev Biol* 247, no. 1 (2002): 165-81.
- Goudevenou, K., P. Martin, Y. J. Yeh, P. Jones and F. Sablitzky. "Def6 Is Required for Convergent Extension Movements During Zebrafish Gastrulation Downstream of Wnt5b Signaling." *PLoS One* 6, no. 10 (2011): e26548.
- Gray, R. S., I. Roszko and L. Solnica-Krezel. "Planar Cell Polarity: Coordinating Morphogenetic Cell Behaviors with Embryonic Polarity." *Dev Cell* 21, no. 1 (2011): 120-33.
- Gross, B., T. Borggrefe, M. Wabl, R. R. Sivalenka, M. Bennett, A. B. Rossi and R. Jessberger. "Swap-70-Deficient Mast Cells Are Impaired in Development and Ige-Mediated Degranulation." *Eur J Immunol* 32, no. 4 (2002): 1121-8.
- Habas, R., I. B. Dawid and X. He. "Coactivation of Rac and Rho by Wnt/Frizzled Signaling Is Required for Vertebrate Gastrulation." *Genes Dev* 17, no. 2 (2003): 295-309.
- Habas, R., Y. Kato and X. He. "Wnt/Frizzled Activation of Rho Regulates Vertebrate Gastrulation and Requires a Novel Formin Homology Protein Daam1." *Cell* 107, no. 7 (2001): 843-54.
- Haffter, P., M. Granato, M. Brand, M. C. Mullins, M. Hammerschmidt, D. A. Kane, J. Odenthal, F. J. van Eeden, Y. J. Jiang, C. P. Heisenberg, R. N. Kelsh, M. Furutani-Seiki, E. Vogelsang, D. Beuchle, U. Schach, C. Fabian and C. Nusslein-Volhard. "The Identification of Genes with Unique and Essential Functions in the Development of the Zebrafish, Danio Rerio." *Development* 123, (1996): 1-36.
- Hall, A. "Rho Family Gtpases." *Biochem Soc Trans* 40, no. 6 (2012): 1378-82.

- Harris, K. P. and U. Tepass. "Cdc42 and Par Proteins Stabilize Dynamic Adherens Junctions in the Drosophila Neuroectoderm through Regulation of Apical Endocytosis." *J Cell Biol* 183, no. 6 (2008): 1129-43.
- Heasman, J. "Morpholino Oligos: Making Sense of Antisense?" *Dev Biol* 243, no. 2 (2002): 209-14.
- Heasman, J., M. Kofron and C. Wylie. "Beta-Catenin Signaling Activity Dissected in the Early Xenopus Embryo: A Novel Antisense Approach." *Dev Biol* 222, no. 1 (2000): 124-34.
- Heerema, A. E., N. W. Abbey, M. Weinstein and B. G. Herndier. "Expression of the Diffuse B-Cell Lymphoma Family Molecule Swap-70 in Human B-Cell Neoplasms: Immunohistochemical Study of 86 Cases." *Appl Immunohistochem Mol Morphol* 12, no. 1 (2004): 21-5.
- Heisenberg, C. P., M. Brand, Y. J. Jiang, R. M. Warga, D. Beuchle, F. J. van Eeden, M. Furutani-Seiki, M. Granato, P. Haffter, M. Hammerschmidt, D. A. Kane, R. N. Kelsh, M. C. Mullins, J. Odenthal and C. Nusslein-Volhard. "Genes Involved in Forebrain Development in the Zebrafish, Danio Rerio." *Development* 123, (1996): 191-203.
- Heisenberg, C. P. and C. Nusslein-Volhard. "The Function of Silberblick in the Positioning of the Eye Anlage in the Zebrafish Embryo." *Dev Biol* 184, no. 1 (1997): 85-94.
- Heisenberg, C. P. and M. Tada. "Zebrafish Gastrulation Movements: Bridging Cell and Developmental Biology." *Semin Cell Dev Biol* 13, no. 6 (2002): 471-9.
- Heisenberg, C. P., M. Tada, G. J. Rauch, L. Saude, M. L. Concha, R. Geisler, D. L. Stemple, J. C. Smith and S. W. Wilson. "Silberblick/Wnt11 Mediates Convergent Extension Movements During Zebrafish Gastrulation." *Nature* 405, no. 6782 (2000): 76-81.
- Hermle, T., M. C. Guida, S. Beck, S. Helmstadter and M. Simons. "Drosophila Atp6ap2/Vhaprr Functions Both as a Novel Planar Cell Polarity Core Protein and a Regulator of Endosomal Trafficking." *EMBO J* 32, no. 2 (2013): 245-59.
- Hilpela, P., P. Oberbanscheidt, P. Hahne, M. Hund, G. Kalhammer, J. V. Small and M. Bahler. "Swap-70 Identifies a Transitional Subset of Actin Filaments in Motile Cells." *Mol Biol Cell* 14, no. 8 (2003): 3242-53.
- Hotfilder, M., S. Baxendale, M. A. Cross and F. Sablitzky. "Def-2, -3, -6 and -8, Novel Mouse Genes Differentially Expressed in the Haemopoietic System." *Br J Haematol* 106, no. 2 (1999): 335-44.

- Huarcaya Najarro, E. and B. D. Ackley. "C. Elegans Fmi-1/Flamingo and Wnt Pathway Components Interact Genetically to Control the Anteroposterior Neurite Growth of the Vd Gabaergic Neurons." *Dev Biol* 377, no. 1 (2013): 224-35.
- Ihara, S., T. Oka and Y. Fukui. "Direct Binding of Swap-70 to Non-Muscle Actin Is Required for Membrane Ruffling." *J Cell Sci* 119, no. Pt 3 (2006): 500-7.
- Izant, JG and H Weintraub. "Constitutive and Conditional Suppression of Exogenous and Endogenous Genes by Anti-Sense Rna." *Science* 229, no. 4711 (1985): 345-352.
- Jaffe, A. B. and A. Hall. "Rho Gtpases: Biochemistry and Biology." *Annu Rev Cell Dev Biol* 21, (2005): 247-69.
- Jenny, A., J. Reynolds-Kenneally, G. Das, M. Burnett and M. Mlodzik. "Diego and Prickle Regulate Frizzled Planar Cell Polarity Signalling by Competing for Dishevelled Binding." *Nat Cell Biol* 7, no. 7 (2005): 691-7.
- Jessen, J. R., J. Topczewski, S. Bingham, D. S. Sepich, F. Marlow, A. Chandrasekhar and L. Solnica-Krezel. "Zebrafish Trilobite Identifies New Roles for Strabismus in Gastrulation and Neuronal Movements." *Nat Cell Biol* 4, no. 8 (2002): 610-5.
- Jones, C. and P. Chen. "Planar Cell Polarity Signaling in Vertebrates." *Bioessays* 29, no. 2 (2007): 120-32.
- Jopling, C. and J. den Hertog. "Fyn/Yes and Non-Canonical Wnt Signalling Converge on Rhoa in Vertebrate Gastrulation Cell Movements." *EMBO Rep* 6, no. 5 (2005): 426-31.
- Kane, D. A., H. M. Maischein, M. Brand, F. J. van Eeden, M. Furutani-Seiki, M. Granato, P. Haffter, M. Hammerschmidt, C. P. Heisenberg, Y. J. Jiang, R. N. Kelsh, M. C. Mullins, J. Odenthal, R. M. Warga and C. Nusslein-Volhard. "The Zebrafish Early Arrest Mutants." *Development* 123, (1996): 57-66.
- Kane, D. A., K. N. McFarland and R. M. Warga. "Mutations in Half Baked/E-Cadherin Block Cell Behaviors That Are Necessary for Teleost Epiboly." *Development* 132, no. 5 (2005): 1105-16.
- Kari, G., U. Rodeck and A. P. Dicker. "Zebrafish: An Emerging Model System for Human Disease and Drug Discovery." *Clin Pharmacol Ther* 82, no. 1 (2007): 70-80.

- Keller, P. J., A. D. Schmidt, J. Wittbrodt and E. H. Stelzer. "Reconstruction of Zebrafish Early Embryonic Development by Scanned Light Sheet Microscopy." *Science* 322, no. 5904 (2008): 1065-9.
- Kilian, B., H. Mansukoski, F. C. Barbosa, F. Ulrich, M. Tada and C. P. Heisenberg. "The Role of Ppt/Wnt5 in Regulating Cell Shape and Movement During Zebrafish Gastrulation." *Mech Dev* 120, no. 4 (2003): 467-76.
- Kim, J. Y., K. Huh, R. Jung and T. J. Kim. "Identification of Bcar-1 as a New Substrate of Syk Tyrosine Kinase through a Determination of Amino Acid Sequence Preferences Surrounding the Substrate Tyrosine Residue." *Immunol Lett* 135, no. 1-2 (2011): 151-7.
- Kimmel, C. B., W. W. Ballard, S. R. Kimmel, B. Ullmann and T. F. Schilling. "Stages of Embryonic Development of the Zebrafish." *Dev Dyn* 203, no. 3 (1995): 253-310.
- Kimmel, C. B. and R. D. Law. "Cell Lineage of Zebrafish Blastomeres. I. Cleavage Pattern and Cytoplasmic Bridges between Cells." *Dev Biol* 108, no. 1 (1985): 78-85.
- King, T. D., W. Zhang, M. J. Suto and Y. Li. "Frizzled7 as an Emerging Target for Cancer Therapy." *Cell Signal* 24, no. 4 (2012): 846-51.
- Kinoshita, N., H. Iioka, A. Miyakoshi and N. Ueno. "Pkc Delta Is Essential for Dishevelled Function in a Noncanonical Wnt Pathway That Regulates Xenopus Convergent Extension Movements." *Genes Dev* 17, no. 13 (2003): 1663-76.
- Kirby, B. B., N. Takada, A. J. Latimer, J. Shin, T. J. Carney, R. N. Kelsh and B. Appel. "In Vivo Time-Lapse Imaging Shows Dynamic Oligodendrocyte Progenitor Behavior During Zebrafish Development." *Nat Neurosci* 9, no. 12 (2006): 1506-11.
- Klein, T. J. and M. Mlodzik. "Planar Cell Polarization: An Emerging Model Points in the Right Direction." *Annu Rev Cell Dev Biol* 21, (2005): 155-76.
- Kloosterman, W. P., A. K. Lagendijk, R. F. Ketting, J. D. Moulton and R. H. Plasterk. "Targeted Inhibition of Mirna Maturation with Morpholinos Reveals a Role for Mir-375 in Pancreatic Islet Development." *PLoS Biol* 5, no. 8 (2007): e203.
- Konantz, M., T. B. Balci, U. F. Hartwig, G. Dellaire, M. C. Andre, J. N. Berman and C. Lengerke. "Zebrafish Xenografts as a Tool for in Vivo Studies on Human Cancer." *Ann N Y Acad Sci*, (2012).

- Kos, R., M. V. Reedy, R. L. Johnson and C. A. Erickson. "The Winged-Helix Transcription Factor Foxd3 Is Important for Establishing the Neural Crest Lineage and Repressing Melanogenesis in Avian Embryos." *Development* 128, no. 8 (2001): 1467-79.
- Krendel, M., F. T. Zenke and G. M. Bokoch. "Nucleotide Exchange Factor Gef-H1 Mediates Cross-Talk between Microtubules and the Actin Cytoskeleton." *Nat Cell Biol* 4, no. 4 (2002): 294-301.
- Kwan, K. M. and M. W. Kirschner. "A Microtubule-Binding Rho-Gef Controls Cell Morphology During Convergent Extension of *Xenopus laevis*." *Development* 132, no. 20 (2005): 4599-610.
- Kwon, T., D. Y. Kwon, J. Chun, J. H. Kim and S. S. Kang. "Akt Protein Kinase Inhibits Rac1-Gtp Binding through Phosphorylation at Serine 71 of Rac1." *J Biol Chem* 275, no. 1 (2000): 423-8.
- Lang, P., F. Gesbert, M. Delespine-Carmagnat, R. Stancou, M. Pouchelet and J. Bertoglio. "Protein Kinase a Phosphorylation of RhoA Mediates the Morphological and Functional Effects of Cyclic Amp in Cytotoxic Lymphocytes." *EMBO J* 15, no. 3 (1996): 510-9.
- Leibfried, A., R. Fricke, M. J. Morgan, S. Bogdan and Y. Bellaiche. "Drosophila Cip4 and Wasp Define a Branch of the Cdc42-Par6-Apkc Pathway Regulating E-Cadherin Endocytosis." *Curr Biol* 18, no. 21 (2008): 1639-48.
- Leibfried, A., S. Muller and A. Ephrussi. "A Cdc42-Regulated Actin Cytoskeleton Mediates Drosophila Oocyte Polarization." *Development* 140, no. 2 (2013): 362-71.
- Leung, C. F., S. E. Webb and A. L. Miller. "Calcium Transients Accompany Ooplasmic Segregation in Zebrafish Embryos." *Dev Growth Differ* 40, no. 3 (1998): 313-26.
- Lieschke, G. J. and P. D. Currie. "Animal Models of Human Disease: Zebrafish Swim into View." *Nat Rev Genet* 8, no. 5 (2007): 353-67.
- Lin, S., L. M. Baye, T. A. Westfall and D. C. Slusarski. "Wnt5b-Ryk Pathway Provides Directional Signals to Regulate Gastrulation Movement." *J Cell Biol* 190, no. 2 (2010): 263-78.
- Linnekin, D. "Early Signaling Pathways Activated by C-Kit in Hematopoietic Cells." *Int J Biochem Cell Biol* 31, no. 10 (1999): 1053-74.



- Liu, Ming, Feng Bi, Xuan Zhou and Yi Zheng. "Rho Gtpase Regulation by Mirnas and Covalent Modifications." *Trends in Cell Biology* 22, no. 7 (2012): 365-373.
- Logan, C. Y. and R. Nusse. "The Wnt Signaling Pathway in Development and Disease." *Annu Rev Cell Dev Biol* 20, (2004): 781-810.
- Malbon, C. C. "Frizzleds: New Members of the Superfamily of G-Protein-Coupled Receptors." *Front Biosci* 9, (2004): 1048-58.
- Mani, M., S. Venkatasubrahmanyam, M. Sanyal, S. Levy, A. Butte, K. Weinberg and T. Jahn. "Wiskott-Aldrich Syndrome Protein Is an Effector of Kit Signaling." *Blood* 114, no. 14 (2009): 2900-8.
- Marlow, F., J. Topczewski, D. Sepich and L. Solnica-Krezel. "Zebrafish Rho Kinase 2 Acts Downstream of Wnt11 to Mediate Cell Polarity and Effective Convergence and Extension Movements." *Curr Biol* 12, no. 11 (2002): 876-84.
- Martin, E., C. Yanicostas, A. Rastetter, S. M. Naini, A. Maouedj, E. Kabashi, S. Rivaud-Pechoux, A. Brice, G. Stevanin and N. Soussi-Yanicostas. "Spatacsin and Spastizin Act in the Same Pathway Required for Proper Spinal Motor Neuron Axon Outgrowth in Zebrafish." *Neurobiol Dis* 48, no. 3 (2012): 299-308.
- Masat, L., J. Caldwell, R. Armstrong, H. Khoshnevisan, R. Jessberger, B. Herndier, M. Wabl and D. Ferrick. "Association of Swap-70 with the B Cell Antigen Receptor Complex." *Proc Natl Acad Sci U S A* 97, no. 5 (2000): 2180-4.
- Matsui, T., A. Raya, Y. Kawakami, C. Callol-Massot, J. Capdevila, C. Rodriguez-Esteban and J. C. Izpisua Belmonte. "Noncanonical Wnt Signaling Regulates Midline Convergence of Organ Primordia During Zebrafish Development." *Genes Dev* 19, no. 1 (2005): 164-75.
- Matusek, T., R. Gombos, A. Szecsenyi, N. Sanchez-Soriano, A. Czibula, C. Pataki, A. Gedai, A. Prokop, I. Rasko and J. Mihaly. "Formin Proteins of the Daam Subfamily Play a Role During Axon Growth." *J Neurosci* 28, no. 49 (2008): 13310-9.
- Mavrikakis, K. J., K. J. McKinlay, P. Jones and F. Sablitzky. "Def6, a Novel Ph-Dh-Like Domain Protein, Is an Upstream Activator of the Rho Gtpases Rac1, Cdc42, and Rhoa." *Exp Cell Res* 294, no. 2 (2004): 335-44.
- McNeill, H. "Planar Cell Polarity and the Kidney." *J Am Soc Nephrol* 20, no. 10 (2009): 2104-11.

- Miller-Bertoglio, V. E., S. Fisher, A. Sanchez, M. C. Mullins and M. E. Halpern. "Differential Regulation of Chordin Expression Domains in Mutant Zebrafish." *Dev Biol* 192, no. 2 (1997): 537-50.
- Mocsai, A., J. Ruland and V. L. Tybulewicz. "The Syk Tyrosine Kinase: A Crucial Player in Diverse Biological Functions." *Nat Rev Immunol* 10, no. 6 (2010): 387-402.
- Moeller, Heinz, Andreas Jenny, Hans-Joerg Schaeffer, Thomas Schwarz-Romond, Marek Mlodzik, Matthias Hammerschmidt and Walter Birchmeier. "Diversin Regulates Heart Formation and Gastrulation Movements in Development." *Proceedings of the National Academy of Sciences* 103, no. 43 (2006): 15900-15905.
- Montero, J. A., L. Carvalho, M. Wilsch-Brauninger, B. Kilian, C. Mustafa and C. P. Heisenberg. "Shield Formation at the Onset of Zebrafish Gastrulation." *Development* 132, no. 6 (2005): 1187-98.
- Montero, J. A. and C. P. Heisenberg. "Gastrulation Dynamics: Cells Move into Focus." *Trends Cell Biol* 14, no. 11 (2004): 620-7.
- Moon, R. T., R. M. Campbell, J. L. Christian, L. L. McGrew, J. Shih and S. Fraser. "Xwnt-5a: A Maternal Wnt That Affects Morphogenetic Movements after Overexpression in Embryos of *Xenopus Laevis*." *Development* 119, no. 1 (1993): 97-111.
- Morcos, P. A. "Achieving Targeted and Quantifiable Alteration of Mrna Splicing with Morpholino Oligos." *Biochem Biophys Res Commun* 358, no. 2 (2007): 521-7.
- Murugan, A. K., S. Ihara, E. Tokuda, K. Uematsu, N. Tsuchida and Y. Fukui. "Swap-70 Is Important for Invasive Phenotypes of Mouse Embryo Fibroblasts Transformed by V-Src." *IUBMB Life* 60, no. 4 (2008): 236-40.
- Myers, D. C., D. S. Sepich and L. Solnica-Krezel. "Bmp Activity Gradient Regulates Convergent Extension During Zebrafish Gastrulation." *Dev Biol* 243, no. 1 (2002): 81-98.
- Myers, D. C., D. S. Sepich and L. Solnica-Krezel. "Convergence and Extension in Vertebrate Gastrulae: Cell Movements According to or in Search of Identity?" *Trends Genet* 18, no. 9 (2002): 447-55.
- Nalbant, P., Y. C. Chang, J. Birkenfeld, Z. F. Chang and G. M. Bokoch. "Guanine Nucleotide Exchange Factor-H1 Regulates Cell Migration Via Localized Activation of Rhoa at the Leading Edge." *Mol Biol Cell* 20, no. 18 (2009): 4070-82.

- Nasevicius, A. and S. C. Ekker. "Effective Targeted Gene 'Knockdown' in Zebrafish." *Nat Genet* 26, no. 2 (2000): 216-20.
- Niehrs, Christof. "The Complex World of Wnt Receptor Signalling." *Nat Rev Mol Cell Biol* 13, no. 12 (2012): 767-779.
- Nusse, R. and H. Varmus. "Three Decades of Wnts: A Personal Perspective on How a Scientific Field Developed." *EMBO J* 31, no. 12 (2012): 2670-84.
- Oates, A. C., A. E. Bruce and R. K. Ho. "Too Much Interference: Injection of Double-Stranded Rna Has Nonspecific Effects in the Zebrafish Embryo." *Dev Biol* 224, no. 1 (2000): 20-8.
- Oberbanscheidt, P., S. Balkow, J. Kuhn, S. Grabbe and M. Bahler. "Swap-70 Associates Transiently with Macropinosomes." *Eur J Cell Biol* 86, no. 1 (2007): 13-24.
- Ocana-Morgner, C., P. Reichardt, M. Chopin, S. Braungart, C. Wahren, M. Gunzer and R. Jessberger. "Sphingosine 1-Phosphate-Induced Motility and Endocytosis of Dendritic Cells Is Regulated by Swap-70 through Rhoa." *J Immunol* 186, no. 9 (2011): 5345-55.
- Ocana-Morgner, C., C. Wahren and R. Jessberger. "Swap-70 Regulates Rhoa/RhoB-Dependent MHCII Surface Localization in Dendritic Cells." *Blood* 113, no. 7 (2009): 1474-82.
- Pan, Y. A., T. Freundlich, T. A. Weissman, D. Schoppik, X. C. Wang, S. Zimmerman, B. Ciruna, J. R. Sanes, J. W. Lichtman and A. F. Schier. "Zebrafish: Multispectral Cell Labeling for Cell Tracing and Lineage Analysis in Zebrafish." *Development* 140, no. 13 (2013): 2835-46.
- Park, H. C., A. Mehta, J. S. Richardson and B. Appel. "Olig2 Is Required for Zebrafish Primary Motor Neuron and Oligodendrocyte Development." *Dev Biol* 248, no. 2 (2002): 356-68.
- Partridge, M., A. Vincent, P. Matthews, J. Puma, D. Stein and J. Summerton. "A Simple Method for Delivering Morpholino Antisense Oligos into the Cytoplasm of Cells." *Antisense Nucleic Acid Drug Dev* 6, no. 3 (1996): 169-75.
- Pearce, G., V. Angeli, G. J. Randolph, T. Junt, U. von Andrian, H. J. Schnittler and R. Jessberger. "Signaling Protein Swap-70 Is Required for Efficient B Cell Homing to Lymphoid Organs." *Nat Immunol* 7, no. 8 (2006): 827-34.

- Pearce, G., T. Audzevich and R. Jessberger. "Syk Regulates B-Cell Migration by Phosphorylation of the F-Actin Interacting Protein Swap-70." *Blood* 117, no. 5 (2011): 1574-84.
- Penzo-Mendèz, Alfredo, Muriel Umbhauer, Alexandre Djiane, Jean-Claude Boucaut and Jean-François Riou. "Activation of G $\beta$  $\gamma$  Signaling Downstream of Wnt-11/Xfz7 Regulates Cdc42 Activity During *Xenopus* Gastrulation." *Developmental Biology* 257, no. 2 (2003): 302-314.
- Pezeron, G., P. Mourrain, S. Courty, J. Ghislain, T. S. Becker, F. M. Rosa and N. B. David. "Live Analysis of Endodermal Layer Formation Identifies Random Walk as a Novel Gastrulation Movement." *Curr Biol* 18, no. 4 (2008): 276-81.
- Pickart, M. A., E. W. Klee, A. L. Nielsen, S. Sivasubbu, E. M. Mendenhall, B. R. Bill, E. Chen, C. E. Eckfeldt, M. Knowlton, M. E. Robu, J. D. Larson, Y. Deng, L. A. Schimmenti, L. B. Ellis, C. M. Verfaillie, M. Hammerschmidt, S. A. Farber and S. C. Ekker. "Genome-Wide Reverse Genetics Framework to Identify Novel Functions of the Vertebrate Secretome." *PLoS One* 1, (2006): e104.
- Poole, A., J. M. Gibbins, M. Turner, M. J. van Vugt, J. G. van de Winkel, T. Saito, V. L. Tybulewicz and S. P. Watson. "The Fc Receptor Gamma-Chain and the Tyrosine Kinase Syk Are Essential for Activation of Mouse Platelets by Collagen." *EMBO J* 16, no. 9 (1997): 2333-41.
- Quemeneur, L., V. Angeli, M. Chopin and R. Jessberger. "Swap-70 Deficiency Causes High-Affinity Plasma Cell Generation Despite Impaired Germinal Center Formation." *Blood* 111, no. 5 (2008): 2714-24.
- Rana, A. A., C. Collart, M. J. Gilchrist and J. C. Smith. "Defining Synphenotype Groups in *Xenopus Tropicalis* by Use of Antisense Morpholino Oligonucleotides." *PLoS Genet* 2, no. 11 (2006): e193.
- Rao, Tata Purushothama and Michael Kühl. "An Updated Overview on Wnt Signaling Pathways: A Prelude for More." *Circulation Research* 106, no. 12 (2010): 1798-1806.
- Rauch, G. J., M. Hammerschmidt, P. Blader, H. E. Schauerte, U. Strahle, P. W. Ingham, A. P. McMahon and P. Haffter. "Wnt5 Is Required for Tail Formation in the Zebrafish Embryo." *Cold Spring Harb Symp Quant Biol* 62, (1997): 227-34.
- Renshaw, S. A. and N. S. Trede. "A Model 450 Million Years in the Making: Zebrafish and Vertebrate Immunity." *Dis Model Mech* 5, no. 1 (2012): 38-47.

- Riento, K. and A. J. Ridley. "Rocks: Multifunctional Kinases in Cell Behaviour." *Nat Rev Mol Cell Biol* 4, no. 6 (2003): 446-56.
- Rohatgi, R., L. Ma, H. Miki, M. Lopez, T. Kirchhausen, T. Takenawa and M. W. Kirschner. "The Interaction between N-Wasp and the Arp2/3 Complex Links Cdc42-Dependent Signals to Actin Assembly." *Cell* 97, no. 2 (1999): 221-31.
- Rohde, L. A. and C. P. Heisenberg. "Zebrafish Gastrulation: Cell Movements, Signals, and Mechanisms." *Int Rev Cytol* 261, (2007): 159-92.
- Roszko, I., A. Sawada and L. Solnica-Krezel. "Regulation of Convergence and Extension Movements During Vertebrate Gastrulation by the Wnt/Pcp Pathway." *Semin Cell Dev Biol* 20, no. 8 (2009): 986-97.
- Rowitch, D. H. and A. R. Kriegstein. "Developmental Genetics of Vertebrate Glial-Cell Specification." *Nature* 468, no. 7321 (2010): 214-22.
- Saburi, S. and H. McNeill. "Organising Cells into Tissues: New Roles for Cell Adhesion Molecules in Planar Cell Polarity." *Curr Opin Cell Biol* 17, no. 5 (2005): 482-8.
- Sanchez-Simon, F. M. and R. E. Rodriguez. "Developmental Expression and Distribution of Opioid Receptors in Zebrafish." *Neuroscience* 151, no. 1 (2008): 129-37.
- Sauzeau, V., H. Le Jeune, C. Cario-Toumaniantz, A. Smolenski, S. M. Lohmann, J. Bertoglio, P. Chardin, P. Pacaud and G. Loirand. "Cyclic Gmp-Dependent Protein Kinase Signaling Pathway Inhibits Rhoa-Induced Ca<sup>2+</sup> Sensitization of Contraction in Vascular Smooth Muscle." *J Biol Chem* 275, no. 28 (2000): 21722-9.
- Schier, A. F. and W. S. Talbot. "Molecular Genetics of Axis Formation in Zebrafish." *Annu Rev Genet* 39, (2005): 561-613.
- Schlessinger, K., A. Hall and N. Tolwinski. "Wnt Signaling Pathways Meet Rho Gtpases." *Genes Dev* 23, no. 3 (2009): 265-77.
- Schofield, A. V., C. Gamell, R. Suryadinata, B. Sarcevic and O. Bernard. "Tubulin Polymerization Promoting Protein 1 (Tppp1) Phosphorylation by Rho-Associated Coiled-Coil Kinase (Rock) and Cyclin-Dependent Kinase 1 (Cdk1) Inhibits Microtubule Dynamics to Increase Cell Proliferation." *J Biol Chem* 288, no. 11 (2013): 7907-17.

- Schulte-Merker, S., R. K. Ho, B. G. Herrmann and C. Nusslein-Volhard. "The Protein Product of the Zebrafish Homologue of the Mouse T Gene Is Expressed in Nuclei of the Germ Ring and the Notochord of the Early Embryo." *Development* 116, no. 4 (1992): 1021-32.
- Schulte, G. "International Union of Basic and Clinical Pharmacology. Lxxx. The Class Frizzled Receptors." *Pharmacol Rev* 62, no. 4 (2010): 632-67.
- Sekiya, R., M. Maeda, H. Yuan, E. Asano, T. Hyodo, H. Hasegawa, S. Ito, K. Shibata, M. Hamaguchi, F. Kikkawa, H. Kajiyama and T. Senga. "Plagl2 Regulates Actin Cytoskeletal Architecture and Cell Migration." *Carcinogenesis* 35, no. 9 (2014): 1993-2001.
- Sepich, D. S., C. Calmelet, M. Kiskowski and L. Solnica-Krezel. "Initiation of Convergence and Extension Movements of Lateral Mesoderm During Zebrafish Gastrulation." *Dev Dyn* 234, no. 2 (2005): 279-92.
- Sepich, D. S., D. C. Myers, R. Short, J. Topczewski, F. Marlow and L. Solnica-Krezel. "Role of the Zebrafish Trilobite Locus in Gastrulation Movements of Convergence and Extension." *Genesis* 27, no. 4 (2000): 159-73.
- Shestopalov, I. A., S. Sinha and J. K. Chen. "Light-Controlled Gene Silencing in Zebrafish Embryos." *Nat Chem Biol* 3, no. 10 (2007): 650-1.
- Shimizu, T., T. Yabe, O. Muraoka, S. Yonemura, S. Aramaki, K. Hatta, Y. K. Bae, H. Nojima and M. Hibi. "E-Cadherin Is Required for Gastrulation Cell Movements in Zebrafish." *Mech Dev* 122, no. 6 (2005): 747-63.
- Shinohara, M., Y. Terada, A. Iwamatsu, A. Shinohara, N. Mochizuki, M. Higuchi, Y. Gotoh, S. Ihara, S. Nagata, H. Itoh, Y. Fukui and R. Jessberger. "Swap-70 Is a Guanine-Nucleotide-Exchange Factor That Mediates Signalling of Membrane Ruffling." *Nature* 416, no. 6882 (2002): 759-63.
- Shu, C. L., Lai Jing Yang, L. C. Su, C. P. Chuu and Y. Fukui. "Swap-70: A New Type of Oncogene." *PLoS One* 8, no. 3 (2013): e59245.
- Simons, M. and M. Mlodzik. "Planar Cell Polarity Signaling: From Fly Development to Human Disease." *Annu Rev Genet* 42, (2008): 517-40.
- Sivalenka, R. R. and R. Jessberger. "Swap-70 Regulates C-Kit-Induced Mast Cell Activation, Cell-Cell Adhesion, and Migration." *Mol Cell Biol* 24, no. 23 (2004): 10277-88.
- Skromne, I. and V. E. Prince. "Current Perspectives in Zebrafish Reverse Genetics: Moving Forward." *Dev Dyn* 237, no. 4 (2008): 861-82.

- Solnica-Krezel, L. "Conserved Patterns of Cell Movements During Vertebrate Gastrulation." *Curr Biol* 15, no. 6 (2005): R213-28.
- Solnica-Krezel, L. "Gastrulation in Zebrafish -- All Just About Adhesion?" *Curr Opin Genet Dev* 16, no. 4 (2006): 433-41.
- Solnica-Krezel, L., A. F. Schier and W. Driever. "Efficient Recovery of Enu-Induced Mutations from the Zebrafish Germline." *Genetics* 136, no. 4 (1994): 1401-20.
- Stein, D., E. Foster, S. B. Huang, D. Weller and J. Summerton. "A Specificity Comparison of Four Antisense Types: Morpholino, 2'-O-Methyl Rna, DNA, and Phosphorothioate DNA." *Antisense Nucleic Acid Drug Dev* 7, no. 3 (1997): 151-7.
- Stern, H. M. and L. I. Zon. "Cancer Genetics and Drug Discovery in the Zebrafish." *Nat Rev Cancer* 3, no. 7 (2003): 533-9.
- Strahle, U. and S. Jesuthasan. "Ultraviolet Irradiation Impairs Epiboly in Zebrafish Embryos: Evidence for a Microtubule-Dependent Mechanism of Epiboly." *Development* 119, no. 3 (1993): 909-19.
- Summerton, James. "Morpholino Antisense Oligomers: The Case for an RNase H-Independent Structural Type." *Biochimica et Biophysica Acta (BBA) - Gene Structure and Expression* 1489, no. 1 (1999): 141-158.
- Swanson, Joel A. and Colin Watts. "Macropinocytosis." *Trends in Cell Biology* 5, no. 11 (1995): 424-428.
- Tada, M. and J. C. Smith. "Xwnt11 Is a Target of Xenopus Brachyury: Regulation of Gastrulation Movements Via Dishevelled, but Not through the Canonical Wnt Pathway." *Development* 127, no. 10 (2000): 2227-38.
- Tahinci, E. and K. Symes. "Distinct Functions of Rho and Rac Are Required for Convergent Extension During Xenopus Gastrulation." *Dev Biol* 259, no. 2 (2003): 318-35.
- Takada, N. and B. Appel. "Swap70 Promotes Neural Precursor Cell Cycle Exit and Oligodendrocyte Formation." *Mol Cell Neurosci* 48, no. 3 (2011): 225-35.
- Takeuchi, M., J. Nakabayashi, T. Sakaguchi, T. S. Yamamoto, H. Takahashi, H. Takeda and N. Ueno. "The Prickle-Related Gene in Vertebrates Is Essential for Gastrulation Cell Movements." *Curr Biol* 13, no. 8 (2003): 674-9.

- Tanegashima, K., H. Zhao and I. B. Dawid. "Wgef Activates Rho in the Wnt-Pcp Pathway and Controls Convergent Extension in *Xenopus* Gastrulation." *EMBO J* 27, no. 4 (2008): 606-17.
- Taniguchi, T., T. Kobayashi, J. Kondo, K. Takahashi, H. Nakamura, J. Suzuki, K. Nagai, T. Yamada, S. Nakamura and H. Yamamura. "Molecular Cloning of a Porcine Gene Syk That Encodes a 72-Kda Protein-Tyrosine Kinase Showing High Susceptibility to Proteolysis." *J Biol Chem* 266, no. 24 (1991): 15790-6.
- Thisse, C., B. Thisse, M. E. Halpern and J. H. Postlethwait. "Goosecoid Expression in Neurectoderm and Mesendoderm Is Disrupted in Zebrafish *Cyclops* Gastrulas." *Dev Biol* 164, no. 2 (1994): 420-9.
- Tokuda, N., K. Kawai, Y. H. Lee, T. Ikegami, S. Yamaguchi, H. Yagisawa, Y. Fukui and S. Tuzi. "Membrane-Induced Alteration of the Secondary Structure in the Swap-70 Pleckstrin Homology Domain." *J Biochem* 151, no. 4 (2012): 391-401.
- Topczewski, J., D. S. Sepich, D. C. Myers, C. Walker, A. Amores, Z. Lele, M. Hammerschmidt, J. Postlethwait and L. Solnica-Krezel. "The Zebrafish Glypican Knypek Controls Cell Polarity During Gastrulation Movements of Convergent Extension." *Dev Cell* 1, no. 2 (2001): 251-64.
- Topczewski, J. and L. Solnica-Krezel. "Cytoskeletal Dynamics of the Zebrafish Embryo." *Methods Cell Biol* 59, (1999): 205-26.
- Tree, D. R., J. M. Shulman, R. Rousset, M. P. Scott, D. Gubb and J. D. Axelrod. "Prickle Mediates Feedback Amplification to Generate Asymmetric Planar Cell Polarity Signaling." *Cell* 109, no. 3 (2002): 371-81.
- Tu, S., W. J. Wu, J. Wang and R. A. Cerione. "Epidermal Growth Factor-Dependent Regulation of Cdc42 Is Mediated by the Src Tyrosine Kinase." *J Biol Chem* 278, no. 49 (2003): 49293-300.
- Tybulewicz, V. L. and R. B. Henderson. "Rho Family Gtpases and Their Regulators in Lymphocytes." *Nat Rev Immunol* 9, no. 9 (2009): 630-44.
- Uckun, Fatih M., Sanjive Qazi, Hong Ma, Lisa Tuel-Ahlgren and Zahide Ozer. "Stat3 Is a Substrate of Syk Tyrosine Kinase in B-Lineage Leukemia/Lymphoma Cells Exposed to Oxidative Stress." *Proceedings of the National Academy of Sciences* 107, no. 7 (2010): 2902-2907.
- Ulrich, F., M. L. Concha, P. J. Heid, E. Voss, S. Witzel, H. Roehl, M. Tada, S. W. Wilson, R. J. Adams, D. R. Soll and C. P. Heisenberg. "Slb/Wnt11 Controls Hypoblast Cell Migration and Morphogenesis at the Onset of Zebrafish Gastrulation." *Development* 130, no. 22 (2003): 5375-84.



- Ulrich, F., M. Krieg, E. M. Schotz, V. Link, I. Castanon, V. Schnabel, A. Taubenberger, D. Mueller, P. H. Puech and C. P. Heisenberg. "Wnt11 Functions in Gastrulation by Controlling Cell Cohesion through Rab5c and E-Cadherin." *Dev Cell* 9, no. 4 (2005): 555-64.
- Uysal-Onganer, P. and R. M. Kypta. "Wnt11 in 2011 - the Regulation and Function of a Non-Canonical Wnt." *Acta Physiol (Oxf)* 204, no. 1 (2012): 52-64.
- Veeman, M. T., J. D. Axelrod and R. T. Moon. "A Second Canon. Functions and Mechanisms of Beta-Catenin-Independent Wnt Signaling." *Dev Cell* 5, no. 3 (2003): 367-77.
- Vigil, D., J. Cherfils, K. L. Rossman and C. J. Der. "Ras Superfamily Gef's and Gaps: Validated and Tractable Targets for Cancer Therapy?" *Nat Rev Cancer* 10, no. 12 (2010): 842-57.
- von Andrian, U. H. and T. R. Mempel. "Homing and Cellular Traffic in Lymph Nodes." *Nat Rev Immunol* 3, no. 11 (2003): 867-78.
- Wallingford, J. B., S. E. Fraser and R. M. Harland. "Convergent Extension: The Molecular Control of Polarized Cell Movement During Embryonic Development." *Dev Cell* 2, no. 6 (2002): 695-706.
- Wallingford, J. B. and R. Habas. "The Developmental Biology of Dishevelled: An Enigmatic Protein Governing Cell Fate and Cell Polarity." *Development* 132, no. 20 (2005): 4421-36.
- Wallingford, J. B. and R. M. Harland. "Xenopus Dishevelled Signaling Regulates Both Neural and Mesodermal Convergent Extension: Parallel Forces Elongating the Body Axis." *Development* 128, no. 13 (2001): 2581-92.
- Wang, H. R., Y. Zhang, B. Ozdamar, A. A. Ogunjimi, E. Alexandrova, G. H. Thomsen and J. L. Wrana. "Regulation of Cell Polarity and Protrusion Formation by Targeting RhoA for Degradation." *Science* 302, no. 5651 (2003): 1775-9.
- Wang, Y. "Wnt/Planar Cell Polarity Signaling: A New Paradigm for Cancer Therapy." *Mol Cancer Ther* 8, no. 8 (2009): 2103-9.
- Wang, Y. H., Y. H. Chen, Y. J. Lin and H. J. Tsai. "Spatiotemporal Expression of Zebrafish Keratin 18 During Early Embryogenesis and the Establishment of a Keratin 18:Rfp Transgenic Line." *Gene Expr Patterns* 6, no. 4 (2006): 335-9.

- Warga, R. M. and C. B. Kimmel. "Cell Movements During Epiboly and Gastrulation in Zebrafish." *Development* 108, no. 4 (1990): 569-80.
- Wei, Y. and T. Mikawa. "Formation of the Avian Primitive Streak from Spatially Restricted Blastoderm: Evidence for Polarized Cell Division in the Elongating Streak." *Development* 127, no. 1 (2000): 87-96.
- Weinberg, E. S., M. L. Allende, C. S. Kelly, A. Abdelhamid, T. Murakami, P. Andermann, O. G. Doerre, D. J. Grunwald and B. Riggelman. "Developmental Regulation of Zebrafish Myod in Wild-Type, No Tail and Spadetail Embryos." *Development* 122, no. 1 (1996): 271-80.
- Wennerberg, K., K. L. Rossman and C. J. Der. "The Ras Superfamily at a Glance." *J Cell Sci* 118, no. Pt 5 (2005): 843-6.
- Westfall, T. A., R. Brimeyer, J. Twedt, J. Gladon, A. Olberding, M. Furutani-Seiki and D. C. Slusarski. "Wnt-5/Pipetail Functions in Vertebrate Axis Formation as a Negative Regulator of Wnt/Beta-Catenin Activity." *J Cell Biol* 162, no. 5 (2003): 889-98.
- Williams, B. B., V. A. Cantrell, N. A. Mundell, A. C. Bennett, R. E. Quick and J. R. Jessen. "Vangl2 Regulates Membrane Trafficking of Mmp14 to Control Cell Polarity and Migration." *J Cell Sci* 125, no. Pt 9 (2012): 2141-7.
- Witzel, S., V. Zimyanin, F. Carreira-Barbosa, M. Tada and C. P. Heisenberg. "Wnt11 Controls Cell Contact Persistence by Local Accumulation of Frizzled 7 at the Plasma Membrane." *J Cell Biol* 175, no. 5 (2006): 791-802.
- Wojnacki, J., G. Quassollo, M. P. Marzolo and A. Caceres. "Rho Gtpases at the Crossroad of Signaling Networks in Mammals: Impact of Rho-Gtpases on Microtubule Organization and Dynamics." *Small GTPases* 5, (2014): e28430.
- Xue, Liang, Wen-Hong Wang, Anton Iliuk, Lianghai Hu, Jacob A. Galan, Shuai Yu, Michael Hans, Robert L. Geahlen and W. Andy Tao. "Sensitive Kinase Assay Linked with Phosphoproteomics for Identifying Direct Kinase Substrates." *Proceedings of the National Academy of Sciences* 109, no. 15 (2012): 5615-5620.
- Yanagi, S., R. Inatome, J. Ding, H. Kitaguchi, V. L. Tybulewicz and H. Yamamura. "Syk Expression in Endothelial Cells and Their Morphologic Defects in Embryonic Syk-Deficient Mice." *Blood* 98, no. 9 (2001): 2869-71.
- Yang, J., Z. Zhang, S. M. Roe, C. J. Marshall and D. Barford. "Activation of Rho Gtpases by Dock Exchange Factors Is Mediated by a Nucleotide Sensor." *Science* 325, no. 5946 (2009): 1398-402.

- Ybot-Gonzalez, P., D. Savery, D. Gerrelli, M. Signore, C. E. Mitchell, C. H. Faux, N. D. Greene and A. J. Copp. "Convergent Extension, Planar-Cell-Polarity Signalling and Initiation of Mouse Neural Tube Closure." *Development* 134, no. 4 (2007): 789-99.
- Yen, W. W., M. Williams, A. Periasamy, M. Conaway, C. Burdsal, R. Keller, X. Lu and A. Sutherland. "Ptk7 Is Essential for Polarized Cell Motility and Convergent Extension During Mouse Gastrulation." *Development* 136, no. 12 (2009): 2039-48.
- Yin, C., M. Kiskowski, P. A. Pouille, E. Farge and L. Solnica-Krezel. "Cooperation of Polarized Cell Intercalations Drives Convergence and Extension of Presomitic Mesoderm During Zebrafish Gastrulation." *J Cell Biol* 180, no. 1 (2008): 221-32.
- Zhang, W., J. Sloan-Lancaster, J. Kitchen, R. P. Tribble and L. E. Samelson. "Lat: The Zap-70 Tyrosine Kinase Substrate That Links T Cell Receptor to Cellular Activation." *Cell* 92, no. 1 (1998): 83-92.
- Ziegenfuss, J. S., R. Biswas, M. A. Avery, K. Hong, A. E. Sheehan, Y. G. Yeung, E. R. Stanley and M. R. Freeman. "Draper-Dependent Glial Phagocytic Activity Is Mediated by Src and Syk Family Kinase Signalling." *Nature* 453, no. 7197 (2008): 935-9.